# Nuclear Fuels & Materials SPOTLIGHT

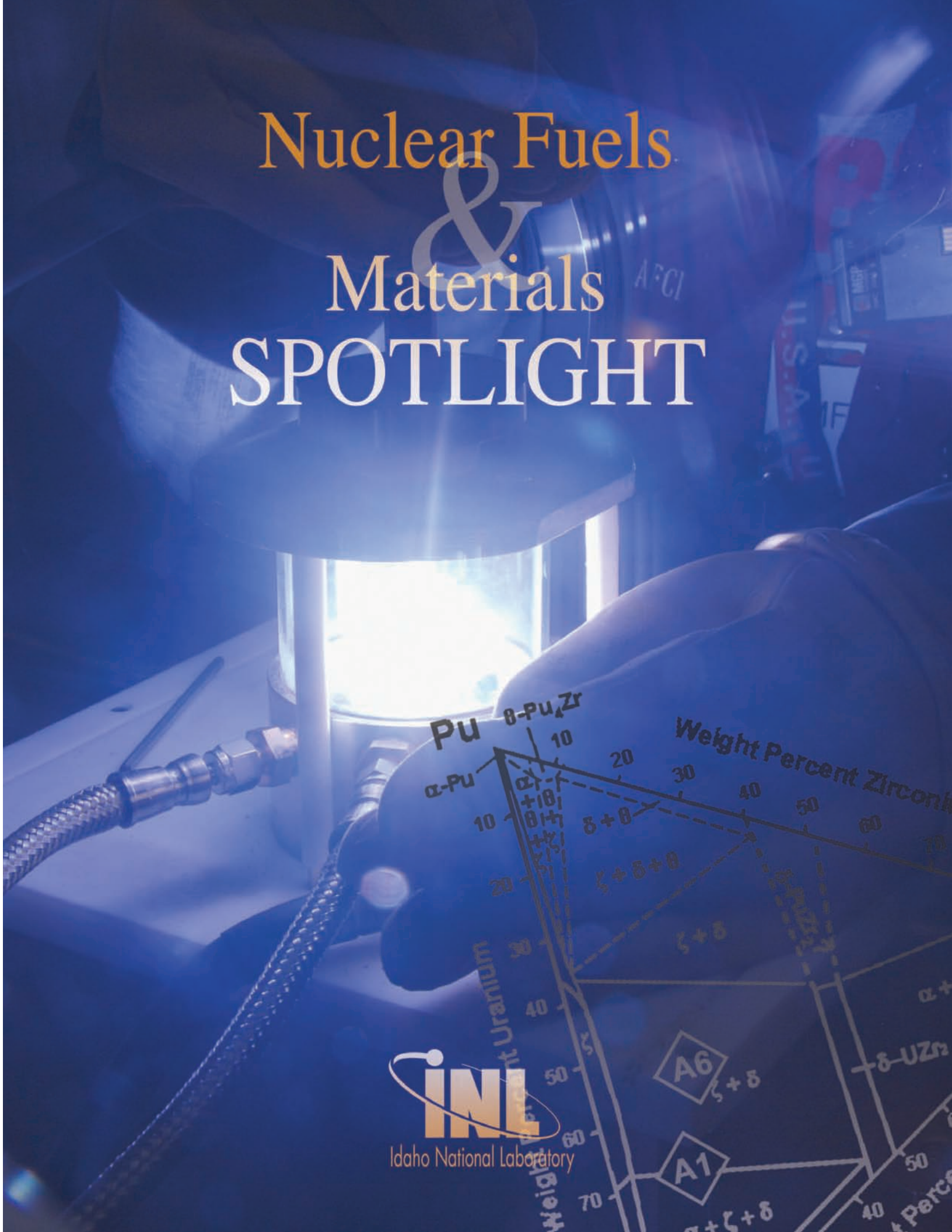


Idaho National Laboratory

# Nuclear Fuels & Materials SPOTLIGHT

March 2009

Idaho National Laboratory
P.O. Box 1625
Mailstop 3878
Idaho Falls, ID 83415-3878

INLNFMSpotlight@inl.gov

Tel: 208-526-9549

Fax: 208-526-2930

www.inl.gov/nuclearfuels

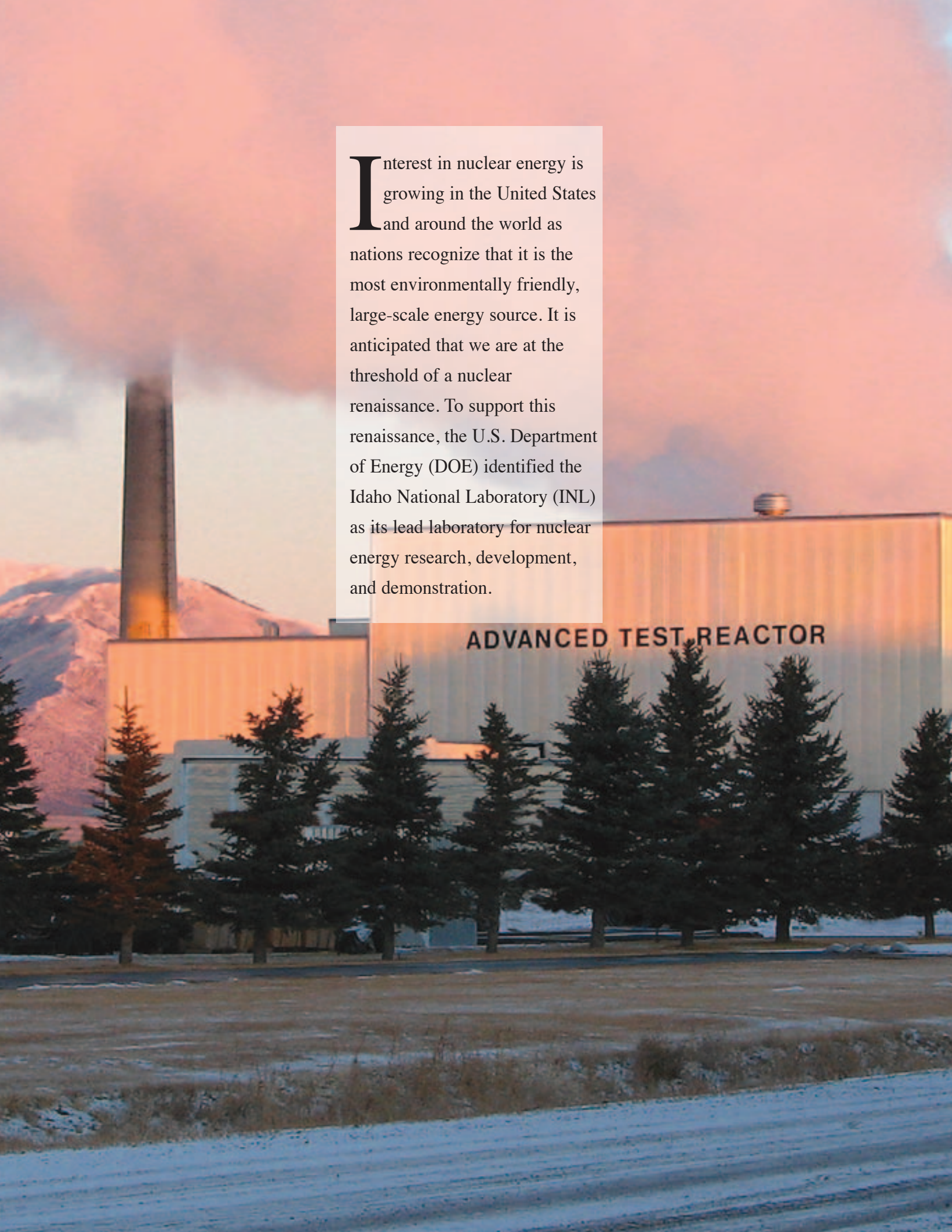


Interest in nuclear energy is growing in the United States and around the world as nations recognize that it is the most environmentally friendly, large-scale energy source. It is anticipated that we are at the threshold of a nuclear renaissance. To support this renaissance, the U.S. Department of Energy (DOE) identified the Idaho National Laboratory (INL) as its lead laboratory for nuclear energy research, development, and demonstration.

# About the Nuclear Fuels and Materials Spotlight

*Kemal O. Pasamehmetoglu*

As the use of nuclear energy grows within the United States and internationally, nuclear fuels and materials research is key to the effort to make nuclear power more affordable and to enhance its safety and reliability. Especially important are developments that can increase burnup and reduce the aging of nuclear materials. The next generation of reactors, depending upon the targeted applications (e.g., process heat and hydrogen production), may use totally different fuel types and materials. Over the longer term, closing the fuel cycle and using recycled materials for nuclear fuel will become a necessity as a means of resource conservation and nuclear waste management.

The INL Nuclear Fuels and Materials Division, established in 2007, will play an important role in meeting these emerging research demands.

The Division will publish an annual *Nuclear Fuels and Materials Spotlight* that will include multiple articles that highlight research areas, capabilities, and expertise of the division. While it is impossible to cover all areas in a single publication in a given year, the *Spotlight* will report on the full spectrum of capabilities, expertise, and accomplishments over multiple years. The objective is to provide a forum for stakeholders and the technical community to get to know the INL Nuclear Fuels and Materials Division. Hopefully, the articles included in each publication will trigger ideas for collaborative research with other national laboratories, universities, industry (both the utilities and nuclear system vendors), and international institutions.

Without feedback from the technical community, sustaining and improving such a publication will be impossible. On behalf of the Nuclear Fuels and Materials Division at the INL, I hope you will find this publication valuable and will provide recommendations for improving it.

*Kemal O. Pasamehmetoglu, PhD*

Director, INL Nuclear Fuels and Materials Division

KEMAL O. PASAMEHMETOGLU received his PhD in Mechanical Engineering from the University of Central Florida in 1986, specializing in nuclear reactor technology with the sponsorship of the U.S. Nuclear Regulatory Commission. He then joined Los Alamos National Laboratory where he worked and served in leadership positions for multiple projects, including the Transient Reactor Analysis Code development, restart analysis for Savannah River K-Reactors, flammable gas mitigation in high-level nuclear waste storage tanks at Hanford, Accelerator Production of Tritium, Accelerator Transmutation of Waste, and Advanced Accelerator Application. While serving as national technical director for advanced fuel development in the Advanced Fuel Cycle Initiative (AFCI), he joined the INL in October 2004. He continues to serve as the national director of advanced fuel development activities, which involves participation by multiple national laboratories and universities. Kemal became the first director of the Nuclear Fuels and Materials Division at the INL in April 2007.

## DISCLAIMER

This information was prepared as an account of work sponsored by an agency of the U.S. Government. Neither the U.S. Government nor any agency thereof, nor any of their employees, makes any warranty, express or implied, or assumes any legal liability or responsibility for the accuracy, completeness, or usefulness of any information, apparatus, product, or process disclosed, or represents that its use would not infringe privately owned rights. References herein to any specific commercial product, process, or service by trade name, trademark, manufacturer, or otherwise, does not necessarily constitute or imply its endorsement, recommendation, or favoring by the U.S. Government or any agency thereof. The views and opinions of authors expressed herein do not necessarily state or reflect those of the U.S. Government or any agency thereof.

INL/MIS-08-14888
**Volume I**

# Table of Contents

Advanced Test Reactor Experiments and Capabilities . . . . . .1

Electron Microscopy of Fuels and Materials . . . . . .11

Metallic Fuels . . . . . .21

Reduced Enrichment for Research and Test Reactors . . . . . .43

Friction Bonding Process Used to Fabricate Fuel Plates . . . . . .45

Silicon as an Alloying Addition to Aluminum for Improving the Irradiation Performance of Fuel Plates . . . . . .51

Advanced Test Reactor In-Canal Ultrasonic Scanner: Experiment Design and Initial Results on Irradiated Plates . . . . . .55

Fuel Performance Modeling . . . . . .63

The Advanced Test Reactor (ATR), at the INL, is one of the world's premier test reactors for studying the effects of intense neutron and gamma radiation on reactor materials and fuels. The physical configuration of the ATR, a four-leaf-clover shape, allows the reactor to be operated at different power levels in the corner lobes to allow for different testing conditions for multiple simultaneous experiments. The combination of high flux (maximum thermal neutron fluxes of $1 \times 10^{15}$ neutrons per square centimeter per second and maximum fast [E>1.0 MeV] neutron fluxes of $5 \times 10^{14}$ neutrons per square centimeter per second) and large test volumes (up to 48 in. long and 5.0 in. diameter) provides unique testing opportunities.

The facility offers three basic experimental configurations. The simplest is the static capsule, wherein the target material is placed in a capsule, or plate form, and the capsule is in direct contact with the primary coolant. The next level of complexity is the instrumented lead experiment, which allows for active monitoring and control of experiment conditions during the irradiation. The highest level of complexity is the pressurized water loop experiment, in which the test sample is subjected to the exact environment of a pressurized water reactor.

Various customers are currently sponsoring experiments in the ATR, including the U.S. government, foreign governments, private researchers, and commercial companies needing neutron irradiation services. The ATR was designated a National Scientific User Facility in 2007, which is enabling greater user access to its capabilities for fuels and materials research. This section provides more details on some of the ATR capabilities, key design features, experiments, and future plans.

# Advanced Test Reactor Experiments and Capabilities

*Frances M. Marshall and S. Blaine Grover*

THE ATR IS one of the most versatile operating research reactors in the United States. The ATR is located at the INL, which is owned by the DOE and currently operated by Battelle Energy Alliance (BEA). The ATR has a long history of supporting reactor fuel and material research for the U.S. Government and other test sponsors. The mission of the ATR is to study the effects of intense neutron and gamma radiation on reactor materials and fuels.

The ATR first achieved criticality in 1967 and is expected to continue operation for several more decades. Current experiments are being conducted in the ATR for a variety of customers, including the DOE, foreign governments, private researchers, and commercial companies that need neutrons. The ATR has several unique features that enable it to perform diverse simultaneous tests for multiple sponsors.

The remainder of this section discusses the ATR design features, testing options, previous experiment programs, and future plans for ATR capabilities and experiments. It also provides some information about the INL and DOE's expectations for nuclear research in the future.

## *ATR Description*

The ATR is a pressurized, light-water-moderated, beryllium-reflected reactor that operates at nominally 2.5 Mpa (360 psig) and 71°C (160°F) and has a maximum operating power of 250 MW. The current operating power is typically closer to 110 MW because of test sponsor requirements, but it is still capable of full power operations. The ATR operates an average of 240 days per year, currently with operating cycles of 6 to 8 weeks, followed by a 1- or 2-week outage for refueling and experiment changes. The core comprises 40 curved-plate fuel elements, each containing 19 curved, aluminum-clad uranium plates arranged in a serpentine configuration around a three-by-three array of primary testing locations called flux traps. These locations have the highest flux locations in the core.

The ATR reactor vessel is constructed of solid stainless steel and is located far enough away from the active core that neutron embrittlement of the vessel is not a concern. In addition, the ATR core internals are completely replaced every 7 to 10 years, with the last change having been completed in January 2005. These two major factors – the stainless-steel vessel and regular change-out of core internals – combined with a proactive maintenance and plant equipment replacement program, have resulted in the ATR operational life being essentially unlimited.

The physical configuration of the ATR (Figure 1) (four-leaf-clover shape) allows the reactor to be operated at different power levels in the four corner lobes to allow for different testing conditions for multiple simultaneous experiments. The horizontal rotating control drum system provides stable axial/vertical flux profiles for experiments throughout each reactor operating cycle unperturbed by the typical vertically positioned control components (see Figure 2 for typical flux distributions). This stable axial flux profile, with the peak flux rate at the center of the core, allows experimenters to have specimens positioned in the core at different known flux rates to receive a range of neutron fluences during the same irradiation periods over the duration of the test program. This control system also allows the reactor to operate different sections of the core at different power levels.

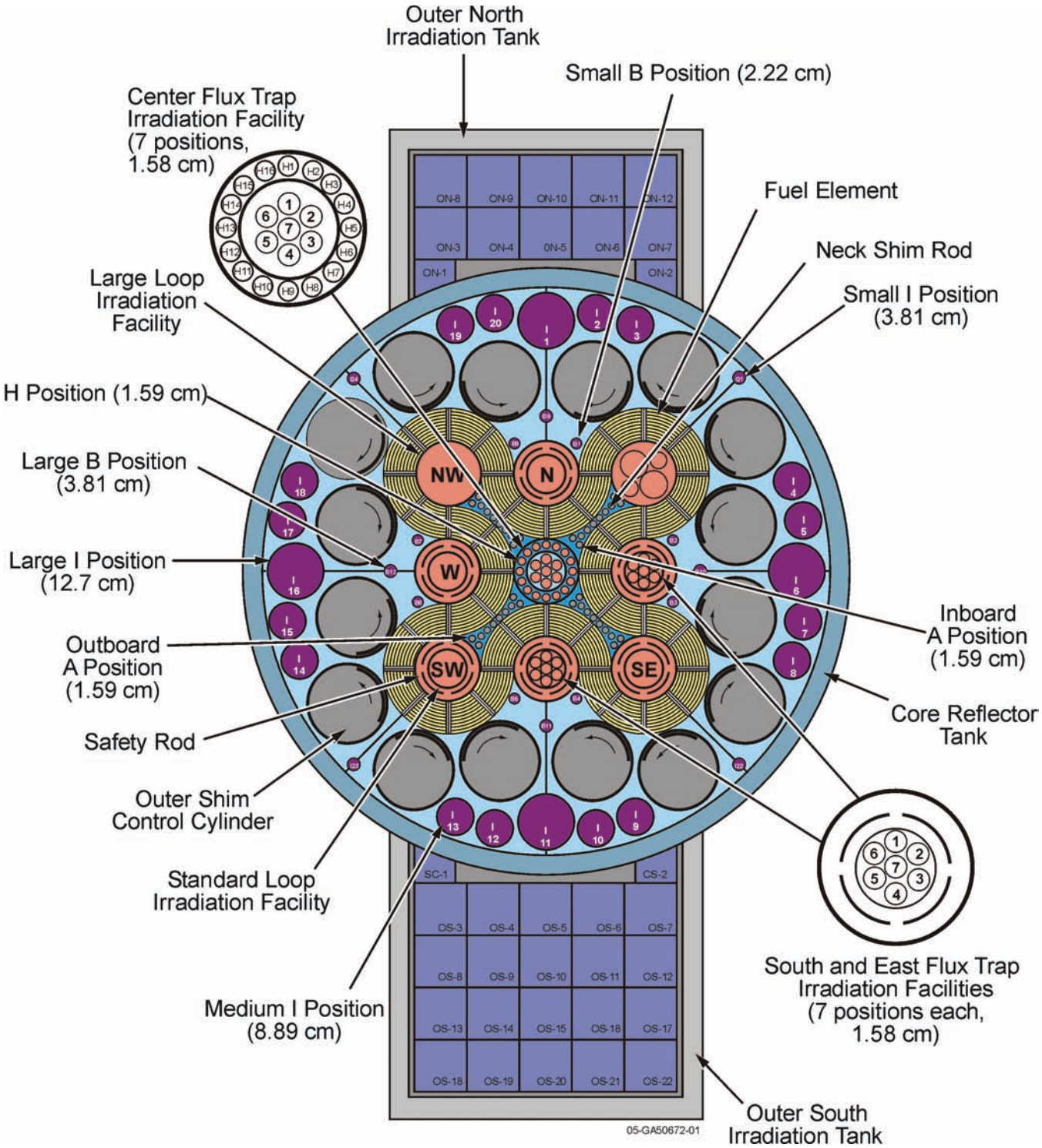


***Figure 1.***

*Map of the Advanced Test Reactor core.*

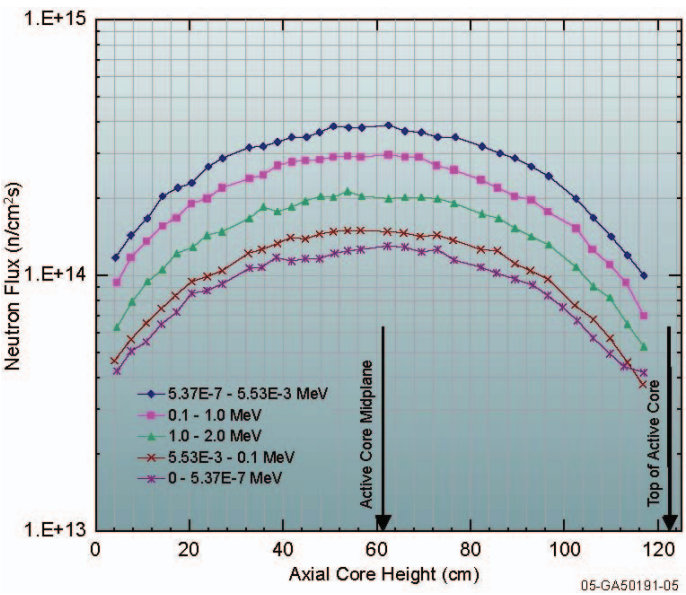


***Figure 2.***

*Unperturbed five-energy-group neutron flux intensity profiles over the active core length of the ATR center flux trap for a total reactor power of 125 $MW_{th}$.*

The ATR design can accommodate a wide variety of testing requirements. The key design features are as follows:

- Large test volumes – 48 in. long (at all testing locations) and up to 5 in. in diameter
- A total of 77 testing positions
- High neutron flux – up to $1 \times 10^{15}$ n/cm$^2$-s thermal and $5 \times 10^{14}$ n/cm$^2$-s fast
- Frequent experiment changes
- Variety of fast/thermal flux ratios (0.1 – 1.0)
- Constant and symmetrical axial power profile
- Power tilt capability between lobes – a ratio of 3:1 between different lobes of the reactor in the same operating cycle
- Individual experiment control
- Simultaneous experiments in different test conditions
- Core internals replacement every 10 years
- Accelerated testing for fuel, up to 20-times-actual burnup rate.

As testing has progressed at the ATR since initial operations, several changes to the reactor and plant have been needed. Some of the changes were implemented to offer more testing capabilities to researchers; other changes have upgraded the plant operating characteristics and increased operational reliability. Changes to the reactor to expand the testing capabilities include addition of the Powered Axial Locator Mechanism (PALM), which allows experiments to be moved axially in and out of the reactor core flux region to simulate reactor startups and other transient conditions. Changes to increase operational reliability include upgrading the instrument and control reactor protection systems (RPS) to more reliable digital systems, resulting in fewer unintentional RPS shutdowns.

## *ATR Test Capabilities*

The ATR uses three basic experimental configurations: 1) the static capsule, 2) the instrumented lead, and 3) the pressurized water loop. The following sections describe each experiment in more detail and include examples of the experiments performed using each type of configuration. An additional experiment configuration, a hydraulic shuttle irradiation system (also discussed below), was being added in 2008.

### *Static Capsule Experiments*

The simplest experiment performed in the ATR is a static capsule experiment. If the specimens are to be irradiated at a specific elevated temperature, then they are sealed in aluminum, zircaloy, or stainless steel tubing with a cover gas and a specially designed insulating gas gap between the specimen and the capsule tube. The sealed tube is then placed in a holder that sits in the ATR test position. A single capsule can be the full 48–in. core height (or shorter) such that a series of stacked capsules may comprise a single test. Capsules are usually placed in an irradiation basket to facilitate the handling of the experiment in the reactor. Figure 3 shows a simplified drawing of the mixed oxide (MOX) irradiation test capsule and basket assembly. Some capsule experiments

contain material that can be in contact with the ATR primary coolant and therefore need the cooling function; these capsules will not be sealed but will remain in an open configuration such that the capsule internals are exposed to and cooled by the ATR primary coolant system. Examples of this are fuel plate testing, in which the fuel to be tested is in a cladding material compatible with the ATR primary coolant chemistry requirements.

Static capsules typically have passive instrumentation, including flux-monitor wires and temperature melt wires for examination following the irradiation. As briefly indicated earlier, limited temperature control can be designed into the capsule through the use of an insulating gas gap between the test specimen and the outside capsule wall. The size of the gap is determined through analysis based upon the experiment temperature requirements, and an appropriate inert gas is sealed into the capsule.

Static capsule experiments are easier to insert, remove, and reposition than more complex experimental configurations. For fuel experiments, it is sometimes necessary to relocate an experiment to a different irradiation location within the ATR to compensate for fuel burnup over the duration of the experiment. A static capsule experiment is also typically less costly than an instrumented one and requires less time for design and analysis prior to insertion into the ATR.

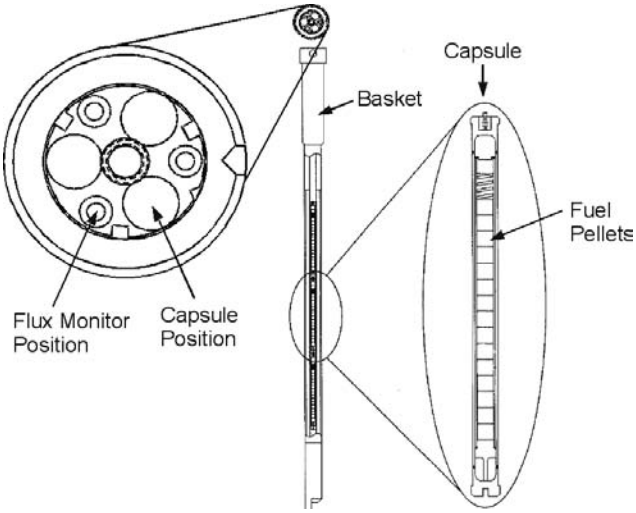


***Figure 3.*** *Static capsule assembly for the MOX experiment.*

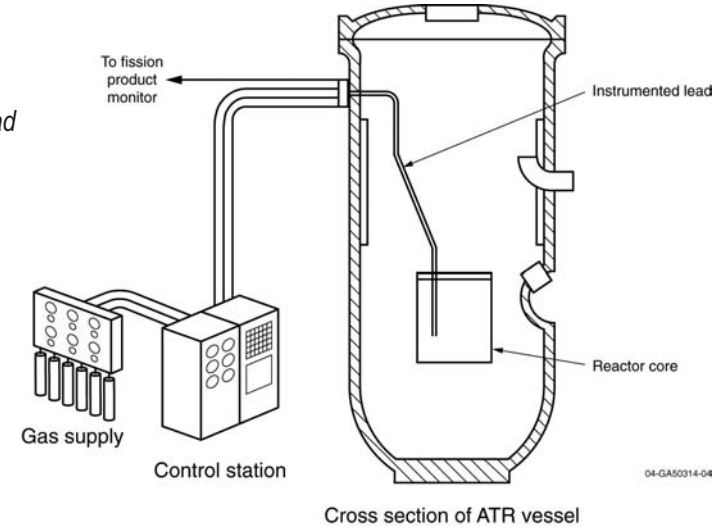


***Figure 4.*** *Example of an instrumented lead experiment configuration.*

### *Instrumented Lead Experiments*

The next level in complexity is an instrumented lead experiment, which provides active monitoring and control of experiment parameters during irradiation. The primary difference between a static capsule and an instrumented lead experiment is an umbilical tube that connects the experiment in the reactor to a monitoring/control system elsewhere in the reactor building.

In a temperature-controlled experiment, thermocouples continuously monitor the temperature and provide feedback to a gas control system that supplies the necessary insulating gas mixture to the experiment to achieve the desired experiment conditions. The thermocouple leads and the gas tubing are located in the umbilical tube. A conducting (helium) gas and an insulating (typically neon or possibly argon) gas are mixed to control the thermal conductance across a predetermined gas gap. The computer-controlled gas blending system allows for the gas mixture to be up to 98% of one gas and as low as 2% of the other gas to allow for a wide range of experiment

temperature ranges. Figure 4 shows a typical instrumented lead experiment.

Another feature of the instrumented lead experiment is the ability to monitor the effluent gas from around the test specimen to determine if changes to the experimental conditions are needed. In a fueled experiment, for example, there is sometimes a desire to monitor for fission gases in order to detect specimen failure. Gas chromatography can also be used to monitor oxidation of an experiment specimen. The instrument leads allow for a real-time display of parameters on an operator control panel. The instrumented leads can also provide an alarm to the operators and experimenters if any parameters exceed test limits. A data acquisition and archive capability can be provided for any monitored experiment parameter. Typically, data are saved for 6 months on a circular first-in, first-out format.

The primary advantage to the instrumented lead experiment is the active monitoring and control of parameters, which is not possible in a static capsule experiment. Additionally, the experiment sponsor does not have to wait until the full irradiation has been completed for all experiment results; the instrumentation provides preliminary results of the experiment and specimen condition.

### *Pressurized Water Loop Experiments*

The pressurized water loop experiment is the most complex and comprehensive type of testing performed in the ATR. Five of the ATR flux traps contain in-pile tubes (IPTs) that provide a barrier between the experiment and the reactor primary coolant system, and are connected to a secondary pressurized water loop coolant system. The IPTs extend through the entire reactor vessel and contain closure plugs at the top of the vessel to allow the experiments to be independently inserted and removed.

The secondary cooling system includes pumps, coolers, ion exchangers, heaters (to control experiment temperature), and chemistry control systems. Loop tests can precisely represent conditions in a commercial pressurized water reactor. As in the instrumented lead experiments, all of the secondary loop parameters are continuously monitored and computer controlled to ensure precise testing conditions. Operator control display stations for each loop continuously display information that is monitored by the reactor operations staff. Test sponsors receive preliminary irradiation data before the irradiations are completed, so there are opportunities to modify testing conditions if needed. The data from the experiment instruments are collected and archived similar to the data in the instrumented lead experiments.

There are two PALM drive units that can be connected to specially configured tests in the pressurized water loop facilities so that complex transient testing can be performed. The PALM drive units move a small test section from above the reactor core region into the core region and back out again – either quickly (in approximately 2 seconds) or slowly, depending on test requirements. This process simulates multiple startup and shutdown cycles of test fuels and materials. Thousands of cycles can be simulated during a normal ATR operating cycle. The PALM drive units are also used to position a test precisely within the neutron flux of the reactor and change this position slightly as the reactor fuel burns.

### *Shuttle Irradiation System*

In 2008, a new facility was added to the ATR – a hydraulic shuttle irradiation system. This system will enable experiments to be inserted into, and removed from, the ATR during the irradiation cycle. Currently, experiments can only be inserted and removed during the outage time, so materials that do not need, or cannot withstand, longer irradiation times are not irradiated in the ATR.

## *Previous and Current Tests in the ATR*

The tests performed in the ATR have been diverse in their designs, objectives, and sponsors. The ATR has supported major nuclear reactor research initiatives for the United States and international collaborations. Some of the more notable experiments are discussed below.

### *Mixed Oxide Fuel*

As part of the nuclear nonproliferation initiatives, it was proposed that weapons grade plutonium be mixed with commercial $UO_2$ and burned in current light water reactors (LWRs). Some testing was needed on the MOX fuel, however. A simple capsule was prepared to contain nine fuel samples, which were exposed to a variety of burnups to simulate LWR burnup profiles. These test capsules were moved from one experiment position to another in the ATR during the irradiation duration to enable a more stable fuel burnup rate during the course of the experiment. Preliminary fuel analysis results were sufficient to enable commercial nuclear power companies to pursue fabrication and use of MOX fuel in commercial LWR power plants.

### *MHTGR Fuel*

In the late 1980s, the United States was interested in designing and deploying smaller high temperature reactors – specifically, the Modular High Temperature Gas Reactor (MHTGR). Several tests for particle fuels were planned in the ATR. One experiment was performed; however, there was evidence of fuel failure so the test was terminated early. Subsequently, the project was cancelled so these tests were also discontinued. The data obtained from this experiment, however, have been valuable in establishing fuel fabrication techniques and a fuel testing program for the Advanced Gas Reactor (AGR) project as part of the Next Generation Nuclear Plant Fuel Research and Development Program.

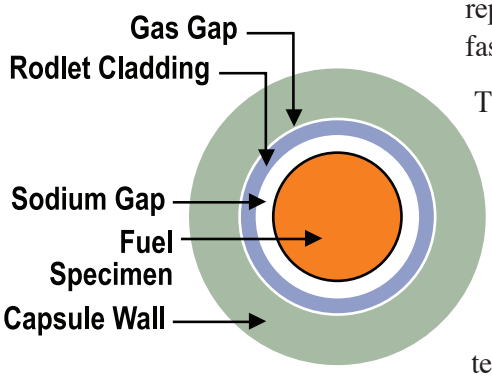


***Figure 5.***
*AFCI capsule cross section.*

### *Advanced Fuel Cycle Initiative Fuel*

As part of work on the AFCI, different fuel types are undergoing irradiation in the East Flux Trap of the ATR. Plans are to continue to irradiate fuel specimens for several more years. The objective of the tests is to support development of fuels to minimize the spent fuel volume needed to be stored in a long-term repository. Because the experiments are taking place in one of the high thermal-flux positions of the ATR and have a maximum linear heat generation rate similar to existing power reactors, a cadmium-lined basket is utilized to reduce the thermal flux and, therefore, reduce the fission rate in the fuel. This approach also increases the fast-to-thermal flux ratio to be more representative of the value of future fast reactors.

These tests are static capsule type experiments consisting of short, internal capsules called rodlets (Figure 5), which contain the fuel specimens. The rodlets are filled with sodium to provide good heat transfer and temperature equalization within the capsule and fuel. An inert cover gas plenum is also included in the top of the rodlet to provide room for swelling and collection of any fission gas releases. Several rodlets are loaded into an outer capsule with a precisely designed gas gap between the rodlets and the capsule wall. The gas gap is filled with a suitable gas to control the heat transfer from the rodlets to the capsule wall and into the ATR

primary coolant, which determines and controls the temperature in the fuel rodlets. The capsules are loaded into an open top basket that positions the capsules in the proper vertical location within the selected position within the East Flux Trap of the ATR.

*Reactor Pressure Vessel Steel*

Several stainless steel samples were irradiated in multiple ATR positions to simulate commercial power plant neutron damage. Some samples were welded before being irradiated, while others were welded after the irradiations. The experiment objectives were to determine the effects of irradiation on welds and weld repairs. Some of the very large experiment specimens required a flux rate that was between the rates of the two positions large enough to accommodate the large specimens. Additional fuel was included as part of the experiment in one of the outer "I" test positions to ensure that the flux received by the experiment was appropriate for the test data needs. This fuel booster provided approximately three times the flux in the test position than would have been provided by the ATR driver fuel alone.

*RERTR Plate Testing*

As part of the Global Threat Reduction Initiative (GTRI), high-enriched uranium fuel is discouraged in all research and test reactors. The Reduced Enrichment for Research and Test Reactors (RERTR) program was initiated to develop and qualify new low-enriched fuels. The ATR has been used as the primary testing location for the new fuel types and will continue to be used until all reactor fuel development is completed and new fuels are fabricated, in approximately 2014. These tests will be static capsule configurations; however, these fuel specimens are in a plate geometry rather than cylindrical pellet, and the fuel plate cladding is in contact with the ATR primary coolant system. These tests are being performed in reflector and flux trap positions.

*Magnox Graphite*

Graphite samples were irradiated to high-density losses from radiolytic oxidation in a high-temperature gas-controlled environment for the Magnox power stations in the United Kingdom in support of life extension studies. Some samples were irradiated in an inert environment, and others in a $CO_2$ environment, to assess the effect of the density loss. The experiment successfully achieved the results the customer wanted. One set of samples was extremely degraded due to oxidation, and the other set of samples in the inert environment was relatively intact.

*Advanced Gas Reactor Fuel*

The AGR Fuel Development and Qualification Program was initiated in 2003, and there will be a total of eight different fuel irradiations throughout the program.

The test train for AGR-1 (Figure 6) consists of six separate capsules vertically centered in the ATR core, each with its own custom-blended gas supply and exhaust for independent temperature control. Each of the six capsules has a diameter of approximately 1.3 in., is 5.2 in. long, and will contain 12 prototypical fuel compacts approximately 0.5 in. in diameter and 1.0 in. long. The fuel compacts are made up of 780-μm-diameter TRISO-coated fuel particles in a graphite matrix compact. The compacts are arranged in four layers in each capsule with three compacts per layer nested in a triad configuration. A graphite spacer surrounds and separates the three fuel compact stacks in each capsule and also provides the inner boundary for the insulating gas jacket. The graphite spacer also contains boron carbide as a consumable neutron poison to limit the initial fission rate in the fuel, providing a more consistent fission rate during the planned 2-year irradiation. In addition to the boron carbide, a thin hafnium shroud is located around the outside portion of the capsule, located toward the center of the ATR core to provide additional neutron absorption and more control of the experiment fission rate.

There are three thermocouples in four capsules (top capsule has five and the bottom capsule has only two due to space limitations) located in the top, middle, and bottom of the graphite holder to measure temperatures during irradiation. For the initial test, high-temperature thermocouples were developed that enabled precise temperature control of the experiment (up to 1,200°C).

Gaseous fission products are monitored by routing the outlet gas from each capsule to an individual fission product monitor system, which includes a high purity germanium (HPGe) spectrometer for identifying specific fission gases and a gross gamma (sodium iodide crystal scintillation) detector to provide indication when a small cloud of fission gases passes through the monitor. This small cloud, or wisp, of fission gases typically indicates when a TRISO fuel coating failure may have occurred.

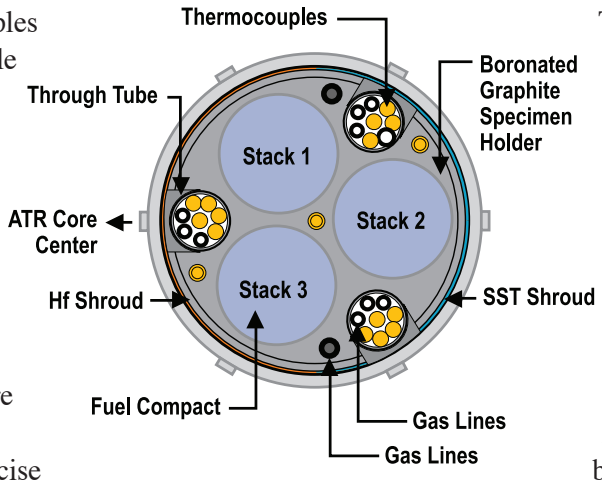


***Figure 6.***

*AGR capsule cross section.*

## *Future Plans for the ATR*

Planned enhancements will increase ATR testing capabilities in the future. One additional pressurized water loop will be reactivated, and there are several organizations interested in performing boiling water reactor (BWR) simulations in the ATR. These tests will require modification of the loop to simulate the BWR conditions (i.e., voids in the core region of the coolant), as well as modifications to the current safety basis and operating processes of the ATR, but that have the potential to yield valuable information about BWR aging issues and design constraints on new BWRs. Preliminary analysis indicates that this testing configuration can be within the ATR safety basis and achieve the necessary conditions for various tests.

The new hydraulic shuttle irradiation system that was added to the ATR in 2008 will enable irradiation of specimens for a short period of time to perform initial feasibility or scoping studies on small amounts of material. This will decrease the cost and time necessary to obtain preliminary data that could be used to develop more complex test programs. Additionally, the shuttle system can be used to irradiate isotope targets that need high fluxes but not high fluences.

In addition to these enhancements, the INL is working to upgrade the irradiation testing infrastructure to enable the ATR to be a center for nuclear fuels and materials research within the DOE complex. This infrastructure includes the experiment assembly capabilities, development of in-reactor instrumentation (e.g., higher temperature thermocouples, creep testing rigs, and additional temperature instrumentation), procurement of a multi-use shipping container for ATR experiments and other irradiation material testing, and upgraded equipment for post irradiation examinations.

The designation of the ATR as a National Scientific User Facility (NSUF) in April 2007 is opening ATR and other INL facilities to a broader range of researchers for work on fuels and materials. The number of experiments sponsored by the DOE through the NSUF is expected to average 15 per year once the ATR NSUF is fully established.

## *Conclusion*

The ATR is a unique and versatile reactor, and the research taking place there today continues the historic role that the INL has played in nuclear reactor development. The ATR will continue operating well into the 21st century as an important contributor to DOE's nuclear research objectives. Additionally, collaborative and complementary capabilities of other research facilities will be vital to achieve the objectives of several national and international initiatives. DOE's commitment to the INL and BEA's commitment to invest in ATR upgrades will ensure that the ATR is ready and available to meet nuclear research needs for diverse experiment sponsors for many years to come.

## *Acknowledgement*

This work was supported by the DOE under DOE Idaho Field Office Contract Number DE-AC07-05ID14517.

## *References*

INL, 2007, "FY 2008, Advanced Test Reactor National Scientific User Facility Users' Guide," INL/EXT-07-13577, Idaho National Laboratory, Idaho Falls, ID.

Grover, S.B., 2008 "The Advanced Test Reactor Irradiation Capabilities Available as a National Scientific User Facility," International Conference on the Physics of Reactors, Interlaken, Switzerland, September 2008.

FRANCES M. MARSHALL (BS, 1982, Nuclear Engineering, University of Virginia; ME, 1999, Chemical Engineering, University of Idaho; Registered PE) is currently the manager of Irradiation Testing for the ATR at the INL, with responsibility for developing the irradiation experiments performed in the ATR. Most recently, Ms Marshall co-led the team to establish the ATR as a NSUF, and she continues to support the transition to full NSUF operation. She held a reactor operator license and worked in the commercial nuclear power industry as a startup and plant system engineer. Ms. Marshall has worked at the INL since 1991 supporting and leading projects in the areas of irradiation experiments, nuclear power plant engineering, regulatory support, power plant performance assessment, and probabilistic risk assessment for the DOE and the Nuclear Regulatory Commission.

S. BLAINE GROVER (BS, 1978, Nuclear Engineering, Idaho State University; Registered PE) has been involved in designing irradiation experiments and associated support systems for the ATR during almost all of his 30-year tenure at the INL. He is currently the technical lead for the ATR irradiation experiments in support of the DOE Next Generation Nuclear Plant (NGNP) program, which includes both fuel and material irradiation testing. Mr. Grover also supports developing new irradiation experiment programs and external customers for the ATR, as well assisting the ATR NSUF.

Nearly all fuels and materials irradiation performance and degradation behavior can be linked to structural changes that occur on the micron and submicron scale. Therefore, it is critically important to have a variety of tools to characterize materials at this scale to improve the fundamental understanding of changes that occur under irradiation. The Electron Microscopy Laboratory (EML), located within the Materials and Fuels Complex at the INL, houses a suite of electron beam instruments primarily dedicated to the structural and chemical characterization (on a micron and nanometer scale) of radioactive nuclear fuels, materials, and waste-forms. Co-located within the EML is a complete set of sample preparation equipment for cutting, grinding, polishing, disc punching, core drilling, dimpling, electro jet-polishing, and precision ion-polishing. Many unique and novel techniques have been developed to prepare challenging activated samples for analysis. Specific examples of analytical scanning and transmission electron microscopy analysis are briefly described in this section.

# Electron Microscopy of Fuels and Materials

*James I. Cole, J. Rory Kennedy, Jian Gan, and Dennis D. Keiser, Jr.*

A ZEISS 960A ($LaB_6$ filament) thermal emission scanning electron microscope (SEM) has been a workhorse for the INL since its installation in 1996. The instrument provides a magnification range up to 200,000x at an accelerating voltage of 30kV, employing analytical detectors that permit, in addition to the standard secondary electron (SE) imaging capabilities, backscatter electron (BSE) imaging and both energy-dispersive spectroscopy (EDS) and wavelength-dispersive spectroscopy (WDS).

Figure 1 shows a result obtained from the Zeiss 960 SEM on an as-cast fuel sample of nominal composition 40U-34Pu-4Am-2Np-20Zr (wt%) prepared in the context of the AFCI. The microstructure is homogeneous throughout the fuel sample and composed of a matrix phase that appears to contain both light and dark contrast sub-phases. Observed within the matrix phase are very dark contrast globular precipitates. Higher magnification images of the sample are shown in Figure 2, where grain boundaries can be identified. The globular precipitates seem to be mostly associated with the dark contrast phase, and the light contrast areas favor the grain boundaries (Figure 2). EDS analysis showed that the light-contrast matrix regions are enriched in plutonium (with possible enrichment in uranium and neptunium), and the darker contrast matrix areas are enriched in zirconium. It appears, therefore, that the grain boundaries are enriched in actinides (particularly plutonium) and the center of the grains are enriched in zirconium.

Higher magnification microstructure images of an as-cast 40Pu-60Zr sample, prepared in the context of the AFCI accelerator-driven system transmutation effort, are shown in Figure 3. The microstructure was shown to be uniform from the center of the sample out to the edge. As in the low-fertile, uranium-bearing fuel sample discussed above, grain boundaries can be observed; however, three distinct phases can be observed here: 1) a relatively large globular phase, 2) an acicular phase, and 3) a matrix phase. The globular

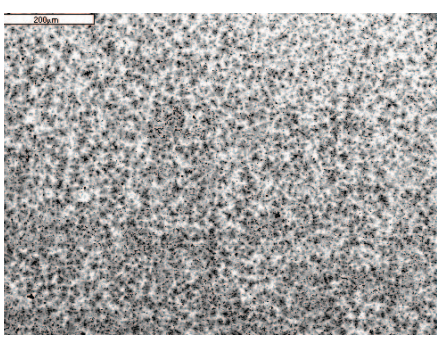

***Figure 1.***
*A BSE image showing the microstructure observed in an as-cast U-34Pu-4Am-2Np-20Zr sample.*

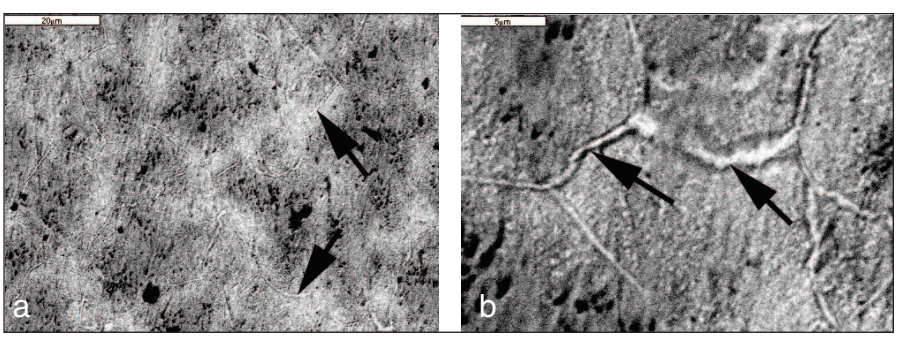


***Figure 2.***
*BSE images showing the grain boundaries (black arrows) in the microstructure observed in an as-cast U-34Pu-4Am-2Np-20Zr sample at two different magnifications.*

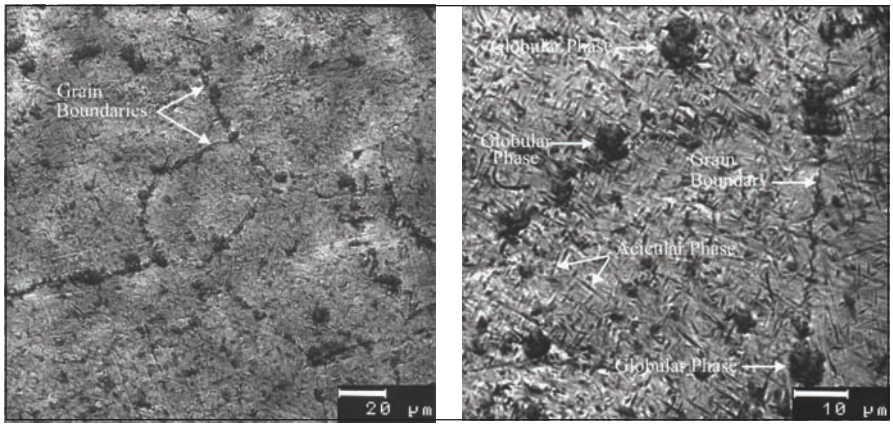


***Figure 3.***

*SEM micrograph of the microstructure observed in an as-cast Pu-60Zr sample.*

phase grows primarily at the grain boundaries, although some random precipitates also form within the individual grains. The individual grains display a Widmanstätten structure where plate-shaped particles (the acicular phase) align along specific crystallographic planes of the matrix crystallites. EDS and WDS analyses revealed the globular phase to be depleted in plutonium, while the two-phase (acicular and matrix) mixture is enriched in plutonium. An even distribution of zirconium occurs over both the globular phase and two-phase mixture. The globular phase and the acicular phase seem to contain some amount of oxygen, with the globular phase being more enriched than the acicular phase. The Widmanstätten structure observed in the two-phase region of the 40Pu-60Zr micrographs may form from the alignment of α-Zr plate-shaped particles (the acicular phase) along crystallographic planes of ill-formed δ-Pu, θ-Pu, or κ-Pu matrix crystallites.

A JEOL 7000F field-emission gun SEM instrument, operational since 2008, can achieve magnifications up to 500,000x with a resolution of 3 nm at 30kV. In addition to enhancing the SE, BSE, EDS, and WDS capabilities, the JEOL 7000F also allows electron backscatter diffraction (EBSD) for orientation imaging microscopy (OIM) analysis. The EBSD detector permits acquisition of crystallographic information by scanning the electron beam over a sample and generating an electron diffraction pattern at each point scanned. The pattern is recorded and indexed to identify the specific crystal orientation and phase at that point. This capability is extremely useful, for example, in evaluating the effect of thermomechanical processing on grain texture. In addition, EBSD combined with EDS enables phase identification and more precise determination of phase distributions within complex microstructures. Figure 4 shows an example of a crystal orientation map of an oxide formation on an Inconel 617 sample following long-term aging at elevated temperatures in air. The small, micron-size crystallites in the oxide, which are difficult to see under standard SEM imaging conditions, are easily discerned from their differences in crystallite orientation.

Fuel cladding chemical interaction is an important aspect of the fuel development programs. The image in Figure 5 was obtained from the interface of a 60U-20Pu-3Am-2Np-15Zr fuel – HT-9 cladding alloy diffusion couple, heated to 650°C for 140 hours. The electron micrograph shows the interdiffusion zone to be a complex mixture of phases developed from the interdiffusion of the cladding constituents into the fuel, and fuel constituents into the cladding. In the base fuel alloy, there is a significant density of zirconium-rich, second-phase precipitates having both globular and stringer-like morphology. X-ray maps illustrated in Figure 6 reveal the distribution of elements within the interdiffusion zone. The maps suggest that the frontal interdiffusion of the fuel into the cladding is actinide dominated, wherein uranium plays a particularly important role and plutonium and neptunium (not shown) track with the uranium. Several distinct phases within the fuel are enriched in iron, chromium, and zirconium; americium appears to concentrate in second-phase particles separate from the other actinide constituents.

The final microscope in the current suite of instruments is a JEOL 2010 transmission electron microscope (TEM) that can operate up to 200kV ($LaB_6$ filament). It is equipped with a Gatan UltraScan 1000 digital

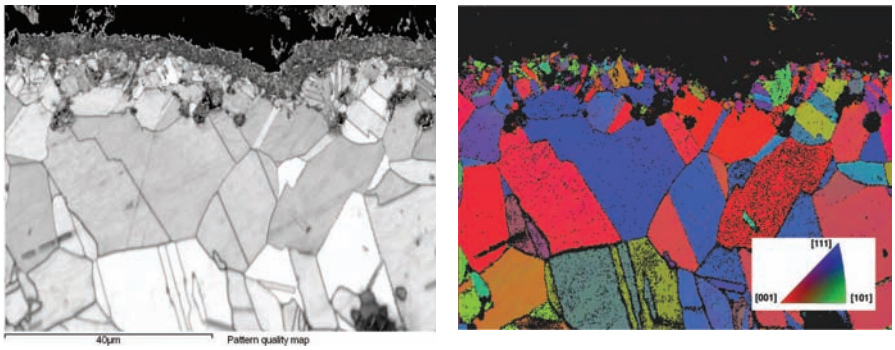


***Figure 4.***

*Image quality map (left) and grain orientation map (right) from an aged Inconel 617 alloy. The image quality map is a representation of the quality of the diffraction pattern formed from each point scanned. Since grain boundaries do not generate indexable patterns, they show up as dark. The grain orientation map is colored to indicate relative grain orientation, as indicated by the legend.*

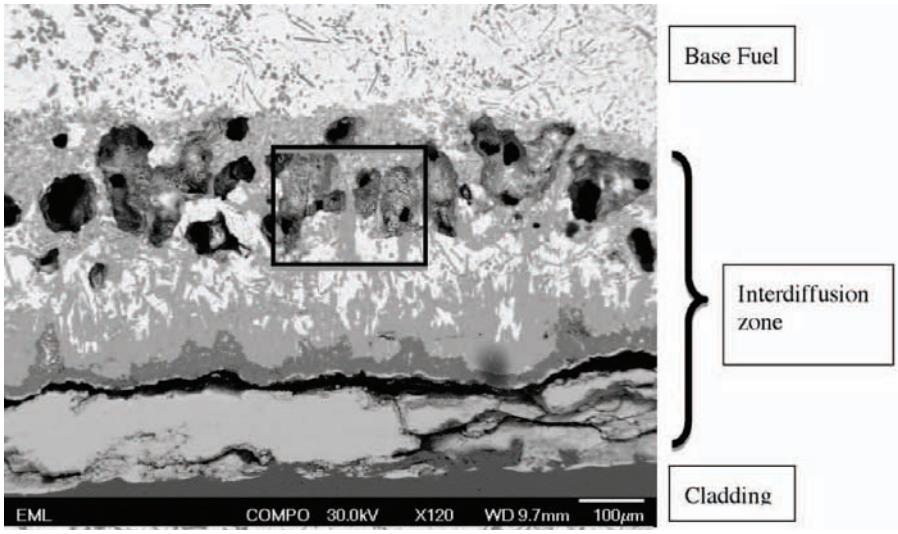


***Figure 5.***

*SEM micrograph of the interaction zone formed from a diffusion couple between 60U-20Pu-3Am-2Np-15Zr fuel and HT-9 stainless-steel cladding heated to 650°C for 140 hours. The rectangular box delineates the region in which a higher resolution elemental X-ray map was collected.*

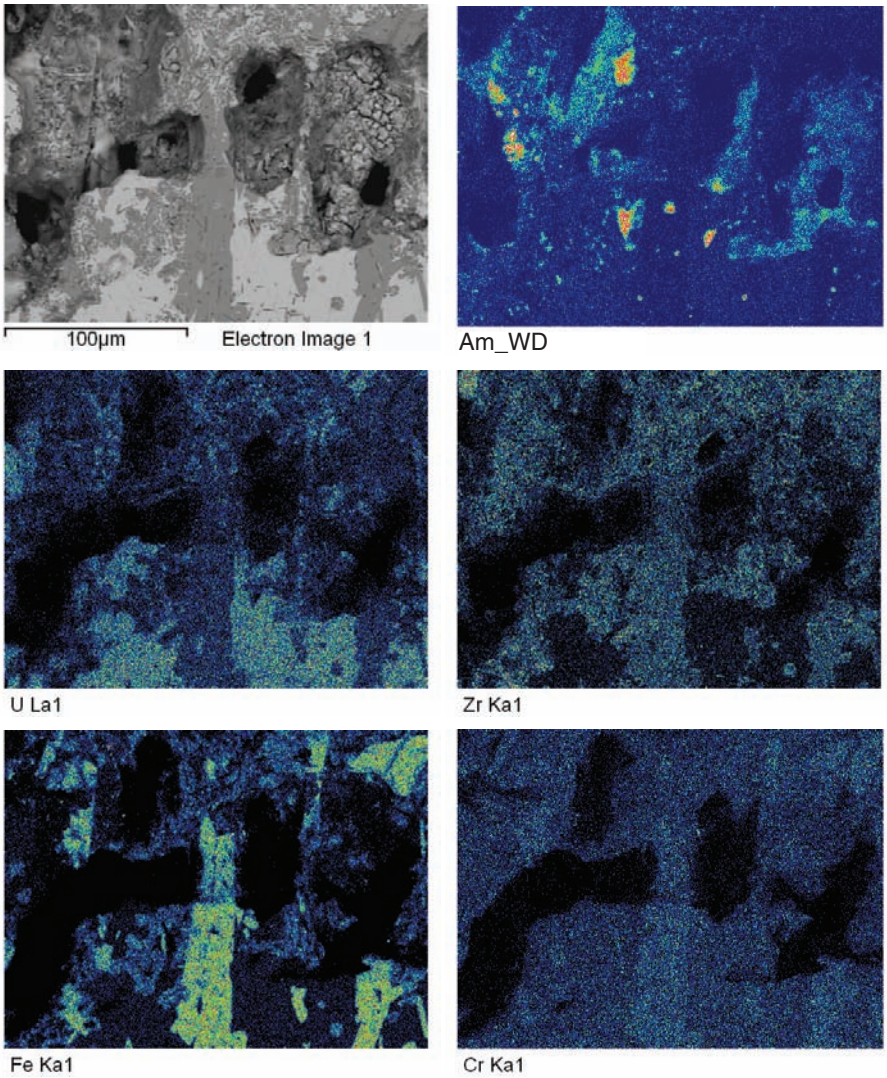


***Figure 6.***

*Elemental EDS and WDS X-ray maps of the rectangular area in Figure 5 showing the distribution of selected elements within the interdiffusion zone. Bright contrast indicates enrichment in the designated element.*

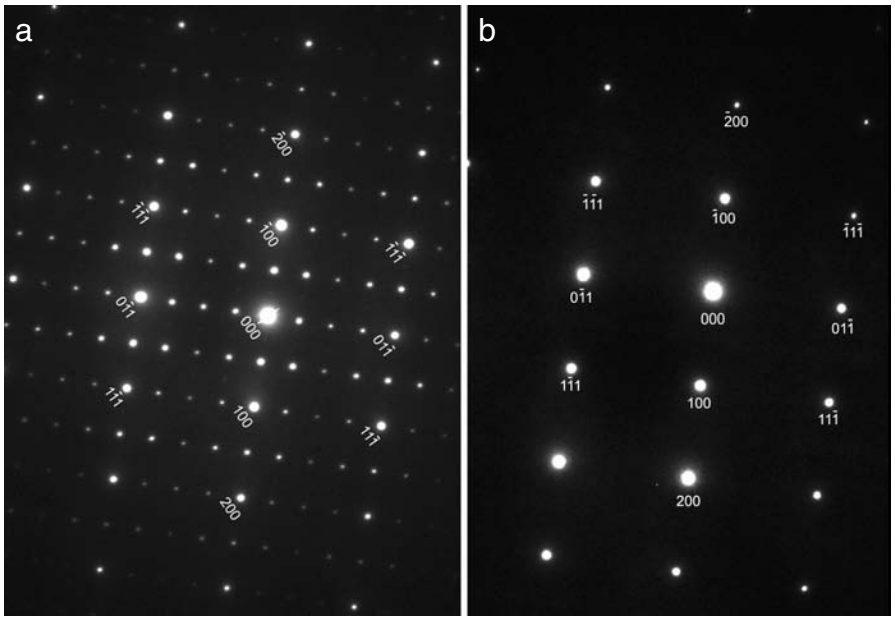


***Figure 7.***

*The [001] zone patterns of a) $U(Al,Si)_3$ and b) $(U,Mo)(Al,Si)_3$ showing ordered $Cu_3Au$ type structure ($L1_2$); see indexed major spots in a) and b). The extra spots in the a) $U(Al,Si)_3$ pattern suggest a super lattice structure since no precipitates were identified.*

camera that produces 2048 x 2048 pixels over a 6.45cm$^2$ imaging area on the TEM screen and an Oxford EDS detector for chemical analysis. There is a scanning TEM unit attached to the microscope.

TEM characterization is an important part of the RERTR program at the INL. Nanometer scale investigations toward understanding the microstructural features of RERTR fuel are presented in Figures 7 and 8.

A variety of phases can potentially form during irradiation of RERTR fuels as a result of fuel/matrix or fuel/cladding interactions. To study the radiation stability of these phases, three depleted uranium alloys were fabricated with compositions of 67u-5Si-28Al, 48U-5Mo-47Al, and 69U-4Mo-20Al-7Si (wt%). In addition to the excess aluminum phase, microstructural analysis revealed the formation of a single $U(Al,Si)_3$ phase in the first alloy, three $UMo_2Al_{20}$, $UAl_4$, and $U_6Mo_4Al_{43}$ phases in the second alloy, and two $(U,Mo)(Al,Si)_3$ and $UMo_2Al_{20}$ in the third alloy. The microstructural stability of these phases under proton irradiation was investigated. A follow-on study using Kr ion irradiation is in progress. The electron diffraction zone axis patterns of $U(Al,Si)_3$ and $(U,Mo)(Al,Si)_3$ are shown in Figures 7a and 7b, respectively. Both phases show an ordered $Cu_3Au$-type structure. The fine spots in the $(Al,Si)_3$ phase suggest a super lattice structure with a lattice spacing eight times that of $U(Al,Si)_3$. No precipitates were identified in either of the two phases. Proton irradiation at 200ºC (up to 3.0 dpa) did not show any discernable changes in the microstructure.

Some interesting features of the $UMo_2Al_{20}$ phase are shown in Figure 8. This phase was identified in both the 48U-5Mo-47Al and 69U-4Mo-20Al-7Si alloys. Although both alloys were prepared by arc casting followed by homogenization treatment at 500ºC

***Figure 8.***

*Bright-field image near zone [011] showing high-density stacking faults in the $UMo_2Al_{20}$ phase in alloy U-5Mo-47Al (a); the streaks in the inset of the diffraction zone pattern are due to the high density of stacking faults on {111} planes. The high-resolution lattice fringe image of the same phase at zone [123] in alloy U-4Mo-20Al-7Si (b) shows the {111} plane projection.*

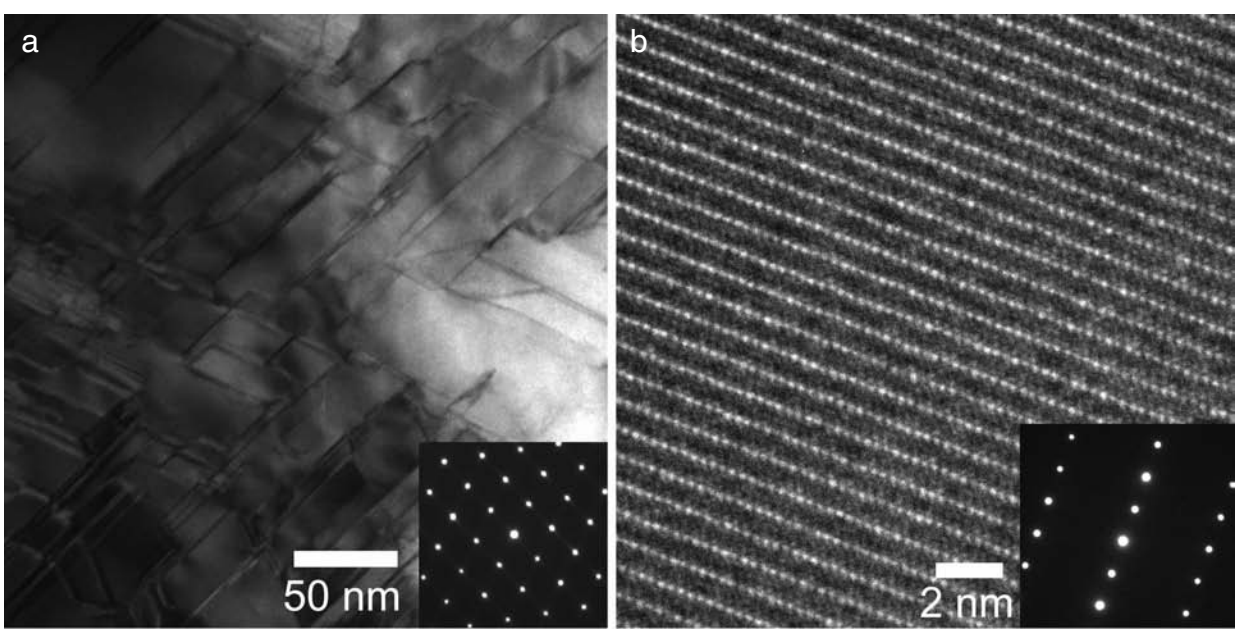

for 200 hours, a high-density of stacking faults was observed in the $UMo_2Al_{20}$ phase in the 48U-5Mo-47Al alloy (Figure 8). The weak streaks in the diffraction pattern in the inset are the result of a high concentration of stacking faults along the {111} planes. In contrast, there are only scattered stacking faults at much lower density in the same phase of the 69U-4Mo-20Al-7Si alloy. Clearly, different microstructures can develop for the same phase depending on the details of the alloy fabrication. These differences may subsequently influence the microstructural development under irradiation.

A high-resolution lattice fringe image of the $UMo_2Al_{20}$ phase near the [123] zone axis in the 69U-4Mo-20Al-7Si alloy is shown in Figure 8b. The line features in the image are {111} plane projections and the spacing between the lines corresponds to the spacing between the {111} planes.

The interesting features of the $UMo_2Al_{20}$ phase are shown in Figure 8. This phase is identified in two different depleted-uranium (DU) alloys: U-5Mo-47Al and U-4Mo-20Al-7Si. Although both alloys were prepared by arc casting followed by a homogenization treatment at 500°C for 200 hours, high-density stacking faults were observed in the $UMo_2Al_{20}$ phase in alloy U-5Mo-47Al (Figure 8[a]). The weak streaks in the diffraction pattern in the inset are the result of high-concentration stacking faults on the {111} planes. There are only scattered stacking faults at a much lower density found in the same phase in alloy U-4Mo-20Al-7Si. This indicates that a different microstructure for the same phase can develop depending on the details of the alloy fabrication, which may influence the microstructural development under irradiation. A high-resolution lattice fringe image of the $UMo_2Al_{20}$

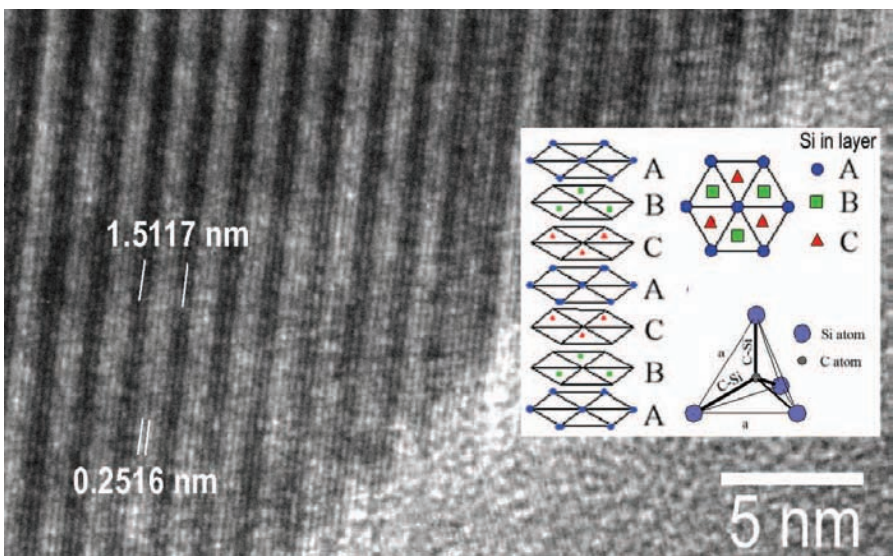


***Figure 9.***
*High-resolution lattice fringe image showing the projection of 6H-SiC basal planes. The six fine fringes between major fringes represent each of the six layers. The inset provides the details on the atomic configuration for the 6H-SiC hexagonal crystal.*

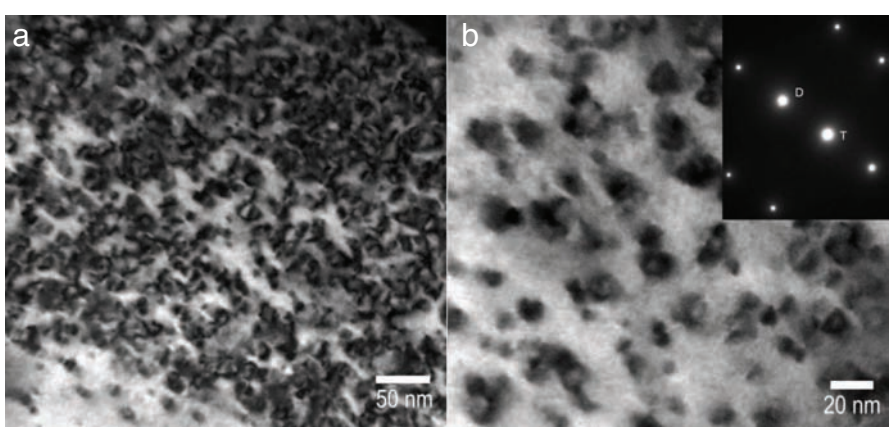


***Figure 10.***
*Low magnification (a) and high magnification (b) bright-field images showing loops in 6H-SiC as a result of Kr ion irradiation at 800°C to a dose of 70 dpa. Dislocation loops were not found in the 10 dpa condition. These loops can affect the mechanical and physical properties of the ceramics.*

phase at the zone [123] in alloy U-4Mo-20Al-7Si is shown in Figure 8(b). The line features in the image are the {111} plane projection, and the spacing between the lines corresponds to the spacing between {111} planes.

Development of fuel matrices and structural materials for application in the Gas-Cooled Fast Reactor requires detailed understanding of the candidate materials and their response to irradiation. The properties inherent to SiC suggest further studies in its application. The high resolution lattice fringe image in Figure 9 shows the basal plane projection of a 6H-SiC hexagonal crystal with a lattice constant of a = b = 0.3080 nm and c = 1.5117 nm. There are six visible lines between the major fringes representing each of the six layers in 6H-SiC. The details of the atomic configuration in 6H-SiC are shown in the inset. The crystal stacking sequence repeats after every six layers. Irradiation of 6H-SiC produces significant microstructural damage. The images in Figure 10 reveal the dislocation loops produced in the microstructure as a result of selective Kr ion irradiation (1.0 MeV Kr ions, 800°C, 70 dpa). Note that no loops were found in the 10 dpa irradiation condition. This result suggests that high-dose irradiation is required to investigate the development of the radiation-induced defects in SiC at high temperature. The formation of a high-density dislocation loop may have significant impact on both the mechanical and physical properties of the SiC-based ceramic materials.

## *Conclusion*

Significant advances have been made in the general materials science community to characterize new and complex materials systems at ever-finer length scales. These characterization techniques are being applied to unique and challenging radioactive fuels and materials at the INL EML. Information gained can be used to support design and modeling efforts that may enhance performance and lead to improved overall life-time prediction capabilities.

JAMES I. COLE (BS, 1989, MS, 1992, PhD 1996, Materials Science, Washington State University) is a Materials Scientist in the Fuel Performance and Design Department at the INL. His research efforts over the last 10 years have focused on radiation effects in reactor structural materials, cladding and structural materials development for advanced reactor systems, and the study of chemical interactions between fast reactor fuels and cladding materials.

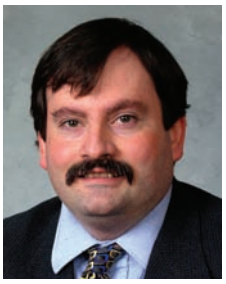

J. RORY KENNEDY (BS, 1982, Colorado State University; MS, 1983; and PhD, 1987, Inorganic Chemistry, Northwestern University) is Manager of the Basic Fuel Properties and Modeling Department at the INL. He has been investigating the synthesis and structure/property relations of materials for over 20 years. Over the last 12 years, his interests have been directed to the fabrication and characterization of materials associated with the nuclear fuel cycle, with emphasis on advanced nuclear fuels.

JIAN GAN (BS, 1982, Physics, Fudan University in China; MS, 1992, Physics, Central Michigan University; PhD, 1999, Nuclear Engineering, University of Michigan) is a Research Scientist in the Basic Fuel Properties and Modeling Department at the INL. He has been actively involved in the research on irradiation effects in materials for more than 12 years, with a focus on investigating microstructure using transmission electron microscopy.

DENNIS D. KEISER, JR. (BS, 1987, MS, 1989, Metallurgical Engineering, University of Idaho; PhD, 1992, Materials Engineering, Purdue University) is a member of the Fuel Performance and Design Department at the INL. He has over 20 years experience researching different issues related to the performance of nuclear fuels and materials. His current research relates to developing low-enriched fuels for application in research and test reactors, developing a better understanding of the diffusion behavior of fuel and cladding components in irradiated fuels, and determining the microstructural development of fuels and materials during irradiation.

Metallic fuels have a history of use that spans the entire nuclear age, from the early plutonium production reactors (1940s) and the first liquid metal fast breeder reactors (1950s) to the most advanced reactor designs of today proposed by industry in support of the Global Nuclear Energy Partnership. Initially, metallic fuels were employed for their ease of fabrication and high heavy-metal density (which led to the most favorable breeding efficiencies in fast reactors). Over subsequent decades of use, metallic fuel technology matured significantly, leading to the realization of major benefits in the areas of fuel reliability and burnup, proliferation-resistant recycling, remote fabrication, and passive reactor safety (Crawford et al., 2007). Such characteristics make metallic fuels a highly competitive technology, especially for use in sodium fast reactors. Research and development activities related to metallic fuel technology have been a major focus of the DOE's research laboratories in Idaho for more than 50 years, and today the INL continues to lead the development of metallic fuels in the United States. This section provides a brief synopsis of the historical progress made on metallic fuel technology, and highlights current activities and recent results in the development of metallic fuels at the INL.

# Metallic Fuels

*Steven L. Hayes, J.Rory Kennedy, Bruce A. Hilton, Randall S. Fielding, Timothy A. Hyde, Dennis D. Keiser, Jr., and Douglas L. Porter*

## *Early Experience with Metallic Fuels*

TWO YEARS BEFORE President Eisenhower's famous "Atoms for Peace" speech in 1953, the Experimental Breeder Reactor (EBR-I), located in the desert west of Idaho Falls, Idaho, had become the world's first nuclear reactor to produce electricity. EBR-I used metallic fuel and was cooled with a liquid sodium-potassium alloy. The design of a typical metallic fuel pin is illustrated in Figure 1. The fuel slug produces heat by nuclear fission, and the heat is conducted through a liquid metal bond to the cladding and then to the reactor coolant. The reactor coolant flows from the bottom to the top of the fuel pin.

During its 12 years of operation, EBR-I employed several different metallic fuel designs, beginning with an initial loading of unalloyed, 93% enriched uranium. The majority of these fuel pins employed solid cylindrical fuel slugs (9.25 mm in diameter) clad in Type 347 stainless steel. This early metallic fuel pin design used liquid metal NaK in the gap between the fuel and cladding to promote efficient heat transfer and keep fuel temperatures low; it was irradiated to a burnup of only 0.35 at.-% (heavy metal).

The next evolution in metallic fuel design in EBR-I made use of a uranium alloy (U-2Zr), still clad in Type 347 stainless steel and still making use of a liquid metal bond. However, in the Mark-III design, the U-2Zr metallic fuel alloy was coextruded with a Zircaloy-2 cladding tube, producing a fuel pin in which the fuel slug was metallurgically bonded to the cladding. This eliminated the need to put a liquid metal bond in the fuel-cladding gap, but in time would prove to be incapable of reaching high burnup due to stresses induced in the cladding by fuel swelling. Eventually, EBR-I demonstrated the use of plutonium-based metallic fuel, and the final fuel loading consisted of a Pu-1.25Al metallic alloy clad in zircaloy.

***Figure 1.*** *Modern metallic fuel pin design.*

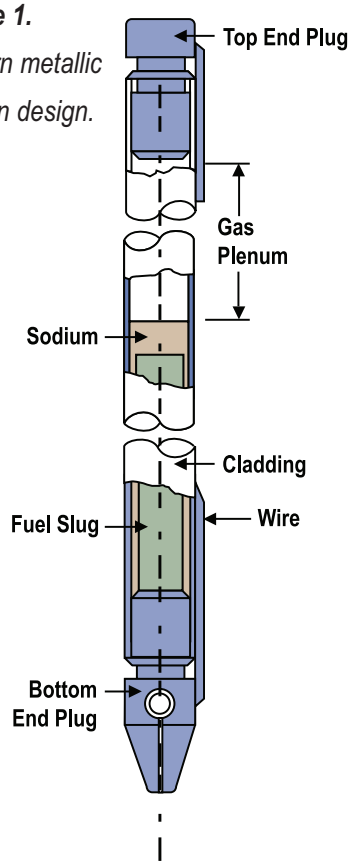


The Dounreay Fast Reactor (DFR) in the United Kingdom, which began full power operation in 1963, also employed a number of metallic fuel designs. These included a U-0.1Cr metallic alloy clad in niobium that employed a sodium bond. Later, U-7Mo and U-9Mo fuel alloys were used. Relatively high burnups of 4 to 9 at.-% were achieved in DFR metallic fuels, considered to be an exceptionally high burnup in early years.

The Enrico Fermi Fast Breeder Reactor, located in Monroe, Michigan, was the first commercial fast reactor. The 200-MWt three-loop design was approved by the Atomic Energy Commission in 1955. Site preparation started in 1956, criticality was achieved in 1963, and operation at 100 MWt began in July 1966. The fuel for the reactor was a U-10Mo metallic alloy, sodium-bonded to zircaloy cladding.

These early metallic fuels were developed using experiments in thermal test reactors (i.e., the Materials Test Reactor in Idaho or CP-5 in Chicago), and the chief fuel performance issue was nonuniform growth of the fuel caused by fuel phase transformations and/or texture created in the fabrication process. These effects sometimes resulted in fuel element bowing or fuel axial growth (causing reactivity anomalies). It was not until these performance issues were understood and corrected/accommodated by design in a subsequent generation of metallic fuel concepts that high burnup became achievable.

Fuel designers at EBR-II engineered fuel designs that could reliably reach 3 at.-% burnup using a U-5Fs (where Fs is a mixture of noble metal elements simulating the fission products carried over in the early melt-refining reprocessing scheme) metallic alloy clad in Type 304 stainless steel and sodium-bonded. By this burnup, however, the fuel began to swell significantly due to gaseous fission products within the fuel. Fuel swelling stressed the cladding, causing breach of the cladding wall.

It was theorized at this time that the swelling problem could be resolved if the fuel had enough space inside the cladding to swell freely to the point where the fission gas could be released through a network of interconnected porosity. The fuel diameter was reduced to 75% smeared density, and the new fuel design achieved 8 at.-% burnup virtually overnight. Figure 2 shows the high percentage of fission gas released as the fuel burnup reaches ~3%, resulting in a dramatically reduced driving force for continued swelling.

Subsequent metallic fuels that used a low smeared density were driven to higher burnups but would eventually fail due to creep rupture of the cladding at or just above the fuel column (where the peak cladding temperature occurred). The much larger volume of released fission gas was overpressurizing the cladding, leading to breach. The gas plenum of these early metallic fuel designs was small. As a final design change, the volume of the gas-collecting plenum above the fuel column was increased, and subsequent metallic fuel pins reliably achieved 20 at.-% burnup without cladding breach.

With the design innovations of a low smeared density fuel pin with a large gas plenum, the final limitation to increased metallic fuel burnup was irradiation-induced swelling of the austenitic stainless steel cladding. Irradiation testing with HT9, a ferritic/martensitic stainless steel, showed it had exceptional resistance to swelling. HT9 was in the process of being qualified as part of a new driver fuel design when EBR-II shut down in 1994. The Fast Flux Test Facility (FFTF) was similarly in the process of qualifying a U-10Zr/HT9 metallic fuel design as the future driver fuel for that reactor at the time of its shutdown.

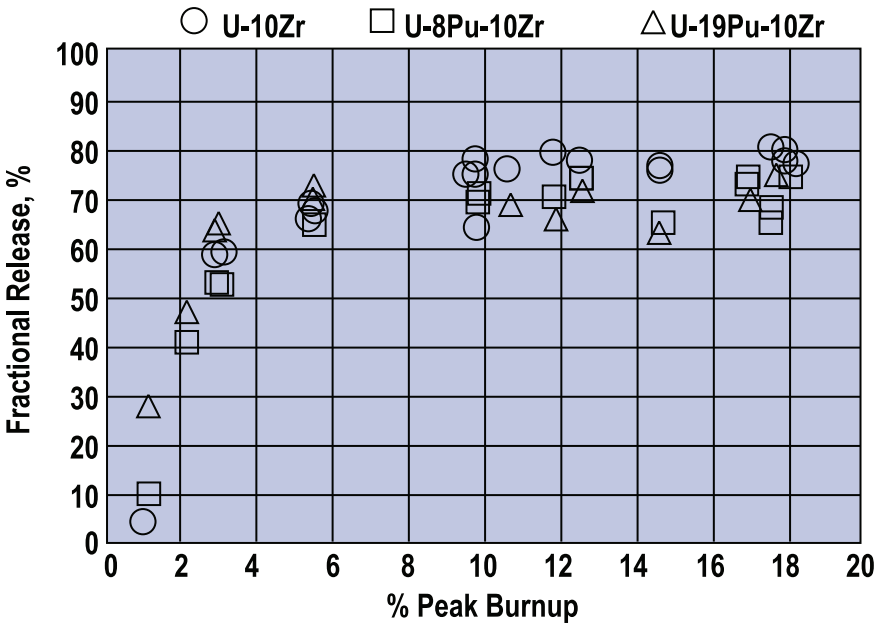


***Figure 2.***
*Fission gas release behavior for a variety of metallic fuels.*

## *Advances in Metallic Fuels for the Integral Fast Reactor*

In the 1980s and 1990s, the composition of metallic fuels under serious development evolved from binary to ternary alloys (i.e., U-xPu-10Zr, with x = 20-30 wt%) in support of the Integral Fast Reactor (IFR) program. The IFR program sought to develop a fast reactor that was passively safe and that made use of a fuel that was easily reprocessed and remotely refabricated, but in a way that was inherently proliferation-resistant (i.e., one in which plutonium was never isolated from other recovered actinides). Metallic fuels fit well with such a concept owing to their high thermal conductivity and thermal expansion (which contributed to reactor safety), compatibility with a pyro-metallurgical reprocessing scheme, and their demonstrated fabrication at engineering scale in a remote hot cell environment.

A substantial plutonium content was incorporated into the metallic fuel alloy to simulate an equilibrium, closed fuel cycle in which plutonium was bred in the blanket region of a fast reactor and added back into the driver fuel at the reprocessing stage. It was also important to demonstrate the concept of transmutation (i.e., burning) of plutonium and minor actinide isotopes (americium, neptunium, and curium) that could be recovered from spent light water reactor fuel in order to reduce its radiotoxicity for a geologic repository. Zirconium was selected as the alloying element, as it appeared to inhibit fuel-cladding interdiffusion as well as increase fuel solidus temperatures.

Using the design innovations developed for the metallic fuel pin used in EBR-II for over 20 years, U-Pu-Zr metallic fuel pins were reliably irradiated to 20 at.-% burnup without cladding breach. When the IFR program ended and EBR-II operations were terminated in 1994, EBR-II was on the verge of a total core conversion to U-20Pu-10Zr metallic fuel. Furthermore, experiments were underway to study the effects of adding americium, neptunium, and curium to the fuel. A low-burnup metallic fuels experiment was completed in which U-20Pu-2.1Am-1.3Np-10Zr was irradiated to 7.6 at.-% burnup. A cross-section of fuel from that experiment, where an electron microprobe was used to determine the redistribution of the major fuel constituents during irradiation (Meyer et al., 2008), is shown in Figure 3.

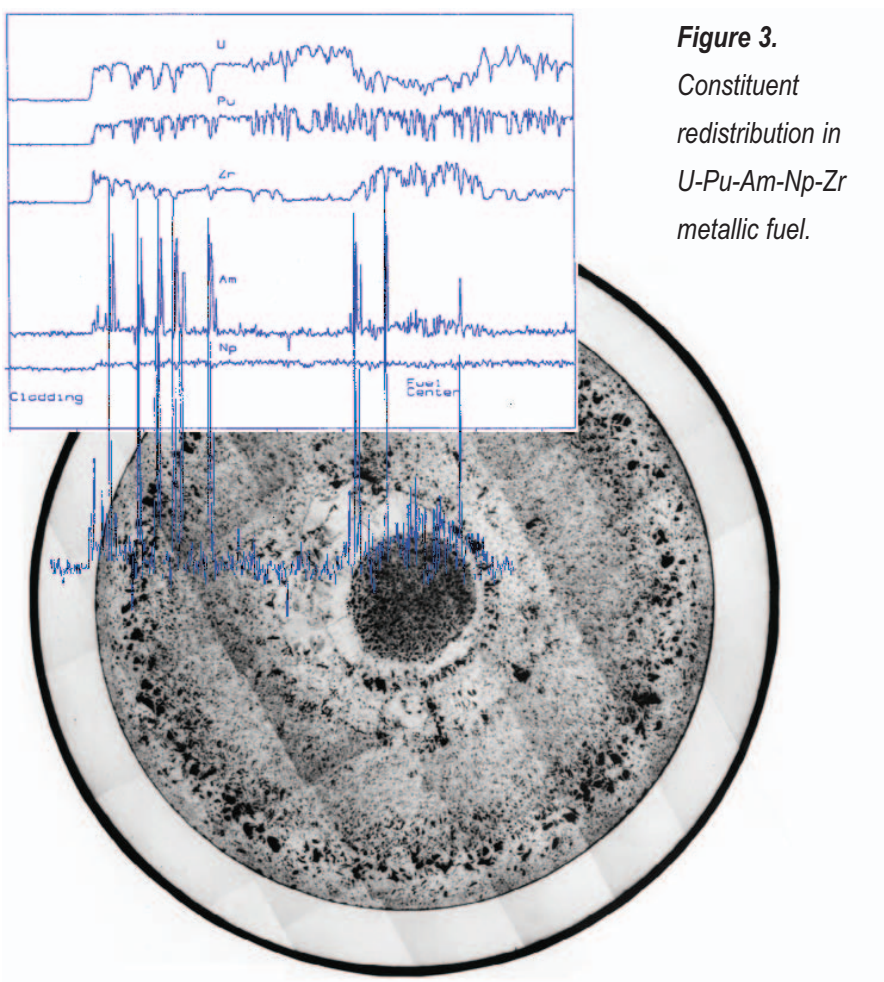


***Figure 3.*** *Constituent redistribution in U-Pu-Am-Np-Zr metallic fuel.*

## *Current Metallic Fuels Research*

### *Metallic Fuels for Actinide Transmutation*

Current research and development activities on metallic fuels focus on their potential use for actinide transmutation in future sodium fast reactors as part of the DOE's Advanced Fuel Cycle research and development (R&D) program. Early factors that led to metallic fuels being identified as a strong candidate for such a mission include the following:

1. Traditional ease of fabrication, especially considering their prior fabrication at an engineering scale in a remote, hot cell environment (Stevenson, 1987)
2. Compatibility with the proliferation-resistant electrochemical recycle scheme
3. Very high burnup potential
4. Passive reactor safety features that derive from attributes inherent to metallic fuels (Chang, 1989).

While the ability to incorporate americium and neptunium into traditional U-Pu-Zr metallic fuel alloys was demonstrated during the IFR program of the 1980s and early 1990s (Trybus et al., 1993), the conventional injection casting fabrication method was not optimized for mitigating loss of the volatile americium constituent in the casting charge. For this reason, significant effort is being applied to the development of an advanced casting system to address this and related issues. The new metallic alloys fabricated as part of the current program are extensively characterized to obtain both fundamental and engineering properties. Finally, the new metallic fuel alloys are incorporated into irradiation experiments to obtain the data needed to assess their in-reactor performance. These activities are summarized in the following subsections.

### *Fabrication of Metallic Fuels*

**Arc-casting Experience**

A previous attempt at casting metallic fuels with americium using the injection casting furnace that had fabricated hundreds of U-Pu-Zr fuels for EBR-II resulted in significant volatile loss of elemental americium during the process (Trybus et al., 1993). That process held the americium-containing fuel alloy under molten and superheated conditions, with a large melt surface exposed to a vacuum for a substantial period of time. It quickly became apparent that a new casting furnace design would ultimately be needed for fabricating metallic fuels with americium.

Before a new casting furnace became available, however, the immediate need was for a method of fabricating small fuel segments that could be used in characterization studies as well as irradiation experiments using miniature fuel rodlets. An arc-casting technique was developed for this purpose. While this technique was never envisioned as a fabrication method suitable for scale-up, it has provided the small fuel specimens required for current research. In arc-casting, metallic-fuel alloys are synthesized and homogenized using a small, commercial, hand-operated arc-melter inside an inert glovebox, as shown in Figure 4.

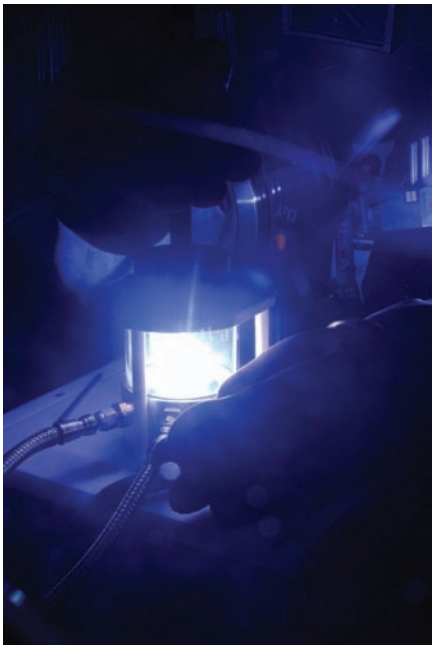

***Figure 4.***
*Arc-melter in use fabricating metallic fuel samples.*

The alloy charge to the arc-melter is considerably less than 50 g, and the total time the fuel alloy is molten is less than a minute. Once homogenization of a fuel alloy is complete, a quartz mold is introduced into the arc-melter, into which the molten metallic fuel alloy is either poured by gravity or drawn by vacuum. Fuel segments up to 0.250 in. in diameter and 1.5 to 2.0 in. in length (see Figure 5) have routinely been cast using this process, with no measurable loss of americium during fabrication.

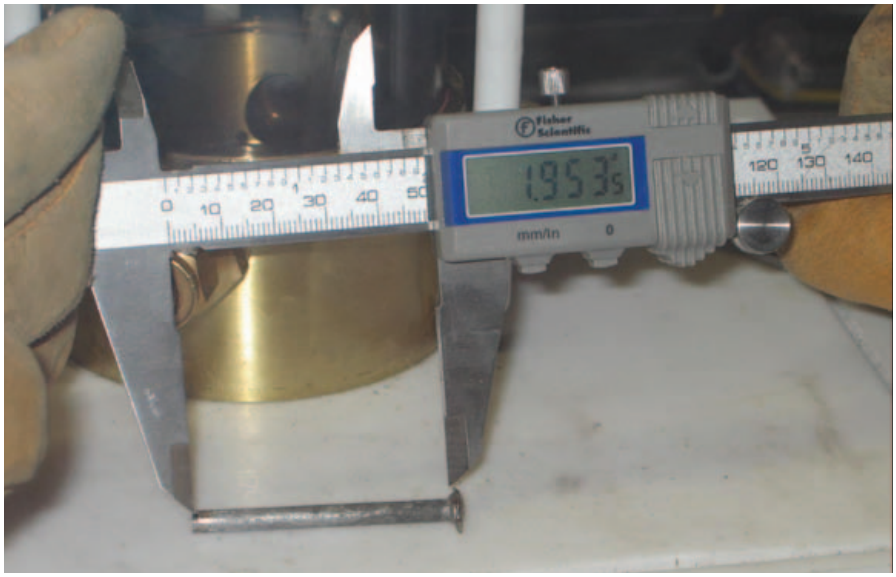


***Figure 5.***
*Typical metallic fuel specimen fabricated by arc-casting.*

*Advanced Casting Research*

Since the late 1950s, metallic fuels have been fabricated at large scale using counter gravity injection casting (CGIC). In CGIC, the fuel material is melted in an induction furnace with glass molds suspended above the crucible. After melting, the furnace and molds are evacuated and the molds are lowered into the molten fuel material. At this time, the furnace is rapidly pressurized, resulting in the molten fuel alloy being forced up into the glass molds where it quickly solidifies. The furnace is then cooled, the molds are removed, and the glass molds shattered to retrieve the metallic fuel slugs.

Well over 100,000 pins have been successfully cast using this method. However, because of the heating cycle duration and the application of a vacuum to a relatively large melt surface, the retention of volatile species (i.e., americium) during casting is a concern for metallic fuel compositions needed for an actinide transmutation mission, as is the amount of waste produced by the one-time use glass molds. For these reasons, an advanced casting prototyping system (designated as the bench-scale casting system [BCS]) has been fabricated to develop bottom pour casting techniques for minor actinide-bearing metallic fuels, which will ensure volatile species retention. It is also being used as a test bed for the development of reusable molds, which will dramatically reduce the quantity of waste generated in the fabrication process.

The BCS is a bottom-pour, pressure-differential-assisted casting system that has an approximate capacity of 300 g of uranium alloy and can simultaneously cast three fuel slugs approximately 250 mm (10 in.) in length and 4.4 mm (.173 in.) in diameter. The furnace is powered by two 10-KW induction power supplies, one used for crucible heating and the other for mold heating. The power supplies are sized such that rapid processing times are achievable. The furnace shell and coils are passively cooled to avoid complications of cooling systems and possible leaks in radioactive areas, as well as coolant leaks into the furnace. A pressure differential can be applied during the casting process by maintaining a positive pressure on the mold while a vacuum or reduced pressure is applied to the mold. Although a hard vacuum is not applied to the mold, a pressure differential of several hundred torr is achieved. Retention of volatile species is achieved by

maintaining the melt continuously under pressure and by rapid casting-cycle times. Initial calculations have shown that very significant volatility reductions can be achieved with the application of only modest overpressure with large gas molecules (i.e., argon).

The BCS is currently operated in a radiological hood and tested with uranium alloys. Future development will focus on casting technique optimization, volatility studies, and reuseable crucible/mold material studies. A schematic of the BCS is shown in Figure 6.

Bottom-pour casting has been used successfully in the casting industry generally, although not for fuel manufacturing. While the BCS is still under operational development, an engineering-scale casting system (ECS) is also under design. This system will be very similar to the BCS, although it will have an approximate casting capacity of 60 pins (~5 kg) and be designed for operation in a totally remote environment. A schematic of a preliminary design of the ECS is shown in Figure 7.

***Figure 6.*** *Schematic of the assembled BCS (showing internal components).*

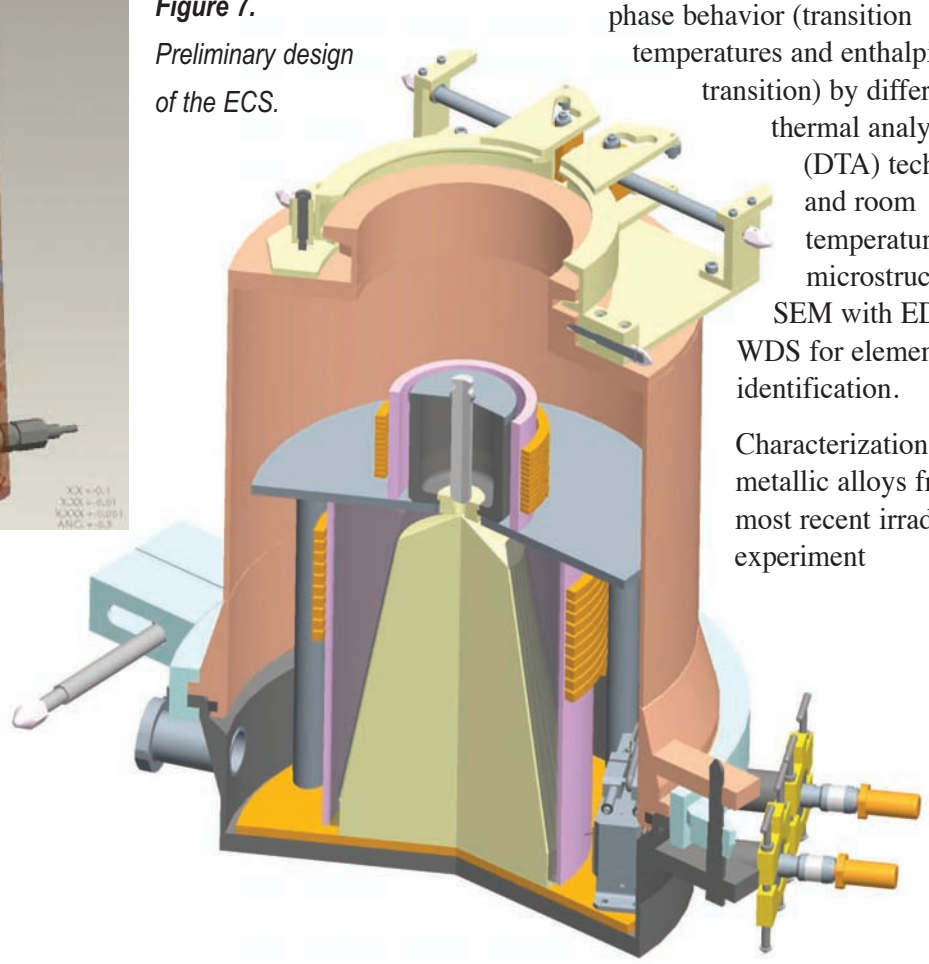

***Figure 7.*** *Preliminary design of the ECS.*

## *Characterization of Metallic Fuels*

### Thermo-physical Properties

INL research activities aimed at understanding the properties and behavior of metallic fuels focus primarily on characterizing unirradiated, as-fabricated fuels in support of irradiation testing. General characterization includes room temperature density by the Arrhenius method, thermal expansion by the dilatometric method, heat capacity by the differential scanning calorimetry (DSC), thermal diffusivity by the laser flash method, room temperature phase identification by X-ray diffraction coupled with Rietveld analysis, thermally induced phase behavior (transition temperatures and enthalpies of transition) by differential thermal analysis (DTA) techniques, and room temperature microstructure by SEM with EDS and WDS for element identification.

Characterization of the metallic alloys from the most recent irradiation experiment

(AFC-2A,B) highlights these capabilities. Two base compositions, 60U-20Pu-3Am-2Np-15Zr and 42U-30Pu-5Am-3Np-20Zr, were fabricated along with companion fuels having additions of lanthanide elements to simulate fission product carryover from electrochemical reprocessing. The X-ray diffraction patterns of the room temperature as-cast, naturally cooled (presumptive non-equilibrium) alloys are shown in Figures 8 and 9, together with the Rietveld refinement analysis results. The samples were prepared as cross-sectional disks from the cast fuel slug and measured only from the fresh cut surfaces. Because the measurements were not performed on powders, the quality of the resulting diffractograms is typically less than optimal. Subtracting out the $LaB_6$ standard, the percent composition of each of the probable phases within the alloys appears in Table 1 along with the refinement residuals.

Both alloys are composed of primarily two phases: the ζ–phase arising out of the U-Pu binary and the δ–$MZr_2$ phase arising out of the U-Zr binary (and perhaps the Pu-Zr binary). A small amount of α-U phase may be present, and some residual nonequilibrium γ-U (high temperature sub-solidus phase) remains. The consistency of composition between each of these base alloys and the companion lanthanide addition alloys is very good. Although an experimentally determined room temperature phase diagram is not available for the U-Pu-Zr system, an approximated diagram is provided in Figure 10 for

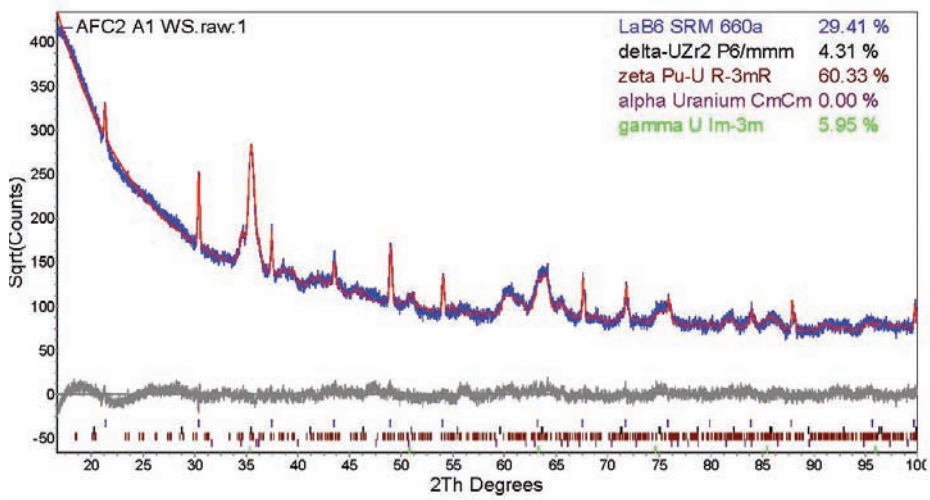


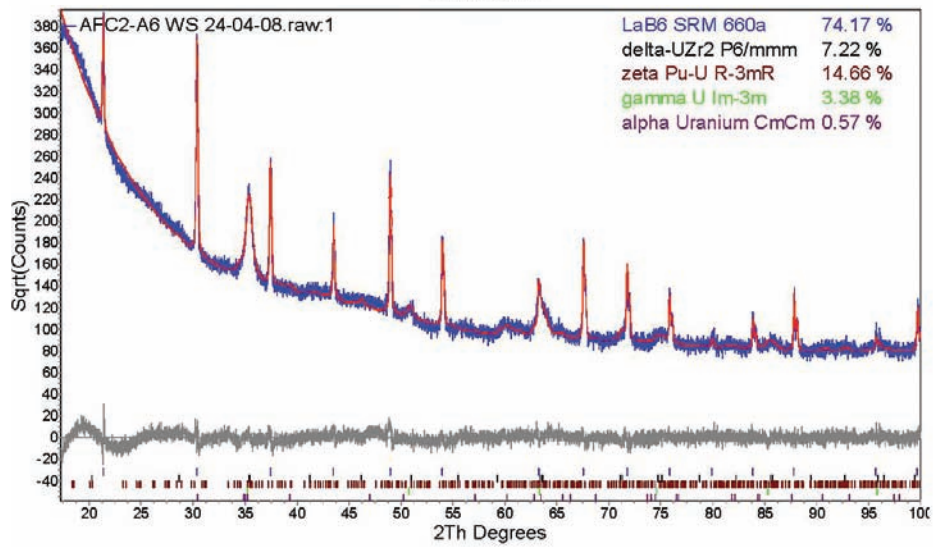


***Figure 8. (top)***

*Rietveld refinement analysis results for the 60U-20Pu-3Am-2Np-15Zr alloy.*

***Figure 9. (bottom)***

*Rietveld refinement analysis results for the 42U-30Pu-5Am-3Np-20Zr alloy.*

| Alloy | ζ-(U,Pu) (%) | δ-(U,Pu)$Zr_2$ (%) | α-U (%) | γ-U (%) | Refinement Residual $R_{wp}$ (%) |
|---|---|---|---|---|---|
| 60U-20Pu-3Am-2Np-15Zr | 86 ± 0.2 | 6 ± 0.1 | 0 ± 0.2 | 8 ± 1.3 | 6.47 |
| 42U-30Pu-5Am-3Np-20Zr | 57 ± 2.3 | 28 ± 2.4 | 2.2 ± 0.7 | 13 ± 1.2 | 6.29 |

***Table 1.***

*Phase contents for the 60U-20Pu-3Am-2Np-15Zr and 42U-30Pu-5Am-3Np-20Zr base composition metal alloys.*

visual illustration of the X-ray diffraction results. Because the minor actinide content of the alloys is small, the five component alloys can be reduced to pseudoternary systems for visualization in two dimensions. This can be accomplished by allowing all the americium to be included with the plutonium (uranium and americium anticipated to show limited mutual solubility) and splitting the neptunium content evenly between uranium and plutonium (both uranium and plutonium show mutual solubility with neptunium). The two base alloys reduce as follows:

60U-20Pu-3Am-2Np-15Zr → 61U-24Pu-15Zr
and
42U-30Pu-5Am-3Np-20Zr → 43.5U-36.5Pu-20Zr

The approximate thermodynamic equilibrium positions for these alloys are indicated in Figure 10. Generally, there is consistency between what is observed and what might be expected, as both alloys are composed of primarily ζ–phase and δ–$MZr_2$ phase with the higher zirconium content alloy having the greater δ–$MZr_2$ content.

The thermally induced phase behavior of the two alloys represented in the traces of Figures 11 and 12 are similar, yet each is distinct. Both show two primary temperature regions through which phase transitions occur: the temperature regions are at about the same temperatures (Table 2), and the transition regions appear to be composed of multiple signals that reveal themselves better in the cooling curves. Included in Table 2 are the determined enthalpies of transition (ΔH) for the general transition regions for the two alloys. The two alloys show that although the higher temperature heats of transition are similar, the lower temperature enthalpies are significantly different.

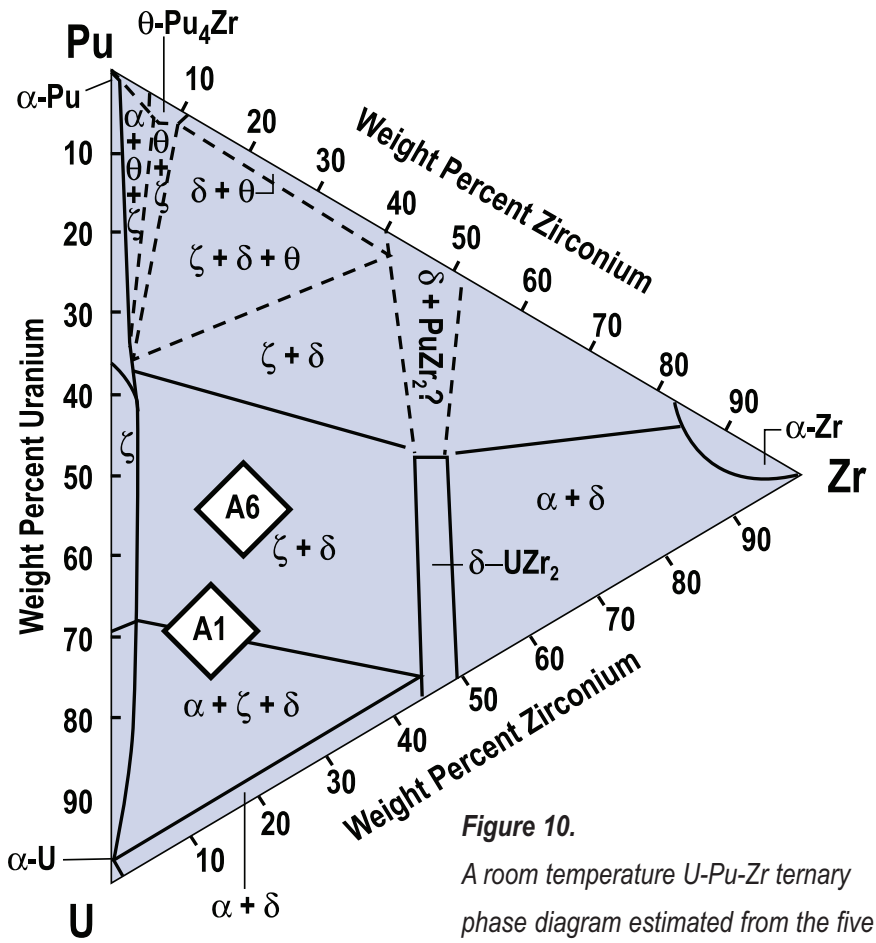


*Figure 10.*
*A room temperature U-Pu-Zr ternary phase diagram estimated from the five isothermal sections from O'Boyle and Dwight (1970) and the three binary phase diagrams of the elements involved. The reduced compositions of alloys 60U-20Pu-3Am-2Np-15Zr (61U-24Pu-15Zr) and 42U-30Pu-5Am-3Np-20Zr (43.5U-36.5Pu-20Zr) are marked as A1 and A6, respectively.*

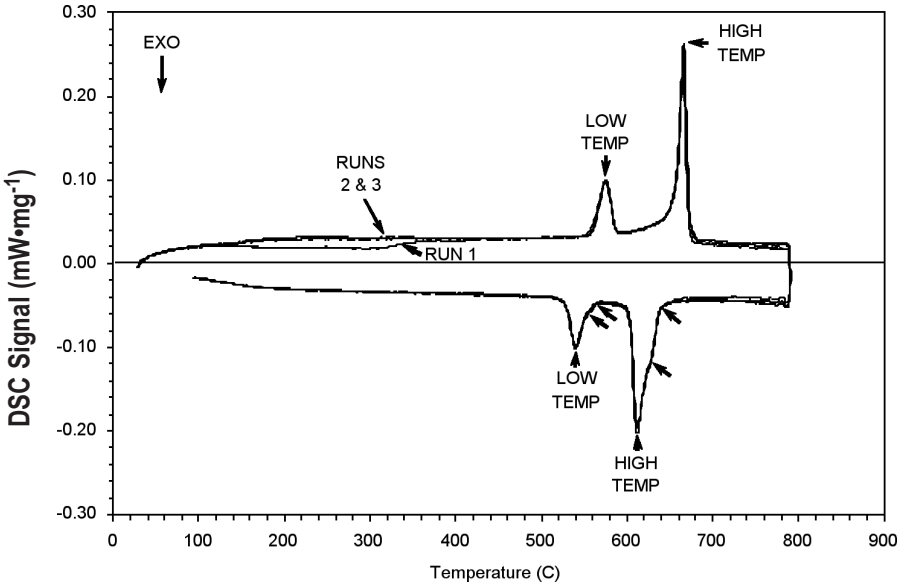


***Figure 11.***
*Heating and cooling traces obtained from the DSC/DTA measurements on the as-cast 60U-20Pu-3Am-2Np-15Zr alloy.*

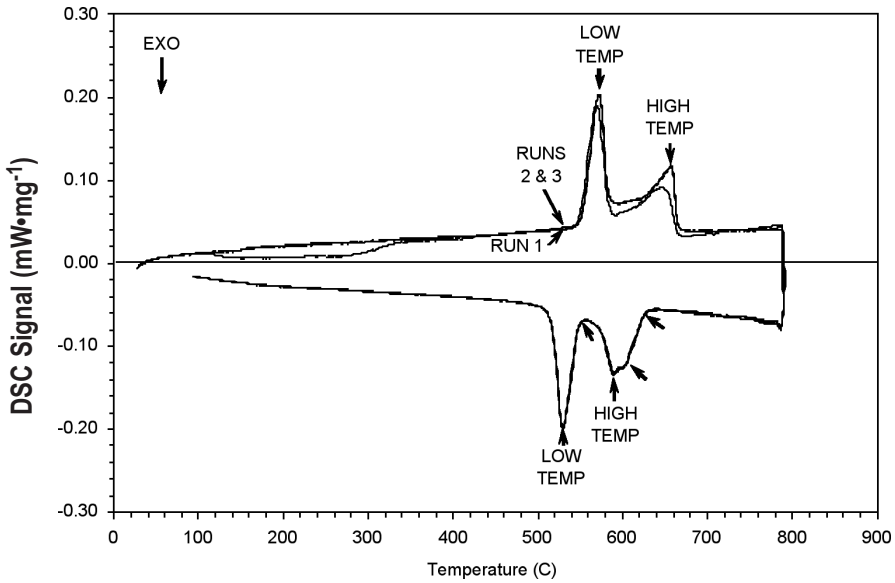


***Figure 12.***
*Heating and cooling traces obtained from the DSC/DTA measurements on the as-cast 42U-30Pu-5Am-3Np-20Zr alloy.*

| **60U-20Pu-3Am-2Np-15Zr** | **Heating** | | **Cooling** | |
|---|---|---|---|---|
| *Transition* | *Low temp* | *High temp* | *Low temp* | *High temp* |
| $T_{tr}$ (K) | 832 ± 1.6 | 929 ± 0.5 | 906 ± 5.8 | 825 ± 0.5 |
| $\Delta H_{tr}$ (J•g$^{-1}$) | 6.9 ± 0.5 | 21.8 ± 0.7 | -20.2 ± 0.4 | -7.1 ± 0.3 |
| **42U-30Pu-5Am-3Np-20Zr** | **Heating** | | **Cooling** | |
| *Transition* | *Low temp* | *High temp* | *Low temp* | *High temp* |
| $T_{tr}$ (K) | 824 ± 1.9 | 900 ± 0.6 | 898 ± 0.4 | 820 ± 0.3 |
| $\Delta H_{tr}$ (J•g$^{-1}$) | 19.6 ± 0.2 | 19.1 ± 1.5 | -18.0 ± 0.2 | -19.6 ± 0.4 |

***Table 2.***
*Transition temperatures ($T_{tr}$) and enthalpies of transition ($\Delta H_{tr}$) determined from differential scanning calorimetry upon heating and cooling of the AFC2 alloys.*

Observing the experimental U-Pu-Zr phase diagram data (O'Boyle and Dwight, 1970), the first transition of the 60U-20Pu-3Am-2Np-15Zr alloy can be interpreted to reflect the transition of the (δ+ζ) phase field directly into the (δ+ζ+γ) field, wherein most of the transition is conversion of δ, which showed to be a minor species from the room temperature X-ray diffraction results and is consistent with the low enthalpy of transition value. This transition is then followed by transition into the (γ+ζ) phase field before 600°C and final transition into the sub-solidus γ-phase field at approximately 640°C.

The thermal phase equilibria transitioning for the 42U-30Pu-5Am-3Np-20Zr may be interpreted with a somewhat more complicated path. The endotherm in the heating curve at about 550ºC may represent first the δ+ζ ↔ δ+ζ+η transition with a narrow δ+ζ+η phase field, followed by the Class II ternary four-phase equilibria reaction δ+ζ+η ↔ δ+ζ+γ, wherein approximately 40% of the material transforms (60δ+20ζ+20η ↔ 45δ+15ζ+40γ) into γ-phase. The subsequent endotherm signal (signals comprising the saddle portion of total DSC signal) represents transversing the δ+ζ+γ field (expected 550ºC - 565ºC) and transitioning into the γ+ζ phase field (expected 565ºC), followed by the transition at approximately 630ºC into the single phase γ field. No other transitions should occur up to the ~1,100ºC solidus.

The importance of the experimental nuclear fuel's thermal conductivity in determining the safety margins and projected fuel performance cannot be overstated. The thermal conductivity of a material at temperature can be computed as the product of its density, heat capacity, and thermal diffusivity. Typically, best results are obtained from a dense material with a homogeneous microstructure. The transmutation metallic fuels produced to date generally show room temperature densities, as determined by the Arrhenius immersion method, that are better than 95% of the theoretical densities (as shown in Table 3). The room temperature density can be combined with thermal expansion data obtained by dilatometric methods to give the material density at temperature.

The temperature dependence of the heat capacity and thermal diffusivity for the fuel alloys is determined and combined with the density to give the fuel thermal conductivity as a function of temperature. Heat capacity is measured by differential scanning calorimetry and thermal diffusivity is obtained with the transient laser flash method. Typically, each of the data sets is fitted to a correlated expression (linear for density and polynomial for heat capacity and thermal diffusivity) and these are carried over to allow the determination of thermal conductivity. The plots in Figure 13 show the averaged measured values for heat capacity (at half-centennial increments) and thermal diffusivity (at centennial increments) for the 60U-20Pu-3Am-2Np-15Zr alloy. The lines representing the polynomial fits are well within the 1σ standard deviations (represented as error bars in plots) determined at each temperature. The plot in Figure 14 illustrates the temperature dependent thermal conductivity result for the 60U-20Pu-3Am-2Np-15Zr test fuel alloy, which itself can be fitted to a polynomial relation (in this case virtually linear). The error bars represented in the plot are shown at the 5% (relative) level, which are taken as conservative. Compounded error estimates obtained from the individual measurements at temperatures generally fall within the 1-6% range at lower temperatures (up to about 600°C) and can increase to 10% or more at higher temperatures (up to 1,200°C). Uncertainty analyses of this type are of increasing importance to the fuel properties and characterization effort at INL as well as the national programs.

| Alloy | Average Density ($g/cm^3$) @ 25ºC | Theoretical Density ($g/cm^3$) | Std. Dev. |
|---|---|---|---|
| 60U-20Pu-3Am-2Np-15Zr | 14.05 | 14.59 | 0.33 |
| 42U-30Pu-5Am-3Np-20Zr | 12.88 | 13.51 | 0.04 |

***Table 3.***

*Average room temperature and theoretical ideal solution densities of the 60U-20Pu-3Am-2Np-15Zr and 42U-30Pu-5Am-3Np-20Zr alloys.*

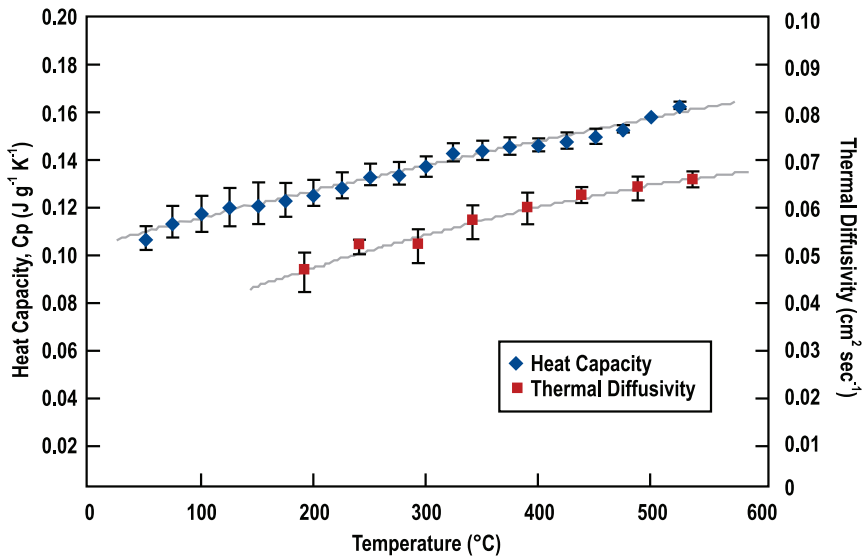


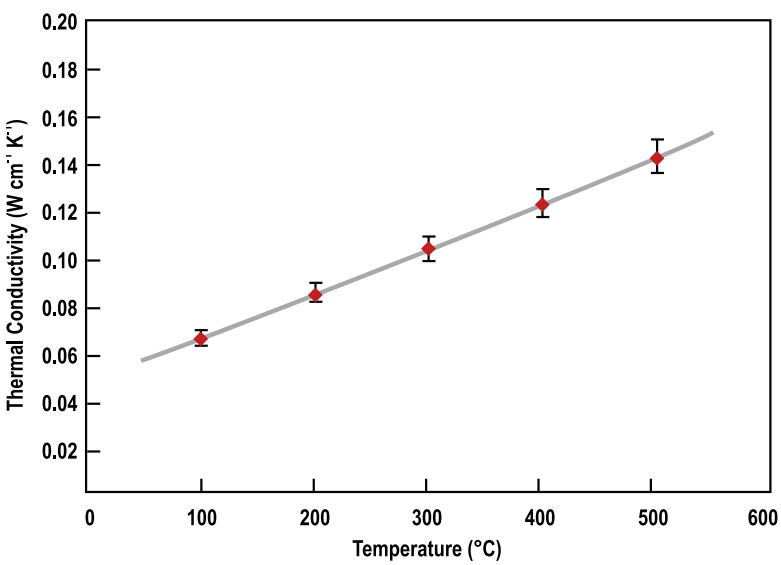


***Figure 13. (Top)***

*Plots showing the temperature dependence of the heat capacity and thermal diffusivity measured for the 60U-20Pu-3Am-2Np-15Zr fuel alloy up to the first phase transition.*

***Figure 14. (Bottom)***

*Plot showing the temperature dependence of the thermal conductivity determined from the fitted expressions for density, heat capacity, and thermal diffusivity from the 60U-20Pu-3Am-2Np-15Zr fuel alloy up to the first phase transition. Error bars are at the 5% level.*

**Fuel-cladding Compatibility**

When a metallic nuclear fuel is irradiated, the fuel swells and eventually contacts the cladding. This typically occurs at around 2 at-% burnup. At this point, interdiffusion can occur between the fuel and cladding, resulting in the formation of interdiffusion zones on the inner surface of the cladding. These zones are comprised of phases that are enriched in fuel and cladding constituents as well as fission products. Having interdiffusion zones present on the inner surface of the cladding can affect the performance of a fuel pin, since these zones can potentially be low melting or can be brittle and exhibit poor mechanical properties. Therefore, it is important to develop understanding of the types of phases that will develop during irradiation of metallic fuels and to determine whether the developed phases are low-melting or prone to cracking.

Much experience was gained during the 30 years of operating the EBR-II reactor in developing an understanding of FCCI in irradiated metallic fuels. Many fuel pins that contained U-Pu-Zr or U-Zr metallic fuel alloys were destructively examined to characterize the fuel-cladding interface (Keiser, 2005). Figure 15 shows the fuel-cladding interface in an irradiated fuel element that had U-Pu-Zr fuel and the austenitic steel D9 as the cladding. Composition analyses that have been performed at the fuel-cladding interface in irradiated fuel elements have shown that lanthanide fission products can be especially

enriched in these locations. Figure 16 shows a location where hardness indents were generated in a FCCI zone. The interaction zone is observed to be decidedly harder than the unreacted cladding.

Diffusion couple experiments are an effective way to improve understanding of how fuel and cladding components will interdiffuse to form phases. Systematic diffusion couple experiments have been performed using fuel and cladding alloys to determine the interdiffusion behavior of specific fuel and cladding constituents. Some examples of such studies can be found in Keiser and Dayananda (1994) and Keiser and Petri (1996). To study the interdiffusion behavior of fuel components, initial tests used simple binary U-Zr alloys followed by more complex U-Pu-Zr alloys, and then fuel alloys that contained fission products (e.g., molybdenum, neodymium, ruthenium, etc.) and minor actinides (e.g., americium, neptunium). To look at the behavior of cladding constituents, simple binary iron-containing alloys were first used (e.g., Fe-Cr and Fe-Ni), followed by more complex Fe-Ni-Cr alloys, and then actual cladding steels (e.g., HT-9, 316SS, D9, HCM12A, ODS, or Alloy 800H). An example of a diffusion structure that formed in an annealed diffusion couple is shown in Figure 17. This diffusion structure formed when a diffusion couple between a 35U-29Pu-4Am-2Np-30Zr alloy and an austenitic Type 422 cladding steel was annealed at 550˚C for 15 hours. Many complex phases can be found in the interdiffusion zone. The current emphasis with diffusion couple testing is to investigate the compatibility of metallic transmutation fuels, which include minor actinides with HT-9 cladding (Cole et al., 2008).

Also of interest, with regard to FCCI, is the development of lined claddings that can be employed to eliminate the FCCI reaction altogether. If lined claddings can be successfully developed, then the potential operating temperature of the fuel element can potentially be increased. The application of liners has also been investigated for improving fuel performance in light water reactors (Frost, 1982). Diffusion couple tests have demonstrated that zirconium and vanadium have the potential to be effective liner materials for eliminating FCCI (Keiser and Cole, 2007). Ultimately, irradiation tests will be required to demonstrate the true effectiveness for these materials as liners. During the IFR program, V-lined cladding was fabricated for irradiation testing, but due to the shutdown of EBR-II in 1994, reactor testing never transpired. During the same program, casting of a U-Pu-Zr

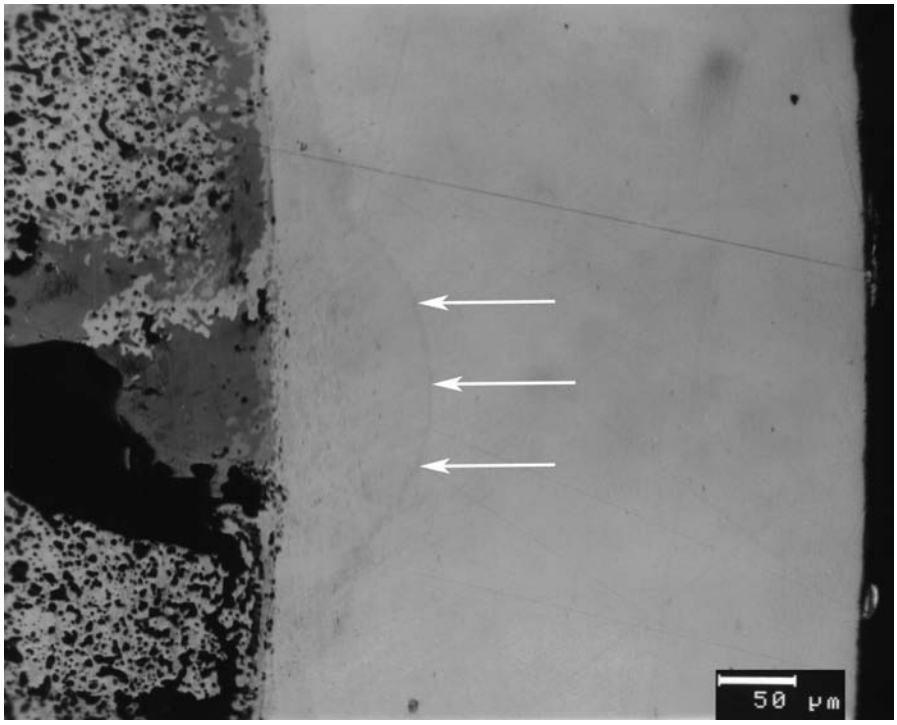


***Figure 15.***
*Optical micrograph showing fuel-cladding interaction (white arrows) adjacent to a large deposit of lanthanide fission products.*

fuel into a zirconium-sheath was performed to see if zirconium on the fuel surface could act as a barrier to FCCI. It was found that the zirconium-sheath cracked during irradiation and proved not to be an effective barrier (Crawford et al., 1993). Having the zirconium as a liner in intimate contact with the cladding should be a more effective way to employ zirconium as an FCCI barrier.

At this point in time, much progress has been made in improving the understanding of FCCI in irradiated metallic fuels.

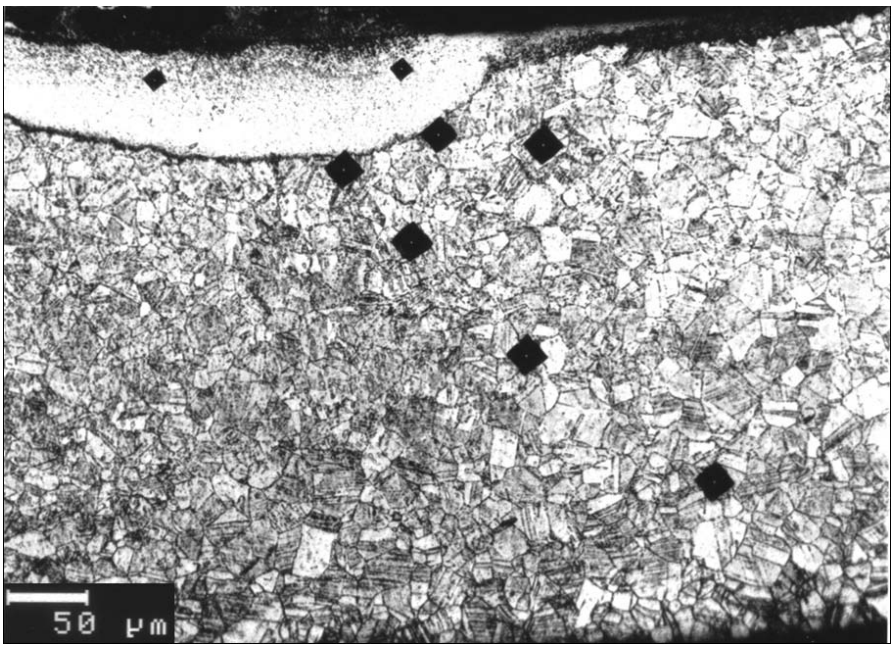


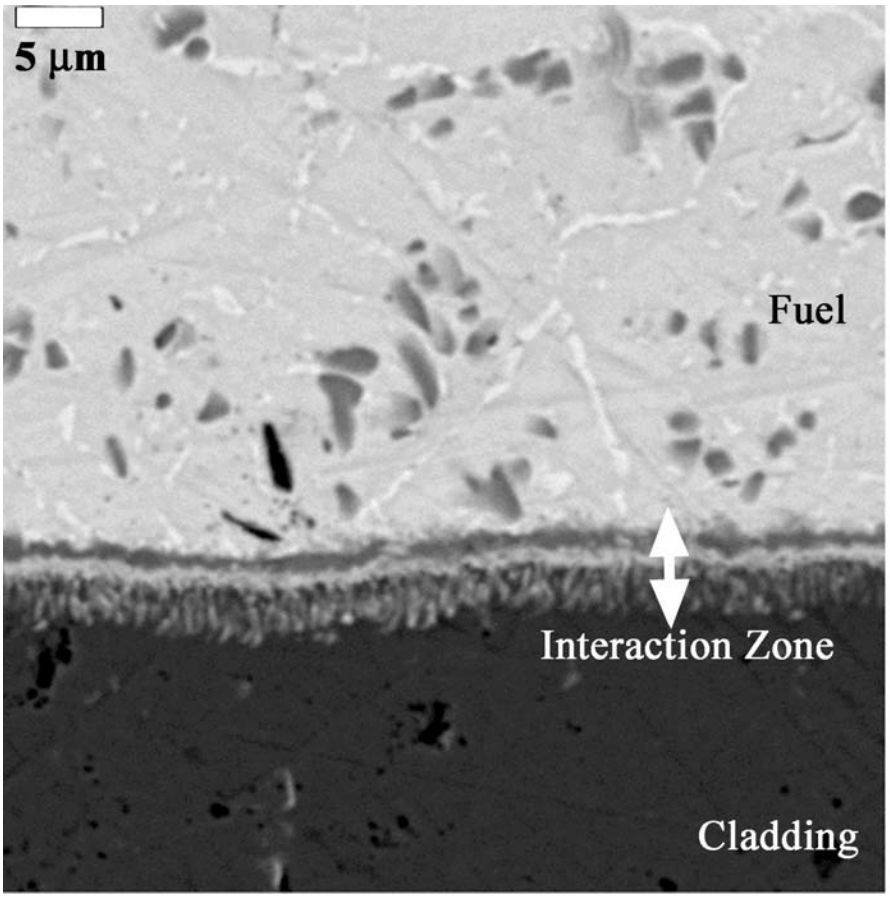


***Figure 16. (Top)*** *Optical micrograph showing the presence of an interaction zone at the fuel-cladding interface. Hardness indents reveal the increased hardness of the interaction zone vis-à-vis the unreacted cladding.*

***Figure 17. (Bottom)*** *Backscattered electron micrograph of the interdiffusion structure that formed in a diffusion couple between a 35U-29Pu-4Am-2Np-30Zr fuel alloy and an austenitic Type 422 cladding steel when annealed at 550˚C for 15 hours.*

It has been determined that the phases that form uranium, plutonium, zirconium, fission products, and cladding constituents; uranium and plutonium are the original fuel alloy constituents that penetrate furthest into the cladding. Of the fission products, the lanthanide fission products penetrate deepest into the cladding, and palladium is the noble metal fission product to penetrate deepest into the cladding. Iron is the cladding component that penetrates deepest into the fuel. In terms of identifying where the largest interdiffusion zones will form in an irradiated fuel element, the combined high temperature and high-power region of a fuel element is consistently found to contain the widest zones. In this region of a fuel element, the interdiffusion kinetics are increased, and the supply of fission products at the fuel/cladding interface is relatively large.

Future work will focus on using diffusion couple experiments to investigate the kinetics of interaction between metallic fuels appropriate for actinide transmutation and the current cladding to be used, HT9. Furthermore, efforts will continue to identify the best barrier materials and to fabricate lined claddings with these materials so that actual irradiation testing can be performed, which is necessary to find the best material for eliminating FCCI altogether.

## *Irradiation Testing of Metallic Fuels*

### Irradiation Testing Strategy

An important aspect of the development of metallic fuels has always been, and continues to be today, the irradiation testing of metallic fuel pins. Historically, such testing was conducted in the experimental fast reactors, EBR-II and the FFTF. Both of these fast reactors, however, were shut down in the early 1990s.

The present lack of a domestic fast flux irradiation capability has of necessity led to a current two-pronged approach to obtaining the necessary irradiation performance data on the new metallic fuel alloys of interest. First, the majority of the fuel performance data are obtained from irradiation experiments conducted in domestically available thermal test reactors, notably the ATR at the INL. Second, a much smaller number of irradiation experiments are conducted in fast reactors available internationally to validate the performance results observed in the thermal-spectrum irradiations and identify any performance differences that may result. In this regard, two metallic fuel pins are currently under irradiation in the Phénix fast reactor in France. The following subsections describe the ongoing irradiation test programs in the ATR and the Phénix and the performance results obtained to date on metallic fuels for actinide transmutation.

### ATR Test Program

The ATR has been used to conduct an extensive test program investigating the irradiation performance of metallic fuels with major additions of the minor actinide elements americium and neptunium. When testing began in 2003, accelerator-driven systems were considered to be a primary application for actinide transmutation fuels, so the early metallic fuels irradiated in the ATR were non-fertile (i.e., uranium-free) fuel alloys. As the national emphasis transitioned to sodium fast reactors as the fast-spectrum device to be used for transmutation, uranium-based metallic fuels were included in the test program. Table 4 summarizes both the recently completed metallic fuel tests and those that are still in progress.

Irradiation testing in the ATR is performed on miniature fast reactor fuel pins, or rodlets. The rodlets are fabricated using archive HT9 cladding tubing 0.230 in. in diameter (0.018 in. wall thickness). Finished rodlets are 6.0 in. in length and have a fuel column height of 1.5 in., giving a plenum-to-fuel volume ratio of >2.0. Due to uncertainties regarding fuel swelling associated with the substantial helium production from americium transmutation in a thermal spectrum, the early experiments (AFC-1 test series) made use of a relatively low fuel smear density of ~0.7; subsequent tests (AFC-2 test series) have returned to the traditional value of 0.75 for metallic fuel. Figure 18 gives a schematic of the metallic fuel rodlet design used in the ATR.

Up to six of these rodlets are included in a secondary stainless steel capsule for irradiation in the ATR. The secondary capsule provides a safety barrier between the metallic fuel (and bond sodium) and the primary coolant should cladding breach occur, and the gap size between the secondary capsule and rodlet cladding is sized to produce peak cladding temperatures in the 500-550°C range. Additionally, the test capsules are irradiated inside a cadmium shroud to reduce neutron flux levels and produce target linear heat generation rates (LHGR) in the test fuels. A photograph of metallic fuel rodlets (just prior to loading into the secondary capsules) appears in Figure 19.

The important variables under study in these ATR tests include the effects of variable plutonium and minor actinide contents, zirconium content, and lanthanide fission product carry-over (from electrochemical recycle) on the performance of these metallic fuel alloys, particularly as they relate to the large historic database generated on U-20Pu-10Zr metallic fuel from EBR-II and the FFTF.

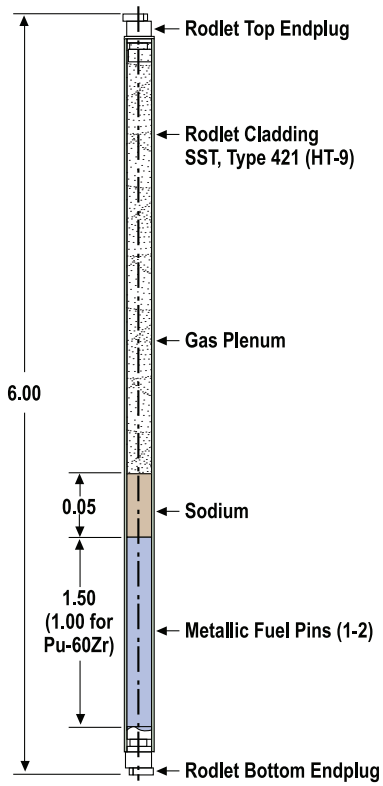


***Figure 18.***
*Metallic fuel rodlet design used in ATR irradiation tests (dimensions in inches).*

| Metallic Fuel Alloy | Experiment | Irradiation Time (EFPDs) | Peak LHGR (W/cm) | Peak Fission Density (fiss/cm$^3$) | Peak Burnup (% fissile) | Status |
|---|---|---|---|---|---|---|
| Pu-40Zr | AFC-1B | 93 | 300 | 5.26E+20 | 5.7 | In PIE |
| | AFC-1D | 593 | 300 | 1.95E+21 | 33.3 | Discharged from ATR |
| Pu-60Zr | AFC-1B | 93 | 300 | 3.51E+20 | 7.0 | In PIE |
| | AFC-1D | 593 | 300 | 1.33E+21 | 39.6 | Discharged from ATR |
| Pu-12Am-40Zr | AFC-1B | 93 | 300 | 4.27E+20 | 5.9 | In PIE |
| | AFC-1D | 593 | 300 | 1.71E+21 | 34.1 | Discharged from ATR |
| Pu-10Np-40Zr | AFC-1G | 644 | 300 | 1.47E+21 | 17.6 | Discharged from ATR |
| Pu-10Am-10Np-40Zr | AFC-1B | 93 | 300 | 3.43E+20 | 5.5 | In PIE |
| | AFC-1D | 593 | 300 | 1.35E+21 | 30.8 | Discharged from ATR |
| U-25Pu-3Am-2Np-40Zr | AFC-1F | 94 | 330 | 5.89E+20 | 6.7 | In PIE |
| | AFC-1H | 706 | 330 | 3.56E+21 | 38.0 | Discharged from ATR |
| U-28Pu-7Am-30Zr | AFC-1F | 94 | 330 | 6.38E+20 | 5.7 | In PIE |
| | AFC-1H | 706 | 330 | 3.97E+21 | 33.4 | Discharged from ATR |
| U-29Pu-4Am-2Np-30Zr | AFC-1F | 94 | 330 | 6.38E+20 | 5.9 | In PIE |
| | AFC-1H | 706 | 330 | 3.93E+21 | 36.2 | Discharged from ATR |
| U-34Pu-4Am-2Np-20Zr | AFC-1F | 94 | 330 | 5.35E+20 | 4.5 | In PIE |
| | AFC-1H | 706 | 330 | 3.48E+21 | 28.3 | Discharged from ATR |
| U-20Pu-3Am-2Np-15Zr | AFC-2A | 219 | 350 | 1.33E+21 | 6.7 | In ATR† |
| | AFC-2B | 219 | 350 | 1.35E+21 | 7.0 | In ATR† |
| U-20Pu-3Am-2Np-1.0Ln*-15Zr | AFC-2A | 219 | 350 | 1.42E+21 | 9.4 | In ATR† |
| | AFC-2B | 219 | 350 | 1.44E+21 | 9.5 | In ATR† |
| U-20Pu-3Am-2Np-1.5Ln*-15Zr | AFC-2A | 219 | 350 | 1.30E+21 | 10.7 | In ATR† |
| | AFC-2B | 219 | 350 | 1.31E+21 | 10.8 | In ATR† |
| U-30Pu-5Am-3Np-20Zr | AFC-2A | 219 | 350 | 1.19E+21 | 8.0 | In ATR† |
| | AFC-2B | 219 | 350 | 1.23E+21 | 8.2 | In ATR† |
| U-30Pu-5Am-3Np-1.0Ln*-20Zr | AFC-2A | 219 | 350 | 1.30E+21 | 9.9 | In ATR† |
| | AFC-2B | 219 | 350 | 1.32E+21 | 10.2 | In ATR† |
| U-30Pu-5Am-3Np-1.5Ln*-20Zr | AFC-2A | 219 | 350 | 1.40E+21 | 11.0 | In ATR† |
| | AFC-2B | 219 | 350 | 1.48E+21 | 11.3 | In ATR† |

* Ln = 6% La, 16% Pr, 25% Ce, 53% Nd
† Reported results through end of Cycle 142B

***Table 4.***
*Summary of metallic transmutation fuel irradiation tests in the ATR.*

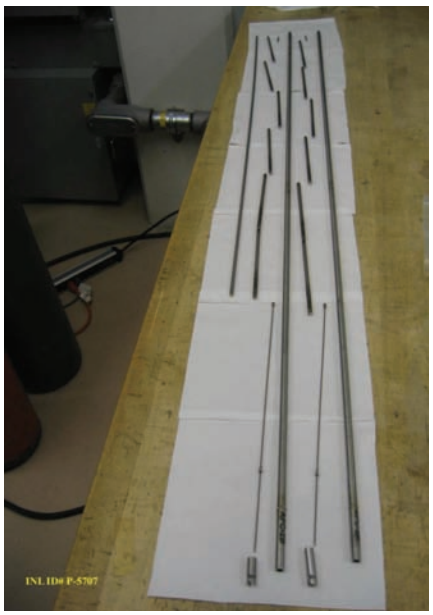


***Figure 19.***
*Two ATR test capsules with 12 metallic fuel rodlets (just before capsule loading).*

**FUTURIX-FTA Experiment in Phénix**

Early in the planning for the ATR test program, two metallic fuel compositions were identified for irradiation in the Phénix fast reactor in France. The compositions selected were Pu-12Am-40Zr and U-29Pu-4Am-2Np-30Zr, and the experiment designed to irradiate them in the Phénix is designated FUTURIX-FTA. Low burnup data on these alloys are already available from ATR irradiations, and experiments to take the same alloys to high burnup are underway. The results from the FUTURIX-FTA metallic fuel pins will provide analogous performance data obtained from a fast-spectrum test. Irradiation of these two metallic fuel pins began in May 2007 and will proceed for 240 effective full-power days, reaching peak burnups in the 10-12 at.-% range; irradiation is anticipated to end in March 2009.

**Irradiation Performance Results**

A number of ATR experiments (Table 4) have been completed that include a variety of non-fertile and low-fertile metallic fuel alloys irradiated to the intermediate burnup level of 7% (6.4 x $10^{20}$ fiss/$cm^3$). Preliminary postirradiation examination (PIE) of these fuels has been completed (Hilton et al., 2006), although specimens are being retained for more specialized examinations pending the availability of some new instruments (e.g., installation is underway of a shielded Electron Probe Micro-Analyzer to measure constituent redistribution within the fuels).

Figure 20 shows a composite of PIE results from a representative non-fertile (Pu-12Am-40Zr) and low-fertile composition (U-29Pu-4Am-2Np-30Zr), including an image of the irradiated fuel rodlet obtained by neutron radiography, rodlet axial fission product distributions obtained by gamma-ray spectroscopy, and optical metallography performed on a transverse section of the fuel/cladding. Significant fuel swelling has not yet begun for the Pu-12Am-40Zr alloy (a), as is evident from the large fuel-cladding gap that still remains. The U-29Pu-4Am-2Np-30Zr alloy (b), seen at a higher fission density, has swollen considerably, with porosity evident within the fuel and the absence of a discernable fuel-cladding gap. These results are consistent with the historic data for U-Zr and U-Pu-Zr metallic fuels, where the onset of swelling has been observed to begin in the range 3 to 6 x $10^{20}$ fiss/$cm^3$ (Hofman et al., 1990). Axial fission product distributions are relatively uniform. This is to be expected for these short fuel columns, which experienced essentially a uniform axial flux profile during irradiation. Furthermore, the cesium-137 profile is contained within the fuel column region, which indicates that fuel swelling has only just begun. In time, a significant fraction of the fission product cesium will be released from the fuel and alloy with the bond sodium, with a large peak observable above the fuel column.

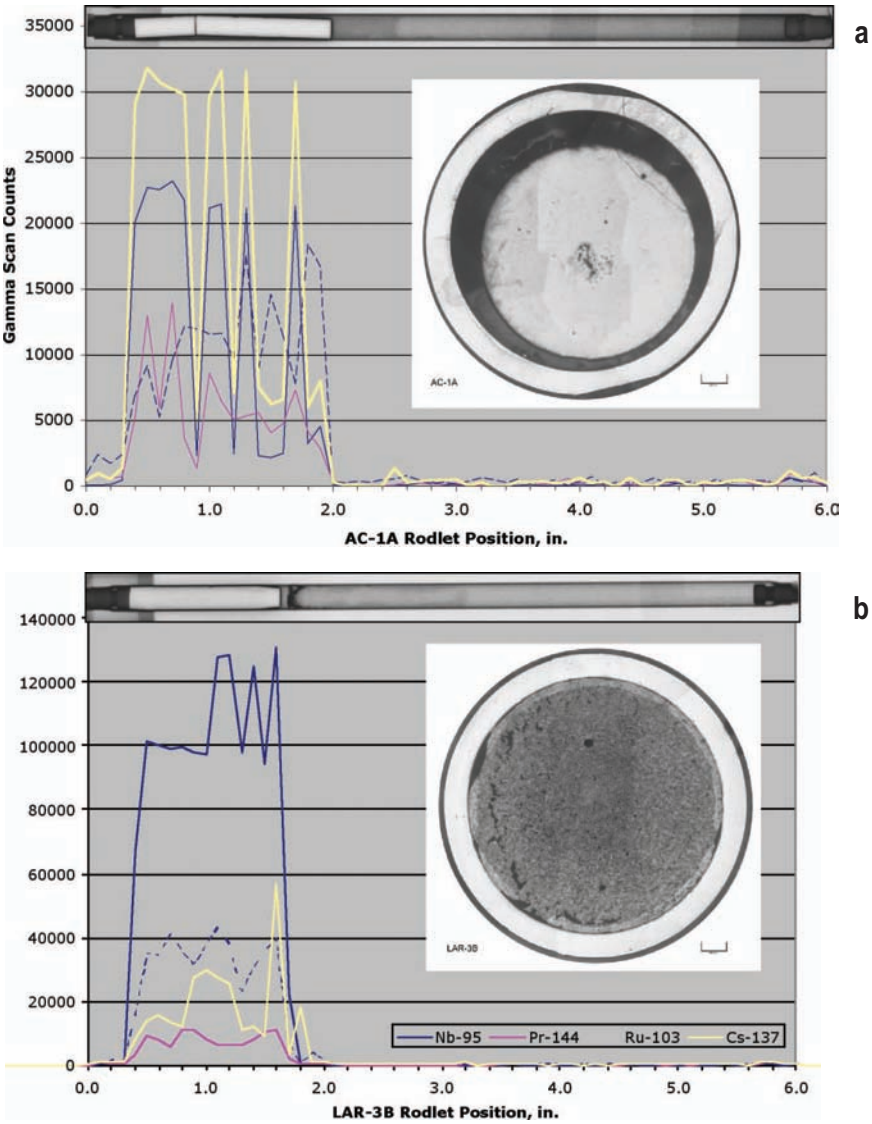


***Figure 20.***
*Fuel swelling and fission product retention in: (a) non-fertile Pu-12Am-40Zr at 4.3 x $10^{20}$ fiss/cm$^3$, and (b) low-fertile U-29Pu-4Am-2Np-30Zr at 6.4 x $10^{20}$ fiss/cm$^3$.*

Figure 21 shows the fission-gas release data from all the metallic fuels alloys. Both non-fertile and low-fertile compositions included in the AFC-1B and AFC-1F irradiation tests are plotted against typical data for U-Pu-Zr irradiations from EBR-II (Hofman and Walters, 1994). The striking feature is that when these data are correlated versus alloy fission density, all the data appear to fall along the same trendline. There may be a slightly longer incubation period to the onset of swelling, and thus, fission gas release for the current metallic fuels with much higher zirconium contents. However, once swelling begins, the fission-gas release behavior appears to converge quickly with the data from previous metallic fuels experiments.

***Figure 21.***
*Fission gas release behavior for metallic fuels.*

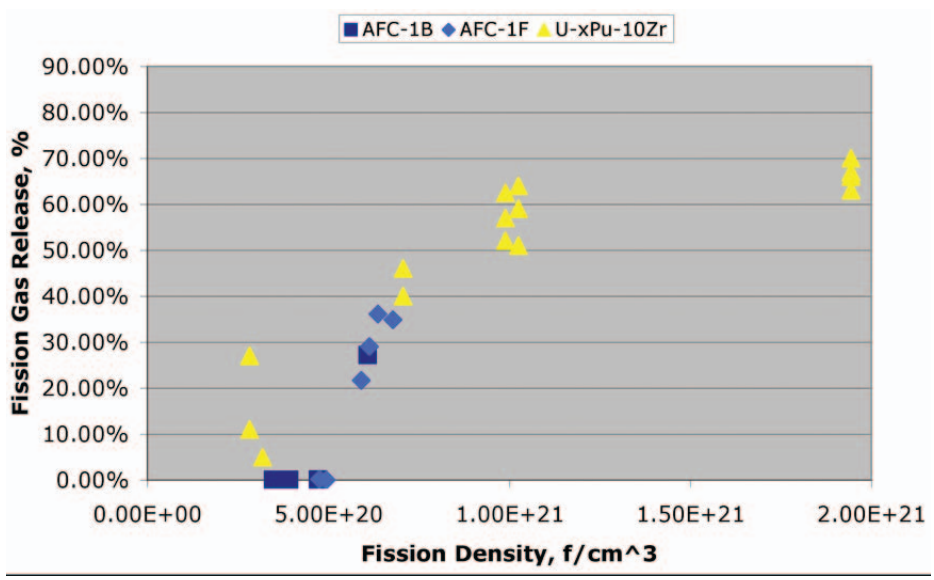

These results, admittedly at an intermediate burnup level, nevertheless seem to indicate that the metallic fuel alloys currently under development, although having significantly higher levels of plutonium, minor actinides, and zirconium than previous metallic fuels, exhibit behavior under irradiation that is remarkably consistent with the large, historic database on U-Pu-Zr metallic fuels.

## *Conclusions and Future Work*

Metallic fuels have a long history of use in sodium-cooled fast reactors. Continued research, development, and design innovation over a period of decades have demonstrated this fuel technology to be safe and reliable to extremely high burnups over a wide spectrum of compositions. Their simple fabrication has historically given them a significant economic advantage over other fuel forms. Research and development on metallic fuels continues today at the INL, with particular emphasis on showing that this fuel technology can incorporate significant quantities of minor actinides for the purpose of efficiently and economically transmuting these elements in a fast-spectrum reactor. New fabrication methods to improve retention of the volatile fuel constituents during the casting process (and reduce waste generation) are being developed, and characterization of the fundamental and engineering properties of advanced metallic fuel alloys is underway. Irradiation testing of the new metallic fuels has so far indicated that the new compositions, although they differ significantly (both in the quantities of plutonium and minor actinides included in the zirconium alloying addition), perform very analogously to the historic U-Zr and U-Pu-Zr fuels when behavior is correlated as a function of fission density.

In the next few years, it is anticipated that a new casting furnace prototype will demonstrate that these new metallic fuel alloys can be fabricated at engineering scale, in a remote environment, with no significant fuel loss or waste generation. Irradiation tests currently underway will provide the performance data needed to assess fuel reliability/burnup capability and identify any unique behaviors that are a result of the new compositions. If these future results are consistent with the intermediate data available at present, metallic fuels are expected to continue to be a strong contender for the fuel technology choice of future fast reactors.

## *REFERENCES*


Chang, Y. I., 1989, "The Integral Fast Reactor," Nuclear Technology, Vol. 88, pp. 129-138.

Cole, J. I., J. R. Kennedy, and D. D. Keiser, Jr., 2008, "An Investigation of Fuel-Cladding Chemical Interaction in Metallic Transmutation Fuels," Transactions of the ANS Embedded Topical Meeting on Nuclear Fuels and Structural Materials for the Next Generation Nuclear Reactors, Vol. 98, Anaheim, CA, June 8-12, 2008.

Crawford, D. C., C. E. Lahm, H. Tsai, and R. G. Pahl, 1993, "Performance of U-Pu-Zr Fuel Cast into Zirconium Molds," Journal of Nuclear Materials, Vol. 204, pp. 148-156.

Crawford, D. C., D. L. Porter, and S. L. Hayes, 2007, "Fuels for Sodium-cooled Fast Reactors: U.S. Perspective," Journal of Nuclear Materials, Vol. 371, pp. 202-231.

Frost, B. R. T., 1982, Nuclear Fuel Elements: Design, Fabrication, and Performance, Pergamon Press, New York, p. 187.

Hilton, B. A., D. L. Porter, and S. L. Hayes, 2006, "Postirradiation Examination of AFCI Metallic Transmutation Fuels at 8 at.%," Embedded Topical Meeting on Nuclear Fuels and Structural Materials for the Next Generation Reactors," American Nuclear Society, Reno, NV, June 4-8, 2006.

Hofman, G. L., R. G. Pahl, C. E. Lahm, and D. L. Porter, 1990, "Swelling Behavior of U-Pu-Zr Fuel," Metallurgical Transactions A, Vol. 21A, pp. 517-528.

Hofman, G. L., and L. C. Walters, 1994, "Metallic Fast Reactor Fuels", in Materials Science and Technology, Vol. 10A, VCH Publishers, New York, pp. 1-43.

Keiser, D. D., Jr., 2005, "Fuel-Cladding Interaction Layers in Irradiated U-Zr and U-Pu-Zr Fuel Elements," Argonne National Laboratory Report, ANL-NT-240.

Keiser, D. D., Jr. and J. I. Cole, 2007, "An Evaluation of Potential Liner Materials for Eliminating FCCI in Irradiated Metallic Nuclear Fuel Elements," Proceedings of the GLOBAL '07 International Conference on Advanced Nuclear Energy and Fuel Cycle Systems, Boise, ID, September 9-13, 2007.

Keiser, D. D., Jr. and M. A. Dayananda, 1994, "Interdiffusion in U-Zr Fuel and Cladding Steels Couples," Metallurgical Transactions, Vol. 25A, p. 1649.

Keiser, D. D., Jr. and M. C. Petri, 1996, "Interdiffusion Behavior in U-Pu-Zr Fuel Versus Stainless Steel Couples," Journal of Nuclear Materials, Vol. 240, pp. 51-61.

Meyer, M. K., S. L. Hayes, W. J. Carmack, and H. C. Tsai, 2008, "The EBR-II X501 Minor Actinide Burning Experiment," ANS Topical Meeting on Nuclear Fuels and Structural Materials for the Next Generation Nuclear Reactors, Anaheim, CA, June 8-12, 2008.

O'Boyle, D. R., and A. E. Dwight, 1970, Proceedings of the 4th International Conference on Plutonium and Other Actinides, Santa Fe, NM, Session 2.

Stevenson, C. E., 1987, The EBR-II Fuel Cycle Story, American Nuclear Society, La Grange Park, IL, chs. 7-9.

Trybus, C. L., J. E. Sanecki, and S. P. Henslee, 1993, "Casing to Metallic Fuel Containing Minor Actinide Additions," Journal of Nuclear Materials, Vol. 204, pp. 50-55.

STEVEN L. HAYES (BS, 1988, MS, 1989, PhD, 1992, Nuclear Engineering, Texas A&M University) is Manager of the Fuel Performance and Design Department at the INL. He has been actively involved in the irradiation testing and modeling of fast breeder reactor fuels, fuels for actinide transmutation, and research reactor fuels for more than 15 years.

J. RORY KENNEDY (BS, 1982, Inorganic Chemistry, Colorado State University; MS, 1983, PhD, 1987, Inorganic Chemistry, Northwestern University) is Manager of the Basic Fuel Properties and Modeling Department at the INL. He has been investigating the synthesis and structure/property relations of materials for over 20 years. Over the last 12 years, his interests have been directed to the fabrication and characterization of materials associated with the nuclear fuel cycle, with emphasis on advanced nuclear fuels.

BRUCE A. HILTON (BS, 1990, Physics, Brigham Young University; MS, 1993, PhD, 1995, Nuclear Materials Engineering, Massachusetts Institute of Technology) is a member of the Fuel Performance and Design Department at the INL. He has 13 years experience in nuclear fuels performance and materials, irradiation testing, and postirradiation examination. Current responsibilities at the INL include technical management of Global Nuclear Energy Partnership/Advanced Fuel Cycle Initiative Postirradiation Examinations (GNEP/AFCI PIE) of advanced nuclear fuels, and advanced LWR nuclear fuels development in the LWR Sustainability Program.

RANDALL S. FIELDING (BS, 2000, MS, 2008, Materials Science and Engineering, University of Idaho) is an engineer in the Fuel Fabrication Department at the INL. He has been active in irradiation experiment assembly, metallic fast reactor fuel fabrication, and dispersion fuel-fabrication research since joining the INL in 2001.

TIMOTHY A. HYDE (BS, 1989, Mechanical Engineering, University of Idaho) is an Engineer/Scientist at the INL with 19 years experience in research and development activities. He has worked in a wide range of technical disciplines, including ceramic and metal alloy fuel development, membrane permeability testing, plasma disassociation of hydrocarbons to grow carbon nano-tubes, aerosol particle measurement, magnetic properties measurement, magnetic alloy development, and numerous experimental and mechanical design projects. These activities have resulted in over 20 publications and numerous awards, including a Research and Development 100 award. Mr. Hyde is a coinventor on numerous Invention Disclosure Reports (IDRs) and is coinventor on two issued patents.

DENNIS D. KEISER, JR. (BS, 1987, MS, 1989, Metallurgical Engineering, University of Idaho; PhD, 1992, Materials Engineering, Purdue University) is a member of the Fuel Performance and Design Department at the INL. He has over 20 years experience researching different issues related to the performance of nuclear fuels and materials. His current research relates to developing low-enriched fuels for application in research and test reactors, developing a better understanding of the diffusion behavior of fuel and cladding components in irradiated fuels, and determining the microstructural development of fuels and materials during irradiation.

DOUGLAS L. PORTER (BS, 1971, MS, 1973, PhD, 1977, Metallurgy and Materials Science, Case Western Reserve University) has conducted research for more than 30 years at the INL, with major interests in irradiation effects on materials and metallic fuel development for fast reactors.

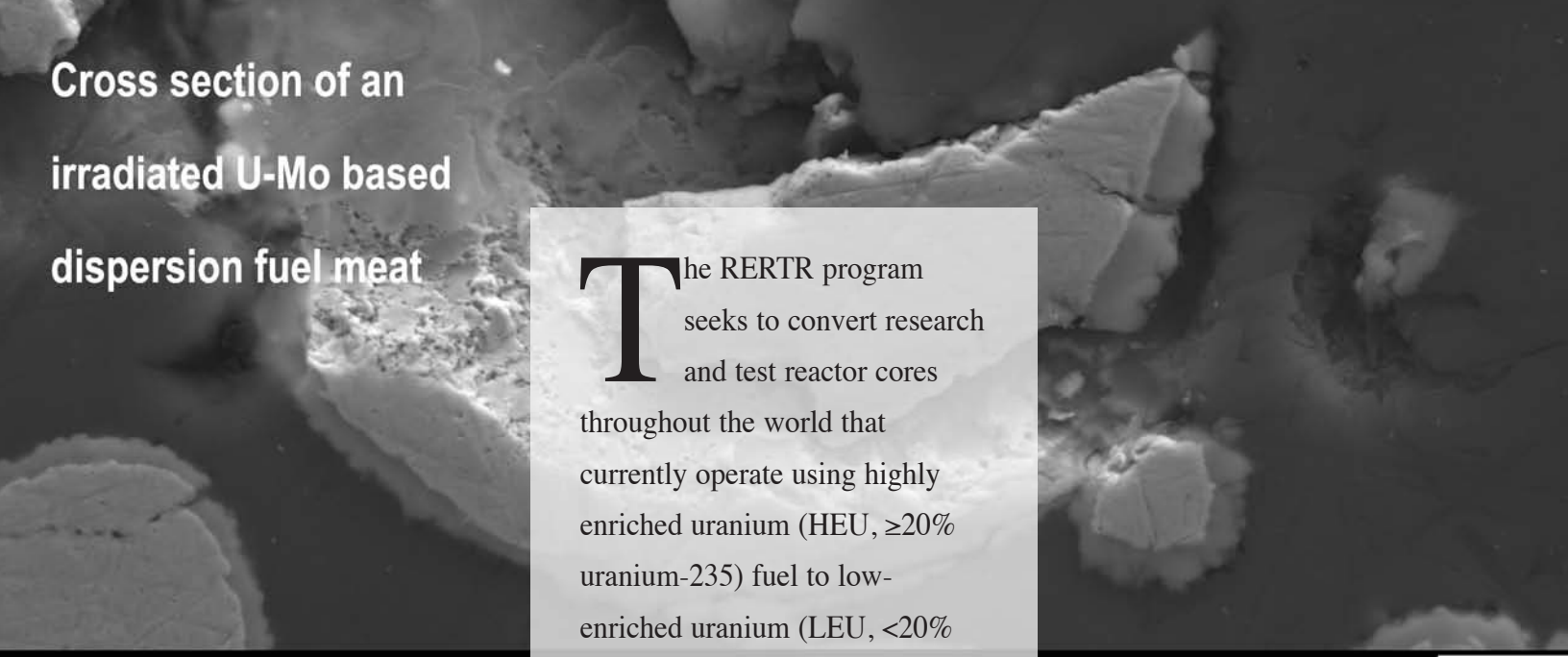


Cross section of an irradiated U-Mo based dispersion fuel meat

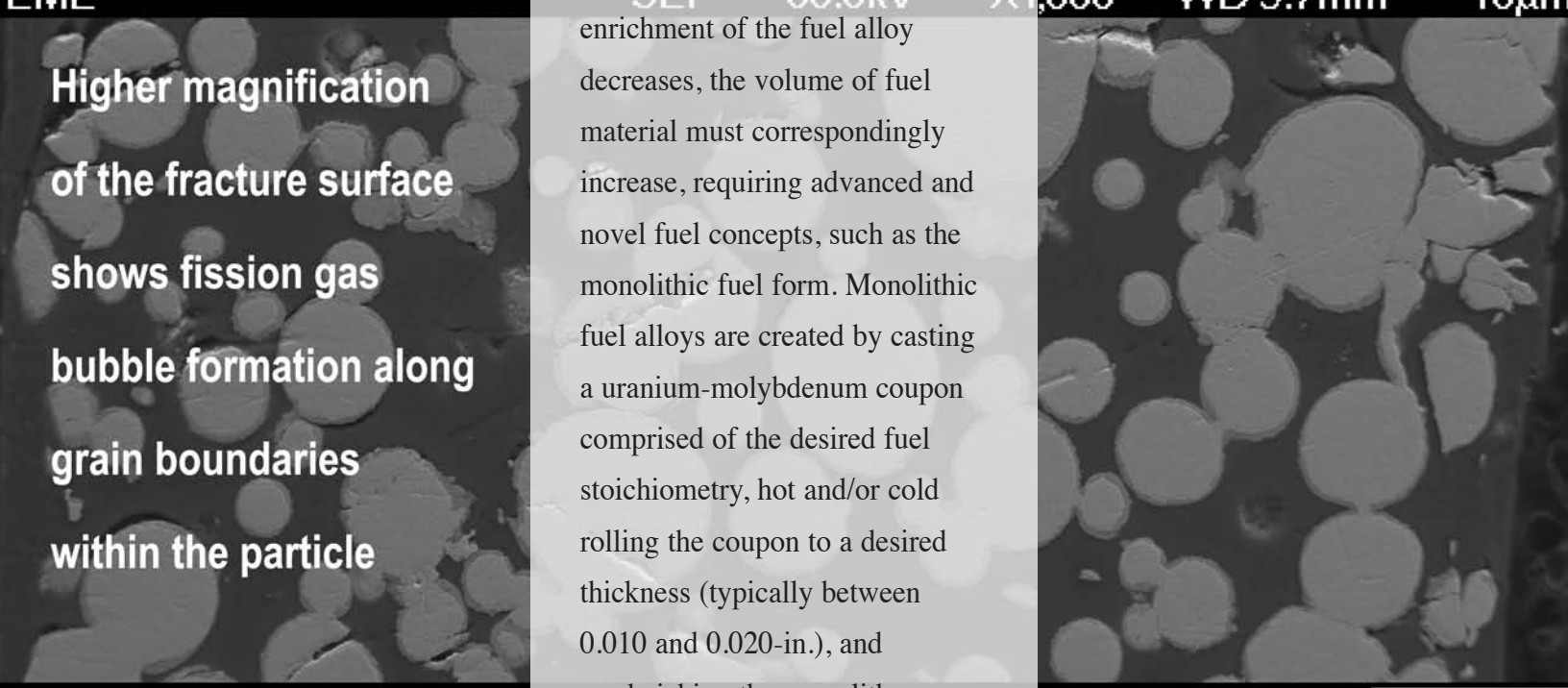


Higher magnification of the fracture surface shows fission gas bubble formation along grain boundaries within the particle

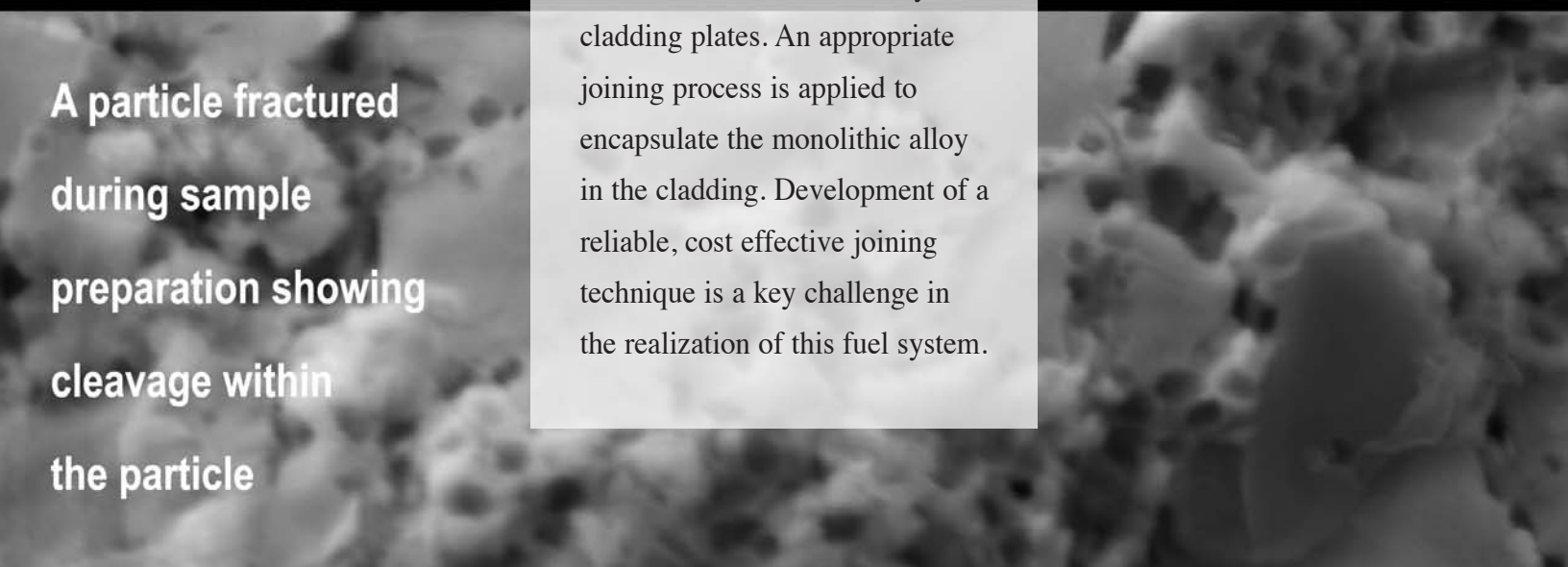

A particle fractured during sample preparation showing cleavage within the particle

The RERTR program seeks to convert research and test reactor cores throughout the world that currently operate using highly enriched uranium (HEU, ≥20% uranium-235) fuel to low-enriched uranium (LEU, <20% uranium-235) fuel. As the enrichment of the fuel alloy decreases, the volume of fuel material must correspondingly increase, requiring advanced and novel fuel concepts, such as the monolithic fuel form. Monolithic fuel alloys are created by casting a uranium-molybdenum coupon comprised of the desired fuel stoichiometry, hot and/or cold rolling the coupon to a desired thickness (typically between 0.010 and 0.020-in.), and sandwiching the monolith between two aluminum alloy cladding plates. An appropriate joining process is applied to encapsulate the monolithic alloy in the cladding. Development of a reliable, cost effective joining technique is a key challenge in the realization of this fuel system.

# Reduced Enrichment for Research and Test Reactors

*Daniel M. Wachs*

THE RERTR PROGRAM marked its 30th anniversary in 2008. From its inception, the program has been tasked with providing the means necessary to enable research and test reactors worldwide to convert from highly enriched nuclear fuel to low enriched nuclear fuel (which is defined by the International Atomic Energy Agency [IAEA] as <20% uranium-235).

High uranium density fuel development has always been a central component of the RERTR program. In its earliest years, the program was focused on expanding the uranium loading limits for the common fuels of the time to enable enrichment reductions (most notably UZrH but also aluminide and oxide-based dispersion fuels). However, these improvements were not sufficient to provide the basis for widespread LEU conversions, and the program initiated the development of new fuels. The $U_3Si_2$ based dispersion fuel was subsequently developed and qualified in the 1980s by the program and provided a uranium density of 4.8 g U/cc.

As a result of this accomplishment, only a handful (less than 30) of civilian research and test reactors worldwide are unable to convert from high- to low-enriched nuclear fuel due to the availability of a suitable LEU fuel. However, these reactors are by the far the greatest civilian consumers of HEU, leading to substantial worldwide commerce in this high-risk material. In the early 1990s, the RERTR program embarked on the development of a replacement fuel for these most challenging reactors. In 2004, the program was refocused and accelerated when the terrorist attacks of September 11 added even more urgency, and the program was absorbed into the National Nuclear Security Administration's (NNSA's) Global Threat Reduction Initiative (GTRI). Aggressive timelines for completion of the fuel development program were put in place, and the INL was tasked with leading a multilaboratory team in the execution of a multi-national mission.

Following an investigation of the irradiation performance of several candidate fuel materials, uranium-molybdenum alloys with between 6 and 12 wt% molybdenum were selected to be the base of fuel development. This fuel offered very high uranium densities and demonstrated excellent irradiation behavior under a wide range of relevant conditions. It was originally envisioned as a dispersion-type fuel capable of almost twice the uranium density (8-9 g U/cc) of any other research reactor fuel available; an alternate monolithic version was later proposed to enable uranium loading up to four times the current state of the art (15-16 g U/cc). While the dispersion version of the uranium-molybdenum-based fuel does not come without challenges, it is a relatively modest change compared to the monolithic version, which represents a dramatic shift from conventional fuel designs and challenges the status quo at many levels.

The development of a new nuclear fuel requires that the developer address multiple issues, including fuel fabrication, irradiation testing, characterization of irradiation performance, fuel performance modeling, and final disposal of the fuel. The INL Nuclear Fuels and Materials Division is uniquely equipped to conduct research in all these areas, leading to a holistic development approach that integrates all the relevant areas of fuel development. Since most R&D programs require several iterations on a fuel concept before development is complete, the natural integration of all these functions in a common location often leads to a meaningful acceleration of R&D

objectives and significant economical advantages. This has clearly been the case for the RERTR uranium-molybdenum fuel development program.

The RERTR fuel development program has faced many challenges along the way that have mobilized the exceptional creativity and technical capability of INL researchers. A sampling of these challenges is described in the following sections. In Subsection I, Dr. Douglas Burkes describes one of the techniques (Friction Bonding) he and his colleagues have developed to fabricate uranium-molybdenum monolithic fuel plates that consist of thin, metallic layers with very different mechanical properties. In Subsection II, Dr. Dennis Keiser describes techniques he and his colleagues developed to investigate the micro-chemical condition of irradiated fuel in order to better understand the interaction of uranium-molybdenum fuels with aluminum and aluminum-silicon alloys during the irradiation of dispersion fuel designs. In Subsection III, Dr. Daniel Wachs and Mr. Jared Wight outline the development of a device designed to allow irradiation testing of prototypic plate-type fuels under conditions well in excess of their prototypic environment, as well as techniques developed for the high fidelity investigation of fuel performance between irradiation cycles. Subsection IV includes a review of fuel performance modeling led by Dr. Pavel Medvedev to support understanding of integrated fuel performance, including the coupling of thermal, hydraulic, mechanical, and chemical behaviors in the monolithic fuel type.

DANIEL M. WACHS (BS, 1995, Mechanical Engineering, MS, 1997, Nuclear and Mechanical Engineering, Oregon State University; PhD 2000, Mechanical Engineering, University of Idaho) is a member of the Fuel Performance and Design Department at the INL. He is currently the National Technical Director for the RERTR Fuel Development Program. His current research interests and technical background include irradiation testing of nuclear fuel and materials, thermal-hydraulic testing and analysis, and reactor system component design for research reactors and liquid metal cooled fast reactors.

# Friction Bonding Process Used to Fabricate Fuel Plates

*Douglas E. Burkes*

THE RERTR PROGRAM has identified several techniques for evaluation and development. The first successful approach was based on extension of the friction stir welding (FSW) technique beyond its original applications. FSW has been in existence since the early 1990s and has routinely been used for joining applications in the aerospace and automotive industries. In general, FSW involves rotating a welding tool (comprised of a shank, shoulder, and pin) at a prescribed speed and tilt, and plunging the weld tool into the workpiece material until the tool intimately contacts the workpiece surface and generates friction.

The friction produces intense heat that bonds the workpiece materials as the weld tool traverses the joint line. The FSW process can be employed to join both similar and dissimilar cast and wrought aluminum, titanium, copper, and magnesium alloys, as well as steels, in multiple configurations, including butt, corner, lap, T, spot, fillet, and hem joints. The process typically produces joints with higher strength, increased fatigue life, lower distortion, less residual stress, and less sensitivity to corrosion compared to conventional fusion welding processes.

A modified FSW process, referred to as friction bonding (FB), is being developed at the INL that allows interfacial bonding between multiple layers of thin metallic materials with dissimilar mechanical properties. This process permits the fabrication of nuclear fuel plates for research and test reactors containing the thin, monolithic fuel alloys. Unlike the traditional FSW process, the interface to be bonded is located perpendicular to the plane of the working tool (Figure 1). The rotating tool face is pressed against the surface layer of material and rotates; the combination of force and rotation creates intimate contact between the fuel and cladding layer while the rotation generates the heat required to initiate metallurgical bonding. The tool is rastered across the entire surface of the fuel plate to establish full bonding of all interracial surfaces.

Recent research on this novel FB process has yielded many significant technical and programmatic contributions over the last several years. The process has been utilized to fabricate a number of fuel plates for various irradiation tests, including 35 mini-plates (25 mm x 100 mm x 1.27 mm) and two full-size fuel plates (57 mm x 600 mm x

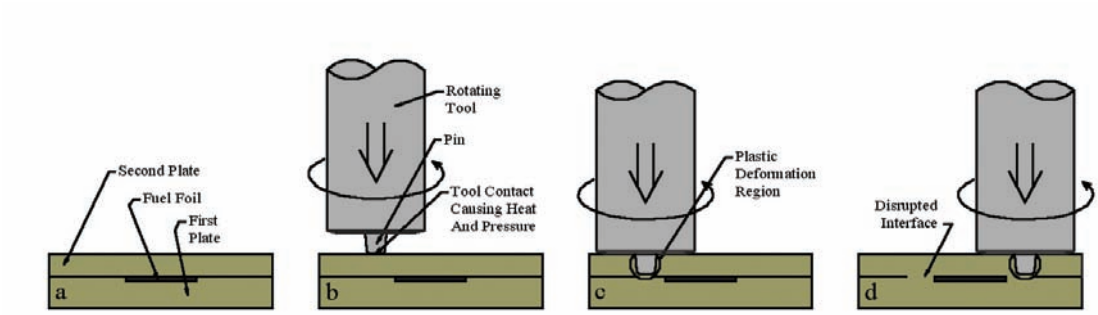


***Figure 1.***

*Schematic of friction-bonding technique developed to enable bonding of aluminum cladding to thin uranium-molybdenum foils.*

1.27 mm). While a few fuel plates in the early experiments showed indications of small delaminations during destructive postirradiation examination (due to fuel chemistry changes during irradiation), most have behaved, and continue to behave, in an expected and normal manner. Techniques to incorporate materials into the fuel/clad interface have successfully demonstrated that they further strengthen the interfacial bond strength. Based on these successes, a prototype FB fabrication unit has been brought online and operation verified for commercial-scale fabrication demonstration.

## *Interfacial Bond Strength Assessment*

The bond strength between the fuel and cladding after fabrication is a critical performance criterion for the monolithic fuel design. In the absence of a recognized standard for this property, the program is developing examination techniques that will provide a better understanding of the impact of various fabrication process parameters and, eventually, operational thresholds for interfacial loads.

As an example of this process, several mini-plates were fabricated employing FB for irradiation in the RERTR-9A experiment (Burkes et al., 2007). Four of the plates were fabricated with a standard steel-faced tool, while the remaining three plates were fabricated with a newer, more robust refractory-faced tool – Anviloy. Beginning-of-life (BOL) bonding was suspected to be better for plates fabricated with the Anviloy-faced tool compared to the steel-faced tool. Pull-tests performed on small samples extracted from the FB fabricated mini-plates confirmed these suspicions, as shown in Figure 2, even though the non-destructive ultrasonic (UT) scans indicated that the interfacial properties were similar (i.e., the sound transmission properties were similar), as shown in Figure 3. However, the stresses occurring during irradiation did not appear to exceed the bond strength for either tool face material or BOL bonding. All seven plates reached the target burn-up without delamination, but the information still helps establish the margins for which the fuel plates can be safely operated.

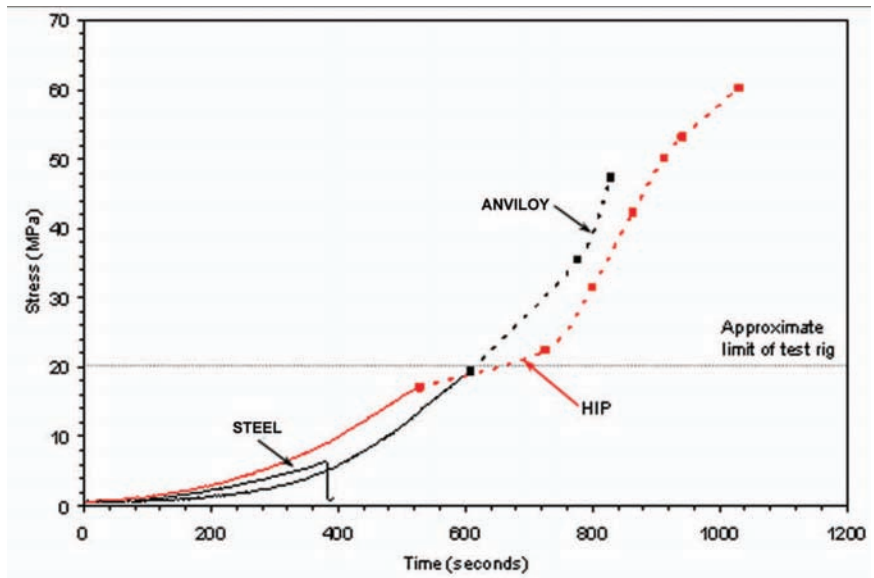


***Figure 2.***

*Pull test results (normal stress) of mini-plates fabricated using HIP, an Anviloy-faced friction-bonding tool, and a steel-faced friction-bonding tool.*

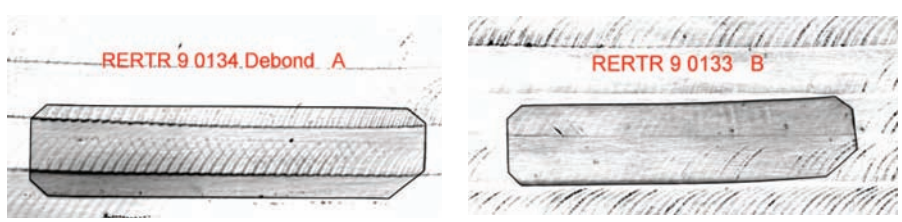


***Figure 3.***

*Ultrasonic testing scans of mini-plates fabricated for the RERTR-9A experiment using a steel-faced tool (left) and an Anviloy-faced tool (right).*

Additional examination was required to assess the impact of chemical alterations to the fuel/clad interface on the fabrication process and BOL bond conditions. Miniplates were fabricated for the RERTR-9B experiment using FB that included a modified Al-2Si layer to minimize formation of the intermetallic interaction layer that forms between the fuel and the cladding at high temperature during irradiation. The modified Al-2Si layer was applied using thermal-sprayed powders of Al-12Si and aluminum to create the inhomogeneous Al-2Si layer, with two different thicknesses: 13 μm and 25 μm. A cross section of the 13-μm-thick thermal-sprayed layer is shown in Figure 4. These two thicknesses were selected based on the recoil zone of fission products in aluminum: 13 μm. A UT scan of a FB plate with the modified silicon interface is provided in Figure 5. The UT scan reveals that the fabrication process is unaffected by the modification to the interface. A second modification to the fuel system was also proposed and evaluated as part of this testing. Fuel plates employing a thin layer (25 to 50 μm) of zirconium at the fuel-clad interface were also fabricated with FB. A metallographic cross section of an example mini-plate is provided in Figure 6 along with an EDX scan of the interface that revealed a molybdenum enrichment zone at the Zr/U-Mo foil interface. All indications were that the FB process was effective in bonding the interfaces of this system.

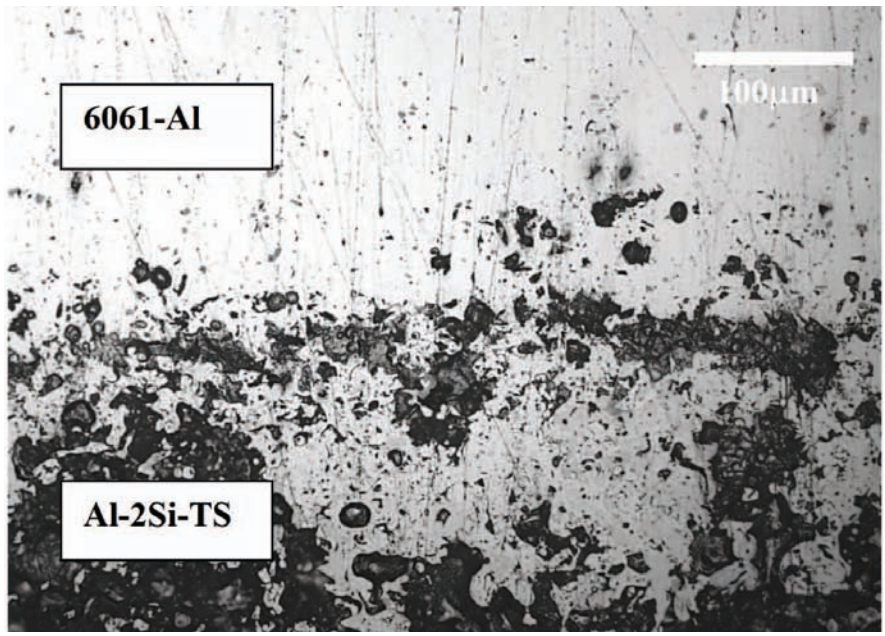


***Figure 4.***
*Cross section of a 13-μm–thick, thermal-sprayed Al-2Si-modified interface.*

***Figure 5.***
*Ultrasonic scan of a mini-plate fabricated employing friction bonding with a 25-μm–thick, thermal-sprayed Al-2Si-modified interface.*

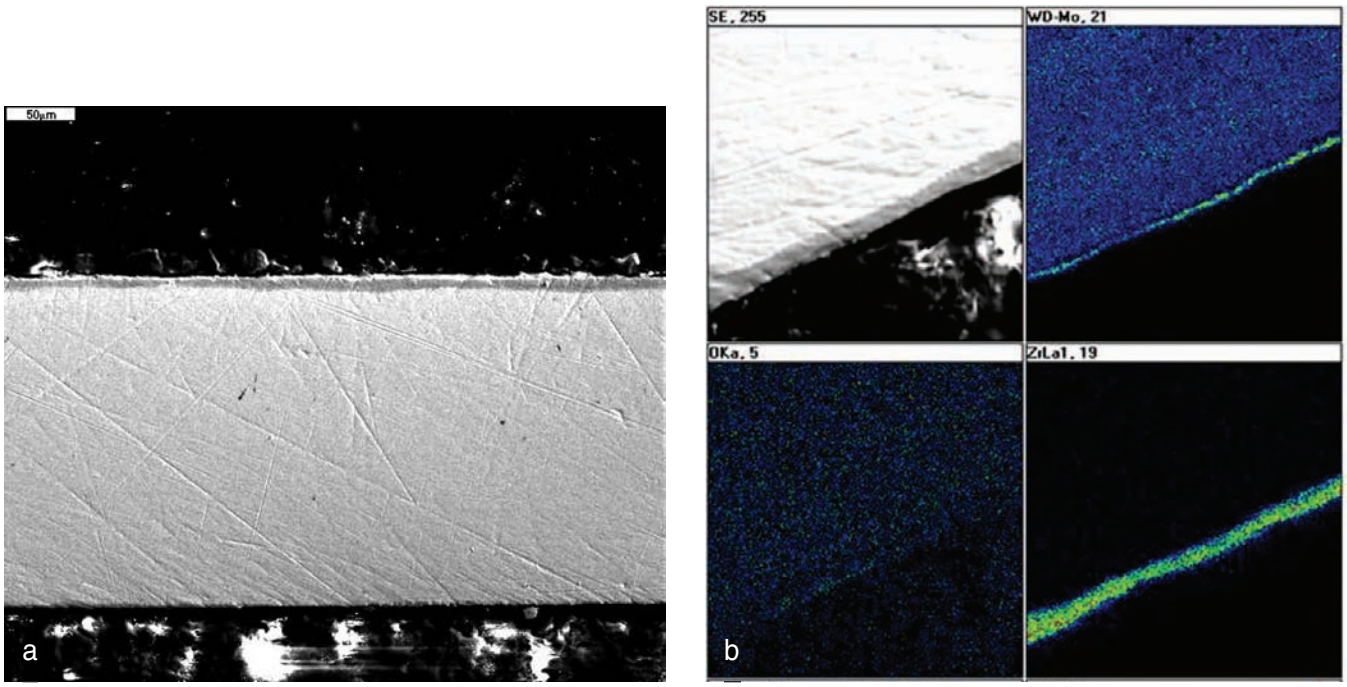


***Figure 6.***

*Metallographic cross section (a) of a mini-plate fabricated using friction bonding with a zirconium interface between the uranium-molybdenum foil and the AA6061 cladding, represented by the dark gray at the top. EDX scans (b) of the interface modification revealed a molybdenum-rich zone between the zirconium diffusion barrier and uranium-molybdenum foil, shown in the top right scan; bottom right is zirconium.*

Finally, two full-size fuel plates were fabricated using FB for the AFIP-2 design: one plate containing the modified zirconium interface and the other containing a silicon interface applied using thermal spray. Scale-up of the fabrication process from mini-plates was achieved generally as anticipated; the fuel plates achieved 80% average burnup during irradiation without incident. Not only did this experiment confirm that the selected modifications would not inhibit the FB process, but it also demonstrated, for the first time, scale-up of fuel fabrication from the mini-plate design to the full-size plate design.

Improvements in the overall processing parameters employed for FB and the onset in development of an operational envelope for the process are ongoing. In particular, research into the relationships between process load, temperature, and concomitant microstructure were investigated. The relationship between process load and the temperature measured at the joint interface is illustrated in Figure 7. Results of this study, specifically the large temperature gradient between the advancing edge of the tool and the retreating edge of the tool, initiated the development of a thermodynamic model (Dixon et al., 2007). A snapshot of an early model run is shown in Figure 8 that basically confirms the temperature gradient across the diameter of the tool face.

Finally, the INL's prototype, full-scale fabrication demonstration unit is now completely online and functional. This piece of equipment, a photograph of which is shown in Figure 9, will allow more fabrication of fuel plates with more consistency and repeatability. Overall, the equipment allows computer controlled feedback, rather than manual operator controlled feedback. The new equipment will also enable the fabrication of long monolithic fuel plates for eventual demonstration of full-scale uranium-molybdenum based monolithic fuel elements in the ATR. The operational envelope established through modeling and experimentation, discussed previously, is currently being validated on the TTI machine.

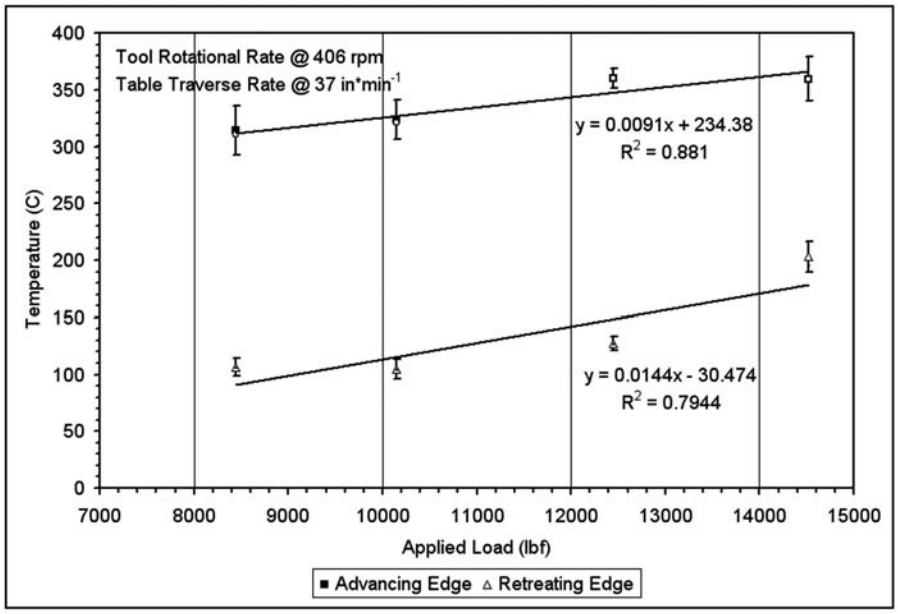


***Figure 7.***
*Temperature measured at the joint interface as a function of applied process load for the advancing edge and retreating edge of the tool. Joint temperature increased with higher process loads, and there is a significant temperature gradient across the diameter of the tool.*

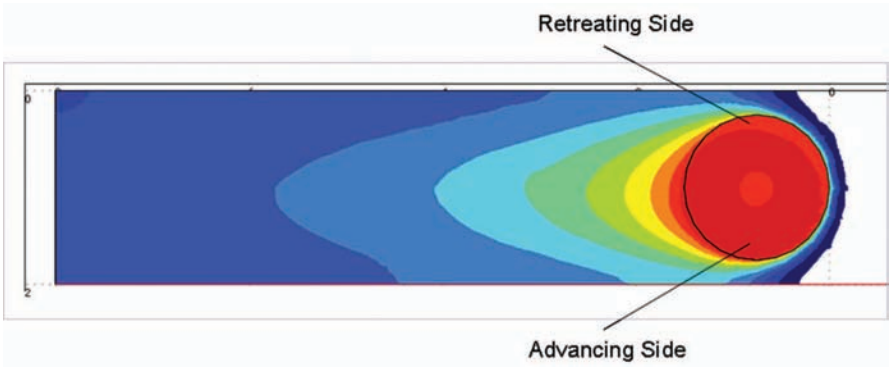


***Figure 8.***
*Thermodynamic model snapshot confirming the temperature gradient across the tool diameter, with the advancing edge having a higher temperature than the retreating edge.*

***Figure 9.***
*Photograph of the TTI machine that will be used for full-scale fabrication demonstration of monolithic fuel plates.*

## *REFERENCES*

Burkes, D. E., N. P. Hallinan, C. R. Clark, "Nuclear Fuel Plate Fabrication Employing Friction Bonding," AWS Welding J., accepted for publication (2008) pp. 3-10.

Burkes, D. E., N. P. Hallinan, K. L. Shropshire, P. B. Wells, "Effects of Applied Load on 6061-T6 Aluminum Joined Employing a Novel Friction Bonding Process," Met. Mat. Trans. A, accepted for publication.

Hallinan, N. P., D. E. Burkes, "Friction Stir Weld Tools, Methods of Manufacturing Such Tools, and Methods of Thin Sheet Bonding Using Such Tools," U.S. Patent Application (2007).

Burkes, D. E., N. P. Hallinan, J. M. Wight, M. D. Chapple, "Update on Friction Bonding of Monolithic U-Mo Fuel Plates," Proc. of 2007 RERTR International Meeting, Czech Republic (2007).

Dixon, J., D. Burkes and P. Medvedev, "Thermal Modeling of a Friction Bonding Process," Proceedings of the COMSOL Conference 2007, Boston, MA (2007) pp. 349-354.

DOUGLAS E. BURKES (BS, 2001, Mechanical Engineering, Texas Tech University; PhD, 2005, Materials Science, Colorado School of Mines) is a member of the Fuel Performance and Design Department at the INL. His current research focuses on development of novel nuclear fuel fabrication processes for application in research and fast reactors, characterization of advanced nuclear fuels, and development of advanced fuel characterization methods and techniques. He has been a member of the Fuel Performance and Design Department since 2006.

# Silicon as an Alloying Addition to Aluminum for Improving the Irradiation Performance of Fuel Plates

*Dennis D. Keiser, Jr.*

EARLY TESTING OF RERTR uranium-molybdenum dispersion fuel plates employed plates with pure aluminum as the matrix in the fuel meat. During irradiation of these fuel plates, large pores developed at the interface between a fuel/matrix interaction layer, which developed due to radiation enhanced diffusion (RED), and the unreacted aluminum matrix. The presence of these pores contributed to the eventual failures of some of the fuel plates.

In order to eliminate the development of this type of failure mechanism, possible alloying additions to the fuel and/or matrix of the dispersion fuel meat were evaluated (Kim et al., 2005). It was determined that silicon had the potential to be an effective addition to the aluminum matrix. The idea was that by adding silicon to the aluminum matrix, different, more radiation-stable phases would form during RED that would perform better during irradiation, and in addition, the overall size of the interaction zones would be reduced. Characterization of irradiated uranium-silicide fuels, which were developed early in the RERTR fuel program for converting some of the research reactors, showed that stable interaction layers had formed during RED of the fuel and matrix (Leenaers et al., 2004). If layers similar to these could be generated in the current RERTR fuels, stable irradiation behavior should result.

To develop an understanding of the silicon diffusion behavior in RERTR fuels, out-of-reactor diffusion couple studies are being performed to see aluminum alloys affects the development of interdiffusion zones in terms of zone width and the types of phases that will form (Keiser, 2007; Perez, 2007). Because these experiments have to be performed at relatively high temperatures (500°C to 600°C) to get measurable diffusion zones in reasonable time periods, these tests are not necessarily representative of the in-reactor phenomena that occur at low temperatures (e.g., 200°C) and under the influence of irradiation (i.e., fission fragments, localized heating, etc). However, these diffusion tests do give an indication of how changing the silicon content in aluminum alloys will affect diffusion behavior. Furthermore, because fuel plates can be exposed to higher temperatures during fabrication, which results in the presence of interaction zones in as fabricated plates, it is important to understand the development of these zones since they will be present in fuel plates going into the reactor.

Diffusion couple experiments that were performed using Al-6061 (0.81 wt% silicon), Al-2Si, Al-5Si, and Al-4043 (4.81 wt% silicon) alloys indicated that the width of the interdiffusion zones that form decreases as the amount of silicon is increased in the aluminum alloy, up to approximately 2.0 wt% silicon. Concentration additions above this value do not seem to reduce the diffusion zone width over what was the case for the alloy with 2.0 wt% silicon. In terms of the phases that develop in the interaction zones, there can be great differences depending on the silicon-containing aluminum-alloy that is employed for the diffusion couple. The presence of minor alloy constituents in the Al-6061 and Al-4043 alloys can affect the nature of the interaction zones.

Diffusion couple tests have also shown that if not enough silicon is available in an aluminum alloy, the diffusion behaviors that are observed may at some point approximate what occurs in the U-Mo-Al system without silicon (Keiser, 2007). Enough silicon has to interdiffuse to the interaction zone to keep silicon-containing phases stable, or they will break down. Therefore, when adding silicon, a minimum amount should be be added to get good behavior.

Another research effort associated with diffusion couple experiments has been the characterization of fuel plates after fabrication. Knowing the times that fuel plates were exposed to higher temperatures provides some information about the kinetics of the interaction between fuel alloys and the matrix. Also, the types of phases that are present in interdiffusion zones can be determined. Characterization of as-fabricated fuel plates is crucial for developing a better understanding of in-reactor behavior since comparison of microstructures before irradiation can be made with those after irradiation. Figure 1 shows the microstructure of an Al-4043 matrix-dispersion fuel plate after fabrication. It shows that silicon-rich layers are already present around the fuel particles before the fuel plate is put into the reactor.

Most postirradiation examination of fuel plates for characterizing the fuel microstructures is done using optical metallography. This technique is effective for identifying features such as swelling behavior because the porosity that develops in the fuel can be characterized. However, as noted, the fuel/matrix interaction zones can have large impacts on fuel behavior, and it is necessary to measure the compositions in these zones to determine the phases that are present in irradiated plates. Since silicon is added to change the phases that form in the interaction zones, it is important to see if different, more stable phases are actually present in irradiated fuel plates because of the presence of silicon. Consequently, samples have been taken from actual irradiated RERTR fuel plates in the form of punchings, mounted longitudinally, and then polished before being inserted into a SEM equipped with an EDS and WDS to conduct microstructural characterization (Janney et al., 2007; Keiser et al., 2008). The samples characterized to date had either low (0.2 wt%) or high (4.81 wt%) silicon. Figure 2 shows the microstructure observed for the low and high silicon samples. The low-silicon plate contained interaction zones that were similar to those that develop in dispersion fuels with pure aluminum as the matrix; the zones in a sample taken from the fuel plate with Al-4043 alloy matrix were relatively narrow and enriched in silicon. The results of these characterizations confirmed that enough silicon has to be present in the matrix to keep silicon-rich layers stable. Therefore, if enough silicon is added to the fuel plate matrix, the interaction zones that are present in a fuel plate irradiated to high burnup will be relatively narrow, and the swelling behavior of these interaction zones will be appreciably improved compared to the zones present in fuel plates without silicon.

Characterization of the surfaces of a fractured sample taken from an irradiated RERTR fuel plate can also be of great value. Such fractured samples are particularly useful because they enable the fine gas bubbles that are present in the fuel to be characterized effectively. These bubbles are typically smeared when polished cross-sections are characterized. Figure 3 shows a few fractured particles that were observed in the fuel meat of an irradiated RERTR fuel plate.

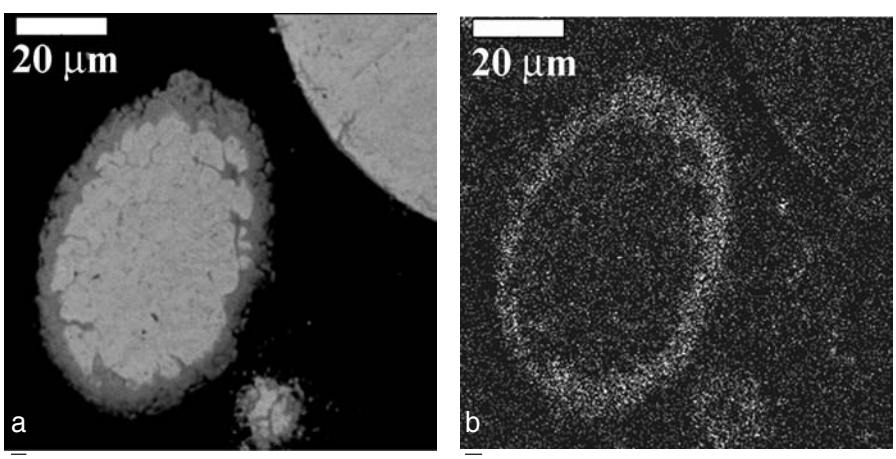


***Figure 1.***

*Backscattered electron micrograph (a) showing white uranium-molybdenum alloy particles in a black Al-4043 matrix and the gray interaction zone around the fuel particles. The silicon X-ray map (b) shows the silicon enrichment in the interaction zone.*

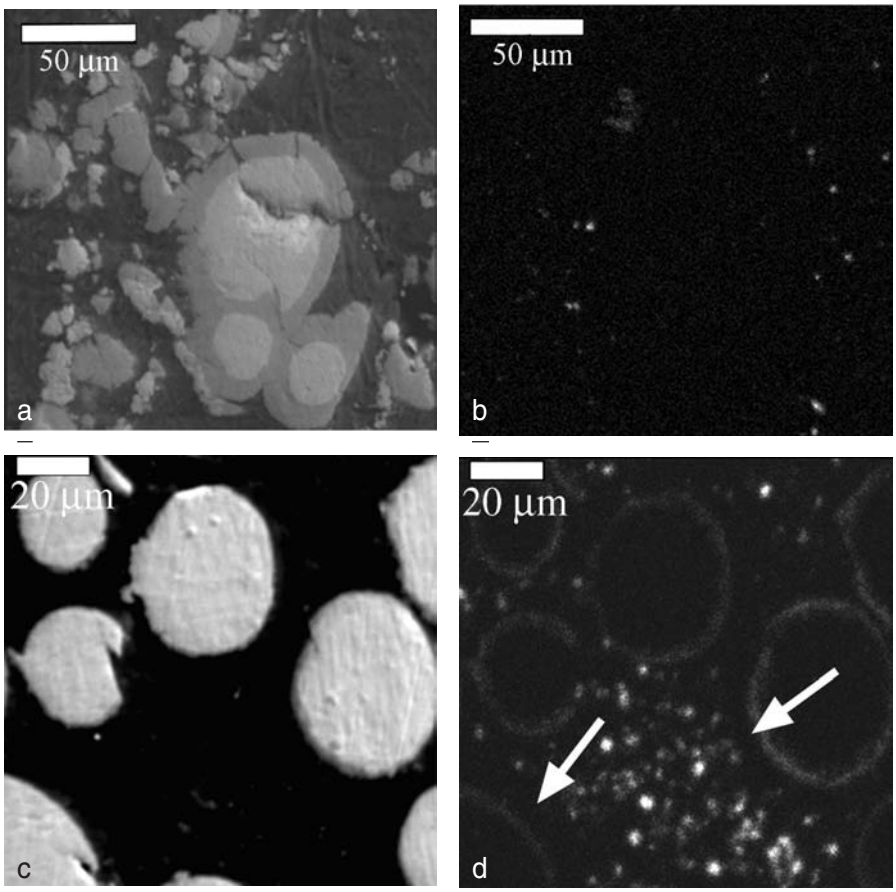


***Figure 2.***

*Backscattered electron images (a) and (c) for an irradiated fuel plate with 0.2 wt% silicon in the matrix and 4.81 wt% silicon in the matrix, respectively, where the bright particles are uranium-molybdenum fuel, the black areas are the aluminum alloy matrix, and the gray regions are the interaction layers. The silicon X-ray map (b) for the low-silicon plate shows negligible silicon in the relatively wide interaction layers, and the silicon X-ray map (d) for the high-silicon fuel plate, where the interaction layers are relatively narrow, contains appreciable silicon The arrows in (d) indicate the areas around fuel particles where recoil zones, which are present around the fuel particles during irradiation, have dissolved the silicon-rich precipitates that are present in the original cladding, creating precipitate-free zones.*

Overall, the addition of silicon to the aluminum matrix in RERTR dispersion fuels is an effective technique for improving the overall irradiation performance of the fuel. Based on this optimal behavior, silicon additions are also being employed to improve another type of RERTR fuel, namely monolithic fuel plates. For an early version of the monolithic fuels, where the uranium-molybdenum foil was in contact with plain Al-6061 cladding, interaction zones developed during irradiation that displayed adverse swelling behavior, which was similar to what was observed in dispersion fuels. Based on the positive effect of adding silicon to the aluminum in dispersion fuels, it is anticipated that the addition of silicon can have a similar positive effect for monolithic fuels.

Different approaches have been tried for adding silicon to the uranium-molybdenum foil/cladding interface (e.g., thermal spraying of the silicon onto the cladding), and irradiated samples are in the process of being characterized. Another approach for dealing with fuel/cladding interaction in monolithic fuel plates is to use zirconium (or possibly niobium or molybdenum) as a diffusion barrier for totally eliminating fuel/cladding interactions. Fuel plates with an applied diffusion barrier have also been irradiated, and early results are promising.

Based on the results of recent reactor tests using dispersion and monolithic fuels with added silicon, the goal of qualifying fuel plates in the next few years for use in research and test reactors seems achievable.

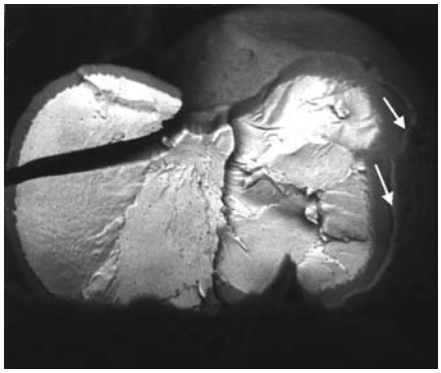

***Figure 3.***
*Backscattered electron micrograph of two uranium-molybdenum particles (white) present in the fuel meat of an irradiated RERTR fuel plate after a sample was fractured for SEM characterization. The white arrows indicate where, based on the fracturing behavior of the interaction zone (gray), an interface may be present between two different phases.*

## *References*


Janney, Dawn E., et al., 2007, Hot Laboratories and Remote Handling Plenary Meeting, Bucharest, Romania, September 20-21, 2007.

Keiser, D. D., Jr., 2007, Defect and Diffusion Forum, 266 (2007) 131.

Keiser, D. D., Jr. et al., 2008, Proc. of the RRFM 2008 International Meeting on Research Reactor Fuel Management, Hamburg, Germany, March 2-5, 2008.

Kim, Y. S., et al., 2005, in: Proc. of the 25th International Meeting on Reduced Enrichment for Research Reactors, Boston, MA, 2005.

Leenaers, et al., 2004, *J. Nucl. Matter.* 327 (2004) 121.

Perez, E., et al., 2007, Defect and Diffusion Forum, 266 (2007) 149.

DENNIS D. KEISER, JR. (BS, 1987, MS, 1989, Metallurgical Engineering, University of Idaho; PhD, 1992, Materials Engineering, Purdue University) is a member of the Fuel Performance and Design Department at the INL. He has over 20 years experience researching different issues related to the performance of nuclear fuels and materials. His current research relates to developing low-enriched fuels for application in research and test reactors, developing a better understanding of the diffusion behavior of fuel and cladding components in irradiated fuels, and determining the microstructural development of fuels and materials during irradiation.

# Advanced Test Reactor In-Canal Ultrasonic Scanner: Experiment Design and Initial Results on Irradiated Plates

*Daniel M. Wachs and Jared.M. Wight*

AN IRRADIATION TEST device has been developed to support testing of prototypic scale plate-type fuels in the ATR at the INL. Optimized experiment hardware and operating conditions provide the irradiation conditions necessary to conduct performance and qualification tests on research reactor-type fuels for the RERTR program.

The irradiation device design allows disassembly and reassembly in the ATR spent fuel canal to enable interim inspections on the fuel plates. An ultrasonic scanner was developed to perform dimensional and transmission inspections during these interim investigations. Example results from the AFIP-2 experiment are presented in this section.

Before implementation of any new nuclear fuel design, the fuel must be tested under a wide range of irradiation conditions. These tests provide the basis for evaluating fuel performance and ultimately the data necessary for a regulator to license a reactor to operate with the fuel. In most cases, this testing envelope must meaningfully exceed the anticipated operating conditions to establish appropriate margins for safe operation. This envelope encompasses a number of key environmental variables that include the thermal, hydraulic, nuclear, and geometric conditions of the experiment. The ATR was specifically designed for this purpose, and it provides the experimenter with the ability to control all these variables over a wide range. The INL Nuclear Fuels and Materials Division (through leadership of the RERTR Fuel Development Program) is utilizing this key asset to develop the nuclear fuels necessary to support the NNSA's GTRI HEU minimization objectives.

The Nuclear Fuels and Materials Division has developed several experimental test trains to enable irradiation testing of nuclear fuel designs in the ATR. The RERTR program focuses on the development of research reactor fuels that operate under conditions that are very similar to the standard ATR coolant environment. Consequently, all the RERTR irradiation test devices are immersed directly in the ATR coolant stream. The first experiments (RERTR-1, -2, and -3) were designed to test the behavior of very small fuel samples (nano- and micro-plates). The size of these samples allowed for testing of a large number of candidate materials and greatly simplified test sample fabrication. The PIE results collected from these screening tests were used to select aluminum clad, uranium-molybdenum alloys for further development. To evaluate performance further, an irradiation test device was developed to test slightly larger scale plates (mini-plates). This scale allowed the experimenter to account for fabrication variables that might appear at a more representative scale while still accommodating a fairly large number of test specimens at a low cost. The sensitivity of fuel performance to various variables was evaluated by testing multiple samples of each type under different irradiation conditions. After extensive testing at the mini-plate scale, a few fuel designs appeared viable enough to justify prototypic testing. Testing at this scale substantially reduced the number of samples that could be tested while simultaneously increasing the cost of testing for each sample. It was, therefore, desirable to develop an irradiation test device that maximized the amount of data that could be collected from each experiment.

The AFIP (ATR full-size-plates in center flux trap position) test assembly, designed specifically for this purpose, provided a versatile testbed for plate-type fuel experiments. The hardware allows the experimenter to subject experiments of various scales to a broad range of

nuclear and thermal-hydraulic conditions. The experimental design allowed disassembly in the ATR canal between irradiation cycles. This made it possible to interrogate the experiment behavior at various stages of irradiation. A complementary set of examination tools has also been developed to collect this data.

## *AFIP Test Hardware*

A basic function of the AFIP test assembly is to enable testing of research-reactor fuel designs at a prototypic scale and under prototypic irradiation conditions. The ATR operates a wide range of irradiation test positions capable of supporting all types of nuclear fuels and materials testing; however, only a few positions are appropriate for the type of testing required for this program (large openings with high neutron flux). The ATR center flux trap (CFT) offers a 3-in.-diameter and 48-in.-long cylindrical cavity with a peak (unperturbed) thermal neutron flux of approximately 4.4 x $10^{14}$ n/cm$^2$/sec and was selected to house the AFIP experiment. Figure 1 shows a cross-section of the ATR.

An insert was necessary to convert the circular opening into a square channel large enough to accommodate a fuel plate at least 2 in. wide. The hardware also provides the structure necessary to control the experiment configuration during testing (i.e., prevent movement or vibration) and handling (before and after irradiation). The hardware must completely constrain the fuel plates during irradiation (without removable screws, bolts, or pins) while still allowing operators to disassemble the experiment (which is submerged under 20 ft of water). A schematic of the experiment cross-section showing the key components of the hardware is provided in Figure 2. Photographs of the hardware components are shown in Figure 3. The experiment can accommodate two fuel plate assemblies with a 2.2-in. plate width. The plate assemblies can accommodate single plates up to 48 in. long or several plates adding up to that total length. The plate assemblies (Figure 4) are held together by a thin rail piece on both sides that extends the full length of the plate assembly. The rail also assures that the coolant-channel gap width remains fixed during irradiation. The fuel plate assemblies are held in position by a ram that is pinned in place by a tapered ram-rod. Four flux monitor wires are also included in the experiment to baseline the nuclear analysis. The experiment is inserted into the ATR CFT through a long in-pile tube that extends above the reactor core. An extension piece

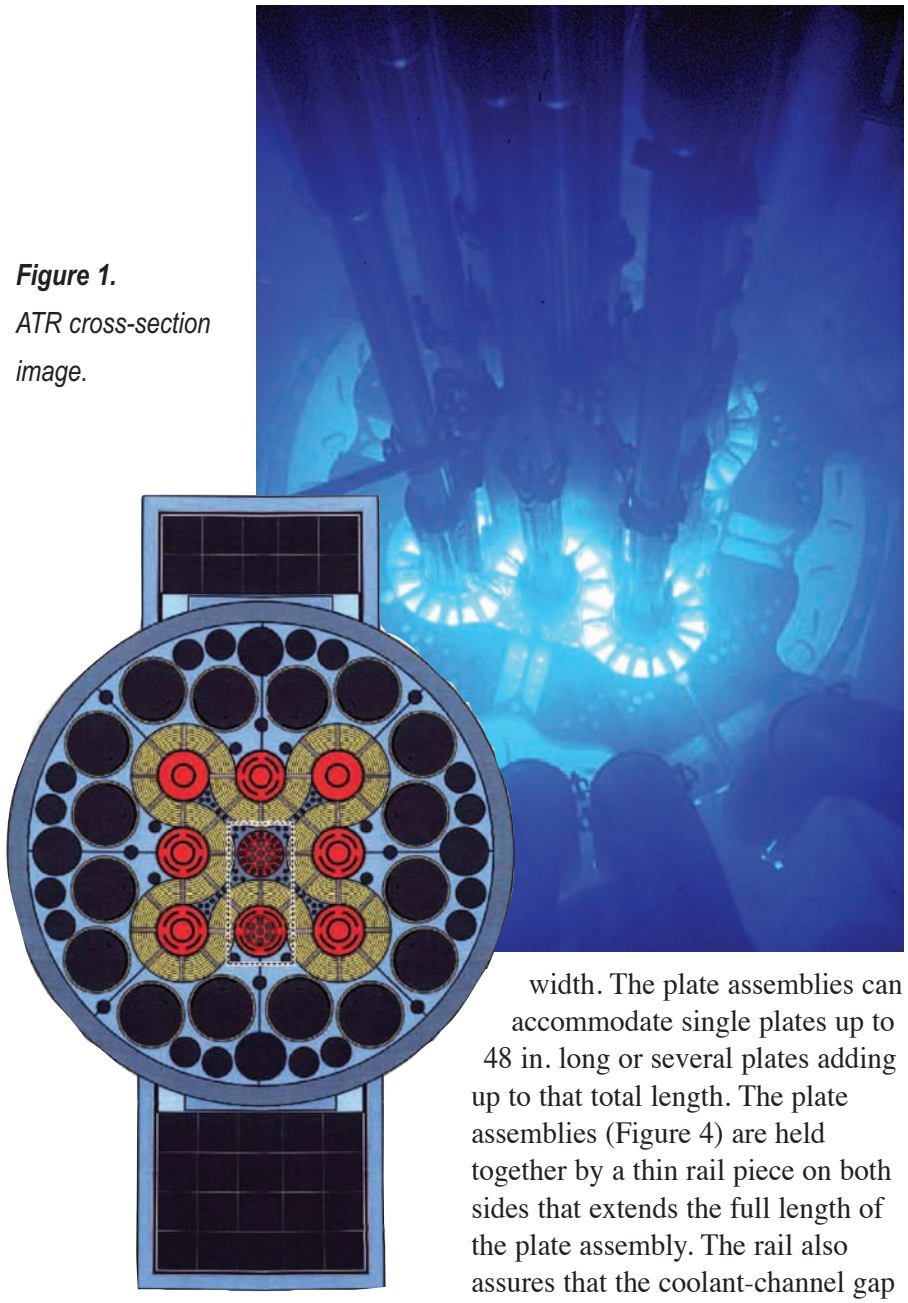

***Figure 1.***
*ATR cross-section image.*

***Figure 2.***

*AFIP test assembly.*

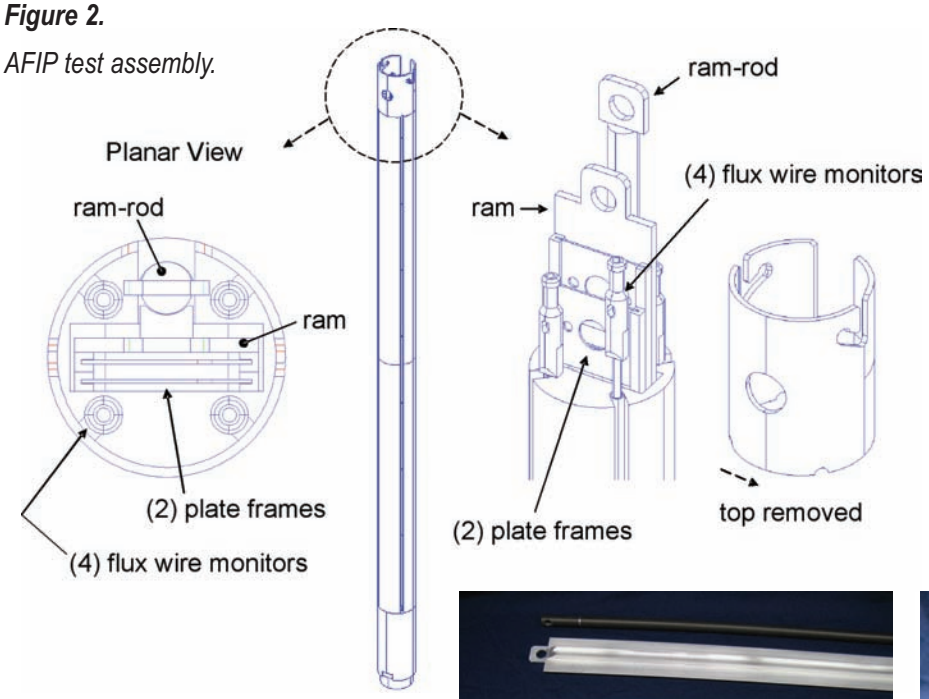


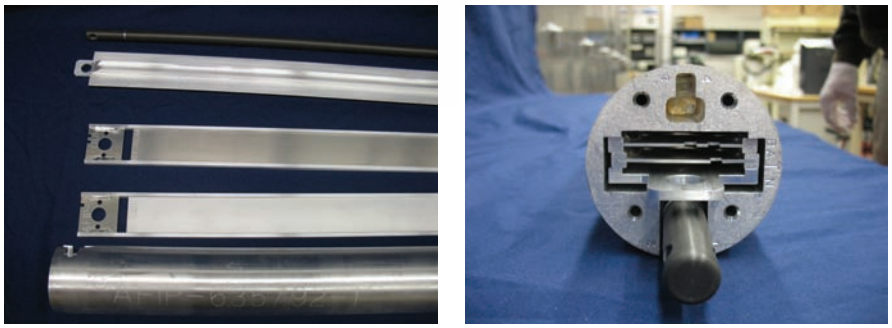

***Figure 3.***

*Test hardware photographs.*

attaches to the top of the experiment hardware to allow loading and unloading of the experiment. The extension also pins the experiment components in place during irradiation.

## *Irradiation Conditions*

The experiment operating conditions are constrained by the allowable ATR coolant conditions. For ATR experiments, the flow instability ratio (FIR) and departure from nucleate boiling ratios (DNBR) must be larger than 2.0. Hydraulic tests and high fidelity thermal models were developed to establish clearly the experiment-operating envelope. A mock-up of the hardware (including nonfueled dummy plates) was fabricated for the hydraulic tests. The ATR typically operates with a core

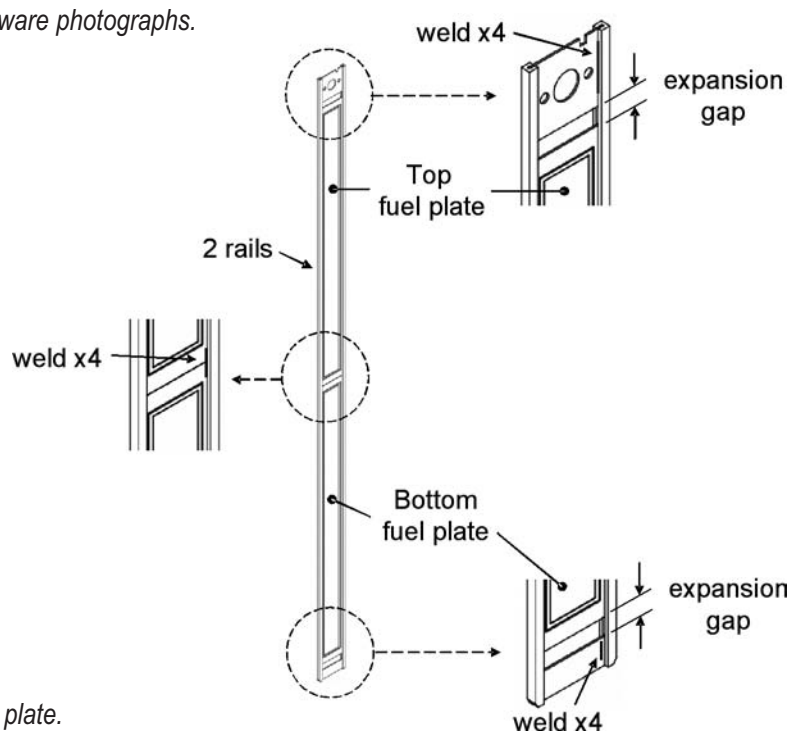


***Figure 4.***

*AFIP fuel plate.*

pressure drop of 77 psi (two-pump mode), where the coolant velocity in the fuel plate channels is roughly 17.4 m/s. The coolant velocity can be increased or decreased by operating in the three-pump mode (100-psi pressure drop) or by inserting an orifice plate at the exit. Thermal analysis confirmed that the experiment could operate at a peak surface-heat flux of at least 500 W/cm$^2$ without exceeding the FIR or DNBR limits. The fuel plate portion of the thermal model is shown in Figure 5.

## *In-Canal Examination*

The most critical performance measure for nuclear fuels is the ability to maintain a stable geometry during irradiation. The conversion of fissile atoms (typically uranium-235) into two fission fragments inevitably leads to growth of the fuel material during irradiation. All nuclear fuels experience this type of behavior on a microscopic scale. The primary challenge of the fuel developer is to identify materials that accommodate fission fragments in a manner that minimizes swelling, and that are geometrically stable at the macroscopic scale during irradiation. This swelling is typically manifest by growth in the plate thickness as a function of fission density. It is also possible that local differences in fission density (and thus, local swelling) could lead to the formation of significant nonuniformities in stress throughout the plate. These stresses could result in overall plate distortion or even delamination of the interface between the fuel and cladding.

Macroscopic shifts in fuel geometry are routinely evaluated after irradiation. However, periodic nondestructive examination that allows this data to be collected several times during the experiment can enhance the value of an individual experiment substantially. This effectively allows the experimenter to transform a single experiment into the equivalent of several experiments, which translates into substantial time and money savings for large experiments.

UT scanning has long been used to inspect fresh fuel plates before irradiation; thus, techniques to determine both the cladding thickness and level of contact (bonding) between fuel and clad layers have been well established. It is also possible to use UT technology to map the surface profile of the plates. Since the UT scanning requires that the fuel plates be submersed in water initially, implementation of the technique for use on irradiated fuel plates in the ATR spent fuel canal is ideal for interim examination. A UT test stand that can be operated remotely with radiation-hardened detectors was developed at the INL for this purpose (Figure 6).

The in-canal UT scanner was first demonstrated as an integral part of the AFIP-2 experiment on full-size monolithic fuel plates. Although significant work had been successfully performed at the miniplates scale, the experiment provided the first opportunity to evaluate the performance of prototypic scale monolithic uranium-molybdenum fuel plates. The examinations yielded unprecedented dimensional resolution for irradiated fuel. Examinations were conducted at

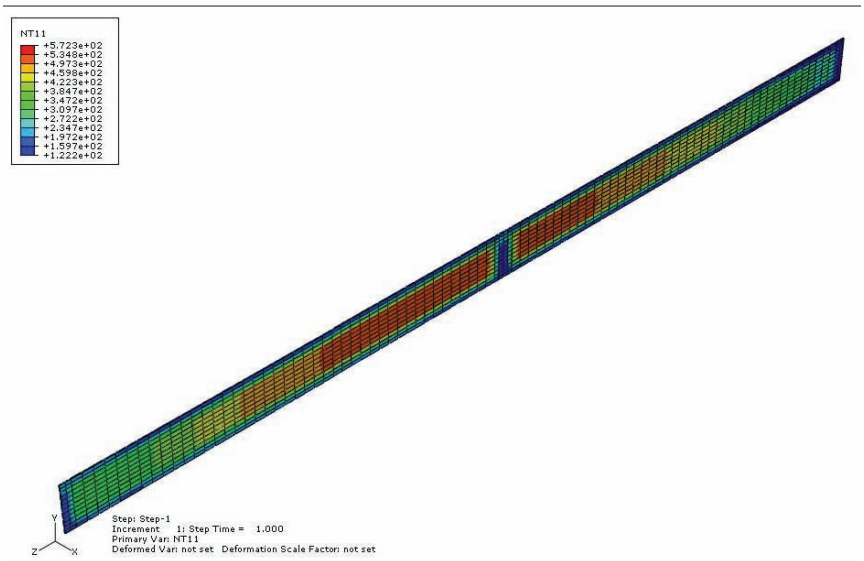


***Figure 5.***

*Fuel surface temperature estimates from thermal analysis.*

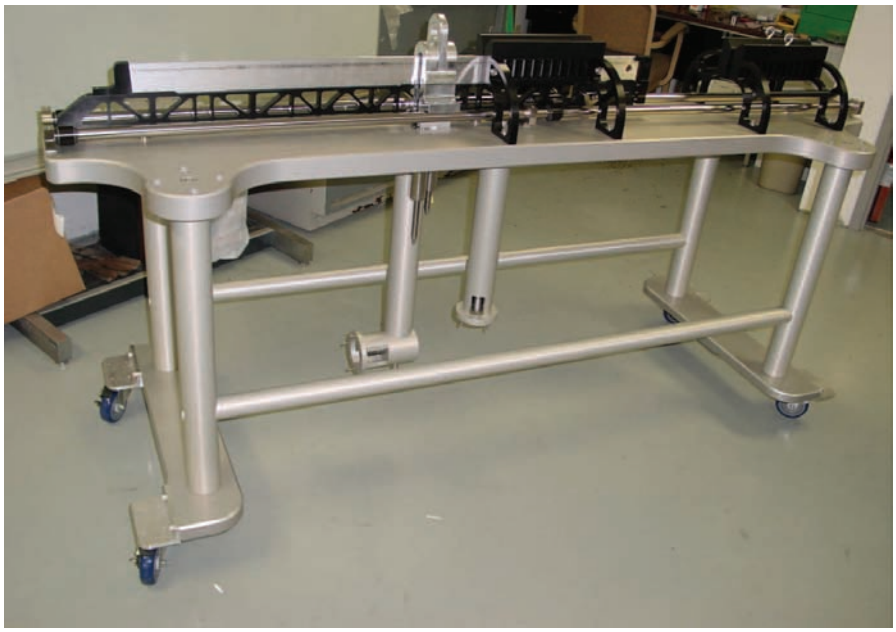

***Figure 6.***
*ATR in-canal UT scanner (prior to installation).*

***Figure 7.***
*Thickness change of one AFIP-2 plate after each irradiation cycle. The right edge of the plate was located at the reactor core centerline and was, therefore, at the highest power/fission density. This location is where the maximum swelling condition occurs. (The highest peak on the far right is from the upper plate.)*

four points: 1) prior to irradiation, 2) after 35 days of irradiation, 3) after 77 days of irradiation, and 4) after 133 days of irradiation. The results clearly show the relationship between swelling and fission density, as the plate thickness mirrors the plate power profile (Figure 7). The measurements (Figure 8) showed that the plate contours remain relatively unchanged during the irradiation (i.e., plate buckling or warping does not occur). Transmission scans were also completed to reveal the formation of any delaminations (Figure 9). However, the scans identified small regions where void densities were large enough to diminish sound transmission in one of the fuel designs. These indications will be an area of focus during destructive examination in the hot cell.

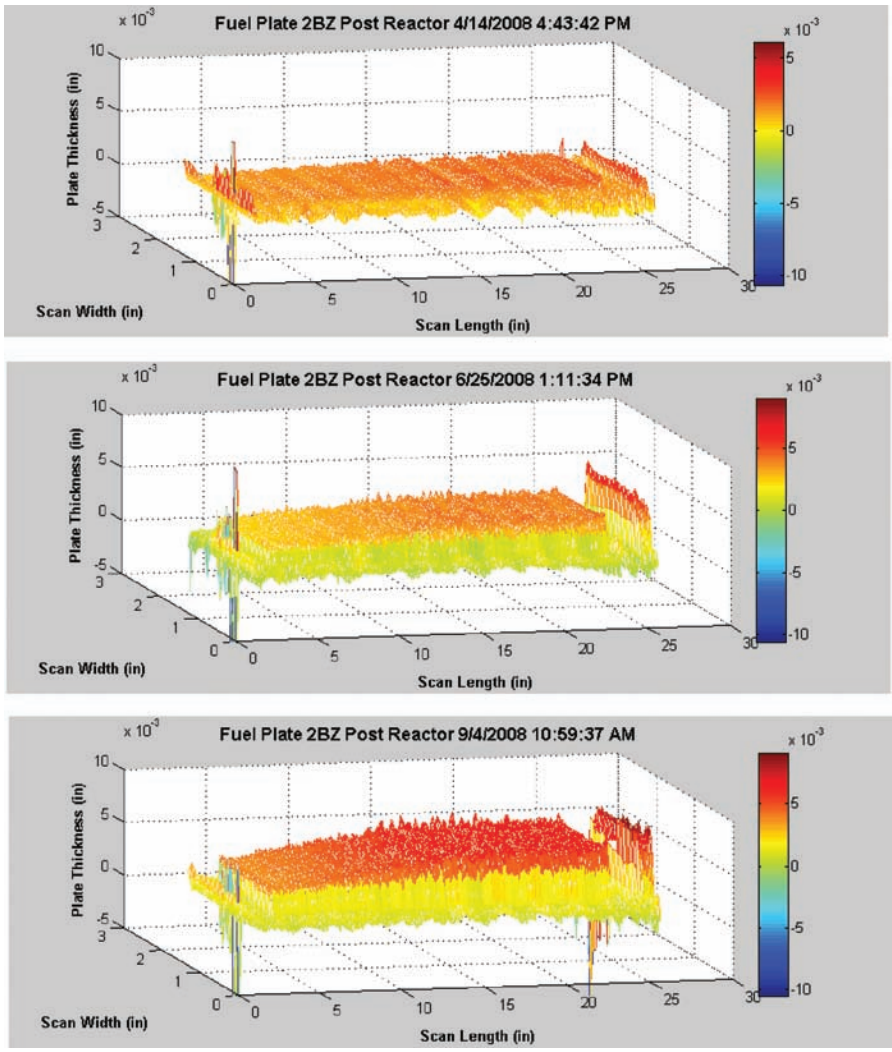

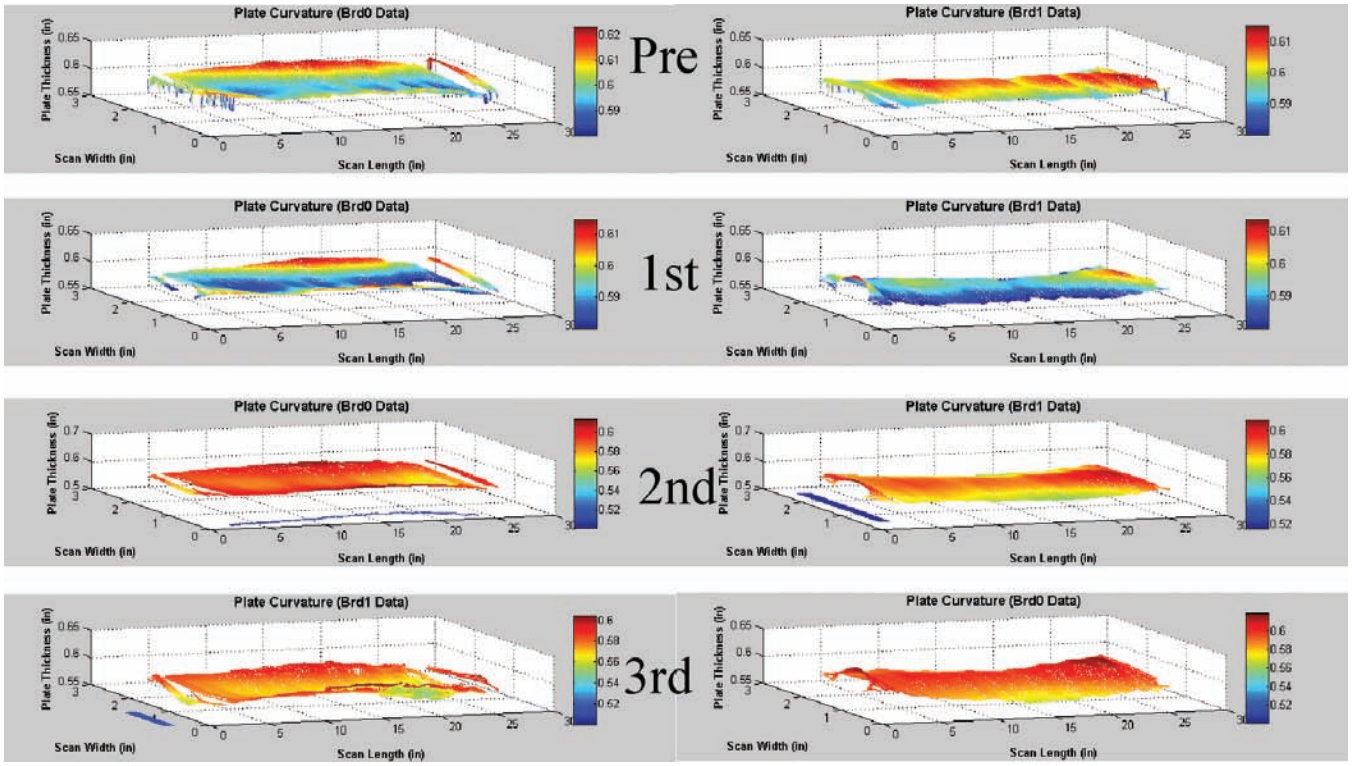


***Figure 8.***

*Surface profiles for one AFIP-2 plate after each irradiation cycle. The images show that the general shape of the plates remains relatively unchanged during irradiation.*

Pre-reactor transmission inspection (01-28-08)

Post-reactor transmission inspection (04-14-08)

Post-reactor transmission inspection (06-25-08)

Post-reactor transmission inspection (09-04-08)

***Figure 9.***

*UT transmission images of one AFIP-2 plate taken from each irradiation cycle. The images show the formation of several small indications in the final cycle.*

## *Conclusions*

The AFIP experiment hardware design enables detailed testing of prototypic scale research reactor fuels designs. The flexible design allows the experimenter to configure the test to achieve a wide range of desired irradiation conditions (i.e., nuclear, thermal-hydraulic, and geometric). The test apparatus also enables collection of a substantial amount of performance data previously unavailable to the experimenter, substantially reducing the cost and length of time required to conduct a fuels development program. Ultimately, this experiment design will be the workhorse capability that enables qualification of new research-reactor fuel designs.

DANIEL M. WACHS (BS, 1995, Mechanical Engineering, MS, 1997, Nuclear and Mechanical Engineering, Oregon State University; PhD 2000, Mechanical Engineering, University of Idaho) is a member of the Fuel Performance and Design Department at the INL. He is currently the National Technical Director for the RERTR Fuel Development Program. His current research interests and technical background include irradiation testing of nuclear fuel and materials, thermal-hydraulic testing and analysis, and reactor system component design for research reactors and liquid metal cooled fast reactors.

JARED M. WIGHT (BS, 2005, Mechanical Engineering, Brigham Young University - Idaho) is an engineer in the Fuel Fabrication Department at the INL. He has been actively involved in the project coordination for irradiation testing of research reactor fuels, hardware design and fabrication of irradiation devices, and engineering of devices needed for fabrication of irradiation samples for 4 years.

# Fuel Performance Modeling

*Steven L. Hayes and Pavel G. Medvedev*

THE INL'S FUEL performance code Plate Lifetime Accurate Thermal Evaluation (PLATE) simulates multiple simultaneous coupled physical phenomena to predict evolution of the fuel temperature and dimensions with burnup. PLATE is used by INL's engineers to analyze fuel behavior during irradiation, and as a testbed for the new fuel performance models, leading to a better understanding of fuel behavior. While the ultimate objective of the RERTR fuel performance modeling effort is to predict the service lifetime of the fuel plates, PLATE represents a critical step towards this goal.

Plate-type fuels are widely used in research and test reactors worldwide. The development of $U_3Si_2$ as the dispersed fuel phase in an aluminum matrix during the 1980s and the current interest and work on uranium alloys as the fuel phase has resulted in fuel systems that undergo substantial chemical interaction between the fuel and matrix phases during irradiation. Results from the PIE of RERTR fuels indicate that the interaction between the fuel and matrix phases occurs readily during irradiation and is a sensitive function of temperature, as illustrated in Figure 1. As the interaction proceeds, a low conductivity reaction-product phase accumulates, with a corresponding depletion of the high-conductivity aluminum matrix phase. This leads to a substantial degradation of fuel meat thermal conductivity with time, and fuel centerline temperatures can increase substantially with burnup even if plate powers decrease. This strong interrelationship between fuel temperature and fuel-matrix interaction makes the development of a simple empirical correlation between the two difficult, since it is unclear what temperature to employ; without a correlation for interaction thickness, it is impossible to calculate fuel temperatures during irradiation. For this reason, a sophisticated thermal model has been developed to calculate fuel temperatures, taking into account the changing volume fractions of fuel meat constituents, including fuel, matrix, and reaction-product phases within the fuel meat, gas generation/swelling in the fuel and

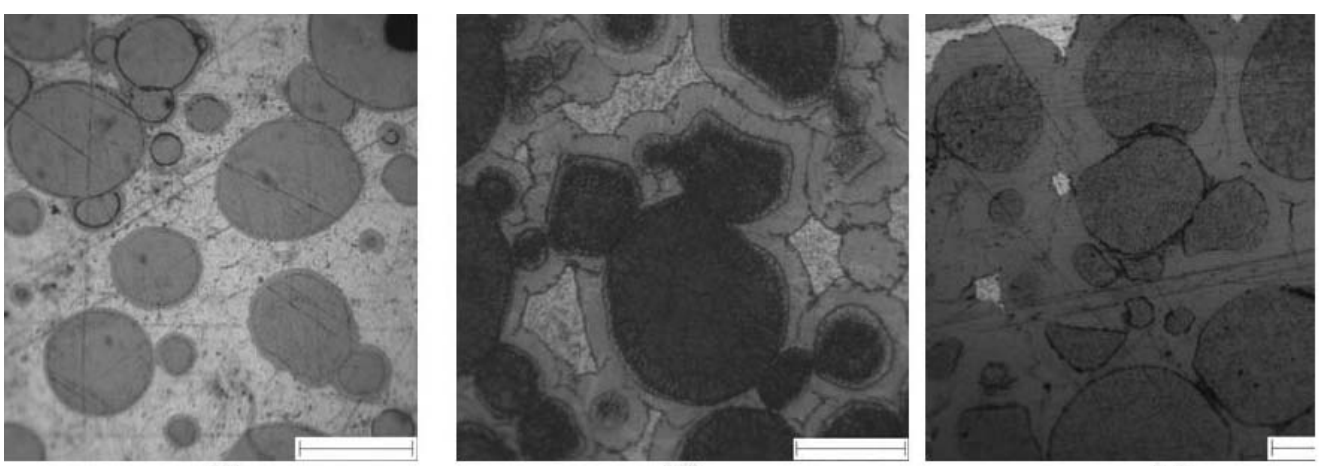

(a) (b) (c)

***Figure 1.***

*Increasing U-Mo/Al fuel-matrix interaction with temperature; (a) U-10Mo at 139°C and 30% burnup, (b) U-10Mo at 203°C and 38% burnup, and (c) U-6Mo at 224°C and 40% burnup (scale=100μm).*

reaction-product phases, and cladding corrosion. Within the framework of this best-estimate temperature calculation, an empirical fuel-matrix interaction-rate correlation has been developed in an integral way. The resulting interaction rate correlation and other associated behavior correlations and models have been implemented within a computer code designated as PLATE, which is now in use to evaluate RERTR fuel plate irradiation performance.

During irradiation, the fuel phase reacts readily with the aluminum matrix. U-Mo/Al fuels loaded at 8 g-U/cm$^3$ and irradiated at high temperature (>200°C) resulted in some cases of the aluminum matrix phase near the fuel centerline being totally depleted due to this reaction by approximately 40% burnup. The stoichiometry of the reaction product has not yet been determined definitively; however, it now appears to be much more aluminum-rich than previously thought. Though it has not been experimentally determined, it is assumed that this aluminide reaction product has a low thermal conductivity (e.g., $UAl_4$ has a very low thermal conductivity of ~0.06 W/cm-°C). Thus, the depletion of the high conductivity aluminum matrix phase and the buildup of a significant quantity of low conductivity reaction-product phase leads to a dramatic decrease in fuel meat thermal conductivity (i.e., reduction by a factor of 2 to 3). Since the reaction rate is an Arrhenius function of temperature, this fuel-matrix interaction can drive an escalating positive feedback thermal response at high temperatures.

Fissions occur within both the fuel and reaction product phases and produce fission product atoms having a larger volume than the fissioned uranium (or plutonium) atoms that produced them. Furthermore, approximately 25% of the fission products are either xenon or krypton gas atoms, some of which coalesce into bubbles over time. These phenomena result in swelling in both the fuel and reaction product phases that increase with burnup. Swelling of the uranium-containing aluminide reaction product in U-Mo/Al fuels is relatively low and does not appear to be very different from the swelling of the reaction product phase in $U_3Si_2$/Al fuels; the swelling of the uranium-molybdenum alloys as a function of burnup, however, is larger than that observed in $U_3Si_2$/Al fuels.

Mechanical constraint minimizes dimensional changes in the width and length dimensions of a fuel plate; as a result, fuel plate swelling is essentially manifest as a thickness increase. Because the coolant channels between fuel plates in most research reactors are normally very small, any fuel plate thickness increases that could substantially decrease the coolant channel size are important to predict for safety evaluations. Fuel plate thickness increases are a composite of three phenomena: 1) cladding corrosion and 2) fuel-matrix interaction, which both produce a reaction product of lower density than the reactants; and 3) the fission product swelling of the uranium-containing fuel and reaction product phases. Fission product swelling is the largest of these components for U-Mo/Al fuels.

The corrosion of the cladding outer surface by the reactor coolant, when extensive, is an important phenomenon to include in fuel modeling. Aluminum cladding corrosion by water results in a reaction product that is a mixture of alumina hydrates, but is often assumed to be either totally or predominantly boehmite ($Al_2O_3 \cdot H_2O$). Boehmite has a low thermal conductivity (~0.002 W/cm-°C), so even relatively thin layers on the cladding surface can lead to significant increases in fuel temperatures; thick boehmite layers (>50μm) can result in fuel temperature increases of 50°C or more.

The fuel performance code PLATE has been developed to model the irradiation performance of high density RERTR fuel plates. Many of its performance predictions are based on empirical correlations developed using data obtained from the extensive fuel testing campaign conducted by the RERTR program during the past decade. However, the heart of the PLATE code is an analytical model for estimating the fuel meat thermal conductivity, as influenced by the changing volume fractions of fuel meat constituents during irradiation. Comparison of PLATE calculations for experimental fuel plates from

various RERTR tests (with measured data obtained during PIE) shows positive overall agreement. Development work on PLATE continues with goals to extend performance correlations outside these parameter ranges, develop more mechanistic irradiation performance models (where possible), extend PLATE to the monolithic RERTR fuels, and couple PLATE with ABAQUS finite element software to analyze the structural integrity of the RERTR fuels.

Analyses made using PLATE have led to a much better understanding of the fabrication and irradiation variables important for acceptable RERTR fuel performance. First, the total fuel surface area should be minimized in order to minimize fuel-matrix interaction. In this regard, spherically shaped fuel particles have an advantage over non-spherical shapes; for any shape, however, the use of small fuel particles (fines) should be avoided. Calculations have also shown that knowledge of the fuel particle size and shape distribution will be necessary to make accurate predictions of fuel plate performance. Second, fuel-matrix interaction is a sensitive function of temperature; thus, efforts should be taken to keep temperatures as low as possible for RERTR fuels. For this reason, cladding surface corrosion must be kept low for this fuel form.

STEVEN L. HAYES (BS, 1988, MS, 1989, PhD, 1992, Nuclear Engineering, Texas A&M University) is Manager of the Fuel Performance and Design Department at the INL. He has been actively involved in the irradiation testing and modeling of fast breeder reactor fuels, fuels for actinide transmutation, and research reactor fuels for more than 15 years.

PAVEL G. MEDVEDEV (PhD, 2004, Nuclear Engineering, Texas A&M University) is a staff member of the Fuel Performance and Design Department at the INL. His interests include nuclear fuel fabrication, testing, and performance.